A Computational Analysis of Dopamine Signaling at the Level of the Varicosity in Rodent Striatum

DISSERTATION

Presented in Partial Fulfillment of the Requirements for the Degree Doctor of Philosophy in the Graduate School of The Ohio State University

By

Katherine Rooney

Graduate Program in Pharmaceutical Sciences

The Ohio State University

2015

Dissertation Committee:

Dr. Lane Wallace, Advisor

Dr. Anthony Young

Dr. Howard Gu

Abstract

Dopamine is a modulatory neurotransmitter that signals the saliency of the environmental input and is involved in the learned formation of responses. Dopamine neurons exist in twelve distinct nuclei throughout the brain, including the substantia nigra pars compacta and ventral tegmental area. The dopamine neurons in these two nuclei send projections to the extended striatum and frontal cortex. These dopamine neurons fire intrinsically at about 5 Hz, creating a baseline low nanomolar extracellular dopamine concentration in the striatum that can be measured using microdialysis. This suggests that baseline dopamine is essential for proper brain function. Dysfunction in the dopamine system leads to diseases such as Parkinson's disease, addiction, schizophrenia and others. Currently, most of what we know about dopamine neurotransmission has been inferred from studies of other neurotransmitter systems. Because dopamine is a modulatory neurotransmitter, it is difficult to study dopamine signaling directly. Greater knowledge of dopamine release, re-uptake and receptor binding is vital in understanding the dopamine system as a whole and would provide valuable data to better treat the disease states associated with dopamine signaling. Herein, I will present research aimed at dissecting the parameters necessary to build a complete computer model of a dopamine varicosity to be used to better understand dopamine signaling.

Chapter 1 introduces the extended striatum, the various neurons and inputs present in the striatum, and the dopamine system in this brain region. This chapter will

focus on the characteristics of each and how each part of the striatum contributes to its overall function. Next, the chapter will discuss in detail the characteristics of the dopamine system as a whole including dopamine transmission, receptors and transporters involved in signaling and the modulatory function of the neurotransmitter.

Chapter 2 presents the findings that dopamine release probability in the striatum is low. A computer simulation of a single dopamine release site was used to determine that less than one vesicle needs to be released per firing event to maintain the reported baseline extracellular concentration. The simulation model was also used to determine the amount of dopamine released to match published data of extracellular dopamine following electrical stimulation *in vitro*. The model suggests that the dopamine release induced by a single electrical stimulation may be as large as two vesicles. Our findings argue that dopamine release at any one particular varicosity is very low.

Chapter 3 presents the findings of a literature review to determine the quantitative details of all aspects in the striatal complex. These details provided evidence that, while the striatum is typically thought of as a dopaminergic area, quantitatively dopamine is a minor system compared to others present in the striatum. While dopamine's number of varicosities and receptors is lower than other systems, we also determined on which elements the receptors are located. We found that dopamine receptors have a diffuse presence. This suggests that dopamine has the capability to modulate the overall output of the striatum.

Chapter 4 presents the findings of a computer simulation of dopamine receptor binding in the vicinity of a single release site under multiple conditions. Baseline, tonic dopamine release results in about half of the dopamine D2 receptors being occupied

while no D1 receptors are occupied. A phasic burst of dopamine has little effect on receptor binding overall. A 30% increase in release probability is necessary to occupy a majority of D1 receptors. In this chapter we also explored the effects of a more complex simulation space and found that as the extracellular dopamine concentration increases, the location of D1 receptors becomes an important factor in receptor binding.

Chapter 5 presents the findings of a computer simulation of dopamine receptor binding in the vicinity of a single release site in the presence of cocaine or amphetamine. The highest dose of cocaine tested (25 mg/kg) only increased D1 receptor binding 4% and almost saturated the D2 receptors in the model. Modeling of the presence of 2 mg/kg amphetamine led to a 13% increase in D1 receptor binding and fully saturated D2 receptors. Our findings argue that the effects of cocaine are more likely due to D2 receptor activation and some of amphetamine's effects may be due to D1 receptor activation.

Finally, chapter 6 summarizes the findings and significance of this dissertation research as well as provides future perspectives. In summary, this dissertation has: (I) summarized the function and overall organization of the striatal complex and dopamine system, (II) determined that dopamine release probability at any one particular release site is low, (III) determined the quantitative details of the elements within the striatum, (IV) studied dopamine D1 and D2 receptor binding under tonic and phasic firing conditions and (V) characterized receptor binding in the presence of the psychostimulants cocaine and amphetamine.

Dedication

This document is dedicated to my family and friends, without whom none of my success would have been possible.

Acknowledgments

I would like to give my sincerest thanks to my advisor, Dr. Lane Wallace, for his guidance and support as a graduate student. I would also like to thank my committee, Dr. Tony Young and Dr. Howard Gu for their scientific discussion and input.

I would also like to thank my fellow graduate students in my program who have been both co-workers and friends. Their knowledge and input as well as their friendship over the years have been invaluable to my development as a scientist.

Finally, I would like to express my gratitude to my family and friends for their unending support. Thank you for supporting my every goal and for your endless amount of patience. Your encouragement and love has made it possible for me to pursue my ambitions.

Vita

November 3, 1988.....Born

2007.....Loveland High School

2011.....B.S. Pharmaceutical Sciences, The Ohio State University

2011 to present .....Graduate Teaching Associate, Department of Pharmacology, The Ohio State University

Publications

1. **Rooney, Katherine E.** and Lane J. Wallace. 2015. "Computational Modeling of Extracellular Dopamine Kinetics Suggests Low Probability of Neurotransmitter Release." *Synapse* 69:515-525.

Fields of Study

Major Field: Pharmaceutical Sciences

Table of Contents

List of Tables

List of Figures

Chapter 1: Introduction

1.1. Overview

The extended striatum, consisting of regions called dorsal striatum, nucleus accumbens core, nucleus accumbens shell, and possibly olfactory tubercle, plays a major role in learning, motivation, and development of habits. Dopamine signaling in the striatum and nucleus accumbens communicates novelty and saliency of the current environmental input and is involved in the learned formation of appropriate responses. Dopamine neurons from the ventral tegmental area (VTA) innervate the nucleus accumbens (ventral striatum), while dopamine neurons from the substantia nigra pars compacta (SNc) innervate the dorsal striatum. The number of dopaminergic cell bodies in VTA and SNC is small, about 20,000-30,000 in mice and 40,000-45,000 in rats (Björklund and Dunnett 2007); however, the axonal projections in the expanded striatum ramify extensively, forming dense, intricate axonal arborizations. The axonal tree from one neuron can influence up to 5.7% of striatal volume. Dopaminergic axons have varicosities (dopamine release sites) distributed along their axons within the expanded striatum, making an estimated hundred thousand varicosities per neuron (Matsuda et al. 2009). Therefore, each dopaminergic neuron has the potential to exert a large influence in

the striatum (Threlfell and Cragg 2011). Most (more than 75%) of striatal dopaminergic varicosities are not associated with synaptic specialization (Descarries et al. 1996). This ultrastructural observation coupled with amperometric experiments (Garris and Wightman 1994) suggest that dopamine signaling occurs through volume transmission. Thus, the neurotransmitter molecules can diffuse and affect receptors within a few micrometers of the release site. Dopamine is retrieved from the extracellular signaling compartment via the dopamine transporter (DAT) (Gether et al. 2006). Dopaminergic neurons fire intrinsically at about 1-5 Hz (Bunney, Aghajanian, and Roth 1973; Koeltzow et al. 1998), suggesting that a baseline dopaminergic tone is important to striatal function. While we know details about the dopaminergic system as a whole, the neurobiology of dopamine release and signaling at the level of the varicosity is still unknown. What dopamine release looks like and how its immediate neighborhood is constructed would have a large impact on the dopamine signal interpretation and ultimate output of the striatum. Using computer models, we are able to construct a plausible model of the dopamine varicosity to better understand vesicular release of dopamine and how different signaling patterns could interact with the immediate neighborhood.

1.2. Extended Striatum

The extended striatum is the primary input for the basal ganglia system and is involved in the planning and modulation of movement as well as being involved in many processes involving executive function. The striatum is composed mainly of medium spiny neurons (MSNs), which are GABAergic in nature. These neurons are the only

output neuron and account for about 95% of the neurons in the striatum (Dubé, Smith, and Bolam 1988). The other 5% of neurons are interneurons. These include at least three different types of GABAergic interneurons as well as a subset of cholinergic interneurons. For the purposes of this dissertation, I will focus on two subsections of the striatum: the dorsal striatum and the nucleus accumbens. The dorsal striatum is mainly associated with motor control while the nucleus accumbens is associated with reward.

The dorsal and ventral striatum (nucleus accumbens shell and core) are extremely similar in cellular composition and there are no well-defined borders between the regions. They are distinguished by their difference in function and the inputs they receive from other brain regions. The dorsal striatum, known as the caudate-putamen in humans, is mainly implicated in procedural and stimulus-response learning (Voorn et al. 2004). This area of the brain is also required for the execution of planned motor behavior and is implicated in the pathophysiology of Parkinson's disease and Huntington's disease (Graybiel et al. 1994).

The nucleus accumbens is thought to play a role in reward and pleasure. This area of the brain receives dopaminergic inputs from the ventral tegmental area, forming one component of the reward pathway. The nucleus accumbens is made up of two distinct regions, the core and the shell. The nucleus accumbens core has been shown to play a role in drug reinforcement (Crespo et al. 2006) and drug-seeking behavior (Ito, Robbins, and Everitt 2004). The shell is more sensitive to addicting drugs, though. Both regions play a role in learned behavior, but the core seems to respond to conditioned reinforcers while the shell seems to enhance certain behavioral responses that are coordinated through the core (Voorn et al. 2004).

1.2.1. Medium Spiny Neurons

The main output neuron of the striatum, the medium spiny neuron, sends projections along two distinct pathways. One projection, known as the direct pathway, sends fibers to the globus pallidus interna/substantia nigra pars reticulata and expresses dopamine D1 receptors. The indirect pathway sends projections to the globus pallidus externa and expresses dopamine D2 receptors. There is only a 5-15% overlap of expression of D1/D2 receptors in MSNs, thus allowing for a distinct segregation of the two pathways (Cerovic et al. 2013).

More than 90% of striatal neurons are known as the medium spiny neuron (MSN). They have been given this name due to the appearance of dense spines on their dendritic processes. These neurons have an inhibitory function. Thus, the output from the striatal complex cannot initiate any behavioral activity. Inhibitory neurons can only modulate activities that are driven either by intrinsic pattern generators or via inputs from other brain regions. The GABAergic output neurons in the striatal complex do not have an intrinsic activity. In the absence of a driving input, they are quiescent. Driving sources are glutamatergic inputs from cortex, thalamus, hippocampus, and amygdala. The cortical inputs form a topological map from the entire cortex (McGeorge and Faull 1989). This suggests that the striatal complex is modulating a wide variety of processes originating in the cortex. These would include executive decision-making from the prefrontal cortex, motor information from the motor areas, and sensory information from visual and auditory cortex areas. The GABAergic output neurons also show substantial collateral

axon innervation of neighboring output neurons, suggesting that activity from multiple areas of the cortex is integrated in the striatum.

1.2.2. Striatal Interneurons

The other 5-10% of cells found within the striatum are interneurons. They consist of four types of GABA interneurons as well as a subset of cholinergic interneurons.

Cholinergic interneurons appear to have a very important role in the striatum. These neurons account for somewhere around 1-2% of total neurons in this brain region. Axons of cholinergic interneurons in the striatum branch profusely (Contant et al. 1996). These neurons are tonically active, providing a constant basal level of acetylcholine in the extracellular environment (Bennett and Wilson 1999). As the only other cholinergic innervation into the striatum is a very small tract from the pedunculopontine nucleus, the vast majority of cholinergic synapses arise from the interneurons. Multiple elements in the striatum express muscarinic and nicotinic cholinergic receptors allowing for cholinergic modulation of the striatal output. Every dopamine nerve terminal has a nicotinic acetylcholine receptor, which could potentially allow for cholinergic modulation of dopamine signaling within the striatum as well.

The remaining interneurons are GABAergic in nature and are divided into four subclasses based on their electrophysiological properties. There are the fast spiking GABAergic interneurons, the low threshold spiking interneurons, the calretinin positive GABAergic interneurons (Tepper and Bolam 2004) as well as tyrosine hydroxylase positive GABAergic interneurons (Ibáñez-Sandoval et al. 2010). The fast spiking

neurons, which are also characterized by their expression of parvalbumin, are thought to make up about 0.7% of the total neurons in the rat striatum (Luk and Sadikot 2001) and are electrotonically coupled via gap junctions (Kita, Kosaka, and Heizmann 1990). The fast spiking interneurons receive a glutamatergic input from the cortex as well as GABAergic input from MSN axon collaterals and a cholinergic input (Tepper and Bolam 2004). The low threshold spiking interneurons express neuropeptide Y, somatostatin and nitric oxide synthase (Smith and Parent 1986). These neurons account for about 0.8% of neurons in the rodent striatum (Rymar et al. 2004) and have the least dense axonal arborization (Kawaguchi 1993). The calretinin neurons account for about 0.8% of neurons in rodent striatum (Rymar et al. 2004) and are relatively sparse in the caudal areas of the striatum (Bennett and Bolam 1993). There are currently no electrophysiological data for these cells and their profile is not known. Finally, the tyrosine hydroxylase GABAergic interneurons are further divided into four subclasses based on their electrophysiological profiles. They were first described in 1987 in the primate (Dubach et al. 1987) and since then have been described in other species such as rats (Meredith et al. 1999), mice (Mao et al. 2001; Petroske et al. 2001) and humans (Porritt et al. 2000; Petroske et al. 2001; Cossette, Lecomte, and Parent 2005). Even though these neurons contain tyrosine hydroxylase, Xenias et al. found they lack the aromatic L-amino acid decarboxylase, dopamine transporter, VMAT2 and dopamine. Also, using voltammetry and optogenetics, they showed that these neurons do not release dopamine when stimulated (Xenias et al. 2015).

1.2.3. Inputs to Striatum

The striatum integrates multiple inputs from other areas of the brain as well. The dorsal striatum receives glutamatergic inputs from the cortex, thalamus and amygdala. The nucleus accumbens receives glutamatergic inputs from cortex, amygdala and hippocampus. There are also dopaminergic inputs originating from the substantia nigra and ventral tegmental area, which innervate the dorsal striatum and nucleus accumbens, respectively (Silberberg and Bolam 2015). The main GABA input to the striatum originates from the four classes of GABAergic interneurons as well as from axon collaterals originating from the MSNs. Finally, there seems to be a small serotonergic input originating from the dorsal raphe.

The corticostriatal glutamatergic input, which accounts for a majority of the inputs to both the D1-expressing and D2-expressing MSNs (Wall et al. 2013), has been shown to map topographically to the extended striatum. The majority of corticostriatal inputs from the frontal cortex, including the motor and sensory cortices, map to the dorsolateral striatum. The visual, cingulate and auditory cortices send projections to the dorsomedial striatum. Finally glutamatergic neurons from the limbic areas of the cortex send projections to the ventral striatum, including the nucleus accumbens (McGeorge and Faull 1989). A visual representation of the corticostriatal inputs is shown in Figure 2, using both coronal and sagittal sections.

1.3. Dopamine

Dopamine is a neurotransmitter found in the brain that is important for voluntary motor control, motivation, reward, learning, attention and memory. Two of the most studied dopaminergic nuclei of the brain are the substantia nigra pars compacta and the ventral tegmental area. Each of these nuclei contains only about 20,000 dopamine neurons, but they have powerful effects on behavior. This suggests that these neurons must have large projection fields to be able to influence brain activity. In fact, dopamine neurons exhibit extensive arborizations in their terminal fields and each neuron can influence up to 6% of the striatal volume (Matsuda et al. 2009). They fire tonically at about 5 Hz and signal through volume transmission which creates a basal dopaminergic tone in the projection areas (Tritsch et al. 2012). The dopaminergic neurons are known to burst simultaneously for about 200 milliseconds when the subject is presented with a natural reinforcer or associated cues (Heien and Wightman 2006).

The dopamine neurons of the VTA are one component of the reward pathway in the brain, which reinforces behavior that is necessary for survival such as eating, drinking and sex. When a reward is presented, dopamine signaling increases (Schultz 2002). This increase modulates circuits involved in memory and behavior, which ensures that these behaviors are repeated.

1.3.1. Volume Transmission

Research suggests that dopamine is able to signal in the striatum via volume transmission. This type of communication is characterized by the ability of the neurotransmitter to diffuse in three-dimensions within the brain extracellular fluid beyond the synaptic cleft. It differs from "wiring transmission" in that it does not occur within a well-defined structure as in synaptic transmission or communication through gap junctions. Release of neurotransmitter from one site is able to influence multiple target cells within a given sphere of influence. Evidence that supports the idea of volume transmission includes the identification of release sites that are outside defined synapses and the presence of receptors located extra-synaptically. Usually volume transmission allows for a constant concentration of neurotransmitter to be present in the area in which it occurs (Agnati et al. 1995).

Dopamine is believed to signal via volume transmission based on multiple pieces of evidence. Published data from no-net-flux micro-dialysis experiments in awake rodents report average baseline levels of dopamine in the low nano-molar range: average of 9.5 nM in rat dorsal striatum (Glick et al. 1994; S. R. Jones et al. 1998; Bianco et al. 2008; Castner, Xiao, and Becker 1993; Chen, Lai, and Pan 1997; Martin-Fardon et al. 1997; Sam and Justice 1996; A. D. Smith, Olson, and Justice 1992), 5.9 nM in mouse dorsal striatum (He and Shippenberg 2000; Käenmäki et al. 2010; Hewett et al. 2010), 4.5 nM in rat nucleus accumbens (Crippens, Camp, and Robinson 1993; Glick et al. 1994; Parsons, Smith, and Justice 1991b; A. D. Smith and Weiss 1999; Kalivas and Duffy 1993; Parsons and Justice 1992), and 4.8 nM in mouse nucleus accumbens (Zapata and

Shippenberg 2002; Käenmäki et al. 2010). Most (60-70%) of striatal dopaminergic varicosities are not associated with synaptic specialization (Descarries et al., 1996). It has also been observed that less than 10% of dopamine D1 and D2 receptors are associated with symmetrical synapses (Zoli et al. 1998). This ultrastructural observation coupled with amperometric experiments (Garris and Wightman 1994) suggests that dopamine signaling occurs through volume transmission. In fact, mathematical modeling suggests dopamine in the nucleus accumbens core is able to travel 6-12 μm before the concentration is reduced by half (Heien and Wightman 2006).

1.3.2. Dopamine Transporter

The dopamine transporter (DAT) is a protein that is involved in the termination of the dopamine signal. This protein binds dopamine in the extracellular space and moves it into the cytosol of the neuron. In the striatum, this transporter is expressed on dopamine varicosities. DAT functions as a symporter, and in order to function, must bind and co-transport two sodium ions and a chloride ion along with a dopamine molecule (Mortensen and Amara 2003).

DAT belongs to the SLC6 family of transporters that couple inward solute transport to downhill movement of Na^+ and Cl^-. This movement occurs as the protein cycles between an outward and inward conformation that bind the substrate and then release it on the opposite side of the membrane. The uptake rate and capacity of DAT are dependent on the kinetics of the conformation changes as well as the number of DAT present on the membrane surface (Vaughan and Foster 2013).

1.3.3. Psychostimulants

The dopamine transporter is a target of many drugs, including drugs of abuse, such as cocaine and amphetamine. Amphetamine is typically used to treat attention disorders, but is also abused. Cocaine can be used as a local anesthetic, but is also used for non-medical reasons. Both drugs cause hyperactivity in humans and rodents. These drugs are thought to exert their effects by blocking and/or reversing the dopamine transporter (Peña, Gevorkiana, and Shi 2015; Zhu and Reith 2008).

Cocaine blocks the dopamine transporter, increasing the time dopamine is in the extracellular space. The presence of cocaine has been shown to increase the dopamine concentration up to 8-fold in the extended striatum (Camp, Browman, and Robinson 1994; Church, Justice, and Byrd 1987). Amphetamine, on the other hand, is thought to exert its actions by not only preventing re-uptake of dopamine, but also by reversing the transporter, causing more dopamine to enter the synapse. Amphetamine has been shown to increase extracellular dopamine concentrations up to 30-fold of baseline in the striatal complex (Badiani et al. 1998; Carboni et al. 2001; Guan and McBride 1988).

Mounting evidence suggests that cocaine and amphetamine work through both dopamine transporter-dependent and independent mechanisms. Psychostimulants have also been shown to bind the serotonin and norepinephrine transporters (Han and Gu 2006). Studies suggest that cocaine and amphetamine can still increase extracellular dopamine in the nucleus accumbens of dopamine transporter knockout mice (Carboni et al. 2001). The authors hypothesized that the presence of norepinephrine transporters

(NET) acted to clear the dopamine in DAT knockout mice in this case and were able to show that the addition of a NET blocker to the knockout animals increased extracellular dopamine in the nucleus accumbens of knockout animals but not wildtype. Further evidence shows that DAT knockout mice still self-administer cocaine and show cocaine-induced place preference (Rocha et al. 1998; Sora et al. 1998). This suggests that while dopamine has been shown to play a role in the effects of psychostimulants, other pathways may also be involved.

1.3.3. Dopamine D1-like Receptors

Dopamine receptors are all G-protein coupled receptors and are divided into two classes: D1-like receptors (D1 and D5 receptors) or D2-like receptors (D2, D3 and D4 receptors). D1-like receptors are coupled to $G\alpha_{olf}$ or $G\alpha_{s}$, which activate adenylyl cyclase and lead to the production of cyclic AMP and activation of protein kinase A. The D1-like receptors are most abundant in the striatum and nucleus accumbens (Savica and Benarroch 2014).

Binding studies of the D1 receptors has revealed that these receptors exist in a high and low affinity state for agonists. There are two theories to describe the affinity state of a G protein-coupled receptor. First, there is a theory that the G protein and receptor form a stable interaction regardless of binding state of the receptor. This interaction leads to a high affinity for the receptor, and, when bound to an agonist, the G protein activates effector proteins without dissociating from the receptor (Hein and Bünemann 2009; Qin et al. 2011). The second theory is the collision-coupling model, in

which the G protein and receptor are uncoupled and move freely throughout the cell membrane. When the receptor binds an agonist, it has a higher affinity for a G-protein, which then binds, activates and dissociates to activate effector proteins (Hein and Bünemann 2009; Skinbjerg et al. 2012). In general, it is believed that the D1 receptor exists mainly in a low affinity state and exhibits a K_d of about 1 μM for dopamine. Richfield et al. determined that about 80% of the D1 receptor exist in the low affinity state (Richfield, Penney, and Young 1989).

1.3.4. Dopamine D2-like Receptors

Dopamine D2-like receptors are coupled to $G\alpha_{i/o}$, which inhibits adenylyl cyclase/cyclic AMP/PKA pathway, and phospholipase A2, which releases arachidonic acid. These signals can be terminated by either activation of a GTPase or phosphorylation of the receptor by a GPCR kinase (Savica and Benarroch 2014). D2-like receptors are found both presynaptically, where they function as autoreceptors, and postsynaptically. These receptors also have two distinct isoforms. The short form consists of 415 amino acids, and the long form has a 29 amino acid insertion in a domain between TM5 and TM6 (Dal Toso et al. 1989; Giros et al. 1989). Usiello et al. found that the long form of the receptor mainly exists on postsynaptic sites, whereas the short form mainly exists presynaptically and functions as an autoreceptor (Usiello et al. 2000). Like the D1 receptors, the D2 receptors are most abundant in the striatum.

It has also been shown that the D2 receptor exists in a high and low affinity state for agonists. Unlike the D1 receptors, the D2 receptors mainly exist in the high affinity

state with an K_d of about 10 nM for dopamine. Richfield et al. found that about 80% of the D2 receptor exist in the high affinity state (Richfield, Penney, and Young 1989). However, multiple studies of the number of high affinity D2 receptors in the striatum suggest the percentage of receptors ranges anywhere from 13-90% (van Wieringen et al. 2012). This wide range could be due to multiple factors such as: agonist used, experimental protocol (intact cells vs. homogenates, composition of media) and analysis of the data (computer assisted vs. by hand). It is still not clear, though, whether the D2 receptors exist in high and low affinity states *in vivo* and what the physiological significance is of the differing affinities (Skinbjerg et al. 2012).

1.3.5. Modulatory Function

Dopamine can only activate G protein-coupled receptors, meaning it cannot cause a direct change in the membrane potential of a neuron. Instead, dopamine serves a primarily modulatory role in the brain. When a D1 receptor is activated, it inhibits potassium channels and increases calcium currents. Activation can also increase the effects of glutamate on NMDA receptors, which further depolarize the membrane and aids in calcium influx. All of these effects usually lead to an increase in excitability for the cell. Another important target of the D_1 receptor–activated pathway is DA- and cyclic AMP–regulated phosphoprotein of 32 kD (DARPP-32). DARPP-32 is a multifunctional protein that integrates multiple neurotransmitter signals to bi-directionally modulate PKA activity (Savica and Benarroch 2014).

When D2 receptors are activated, the $G\alpha_{i/o}$ subunit inhibits the adenylyl

cyclase/cyclic-AMP/PKA pathway and promotes DARPP-32 dephosphorylation. The βγ subunits can also activate inwardly rectifying potassium channels and inhibit calcium channels. D2 activation has been shown to reduce the activity of NMDA receptors, as well. When the D2 receptors are present on postsynaptic cells, these effects exert an inhibitory effect. D2 receptors can also be found on presynaptically, where they decrease neurotransmitter release by inhibiting calcium channels (Savica and Benarroch 2014).

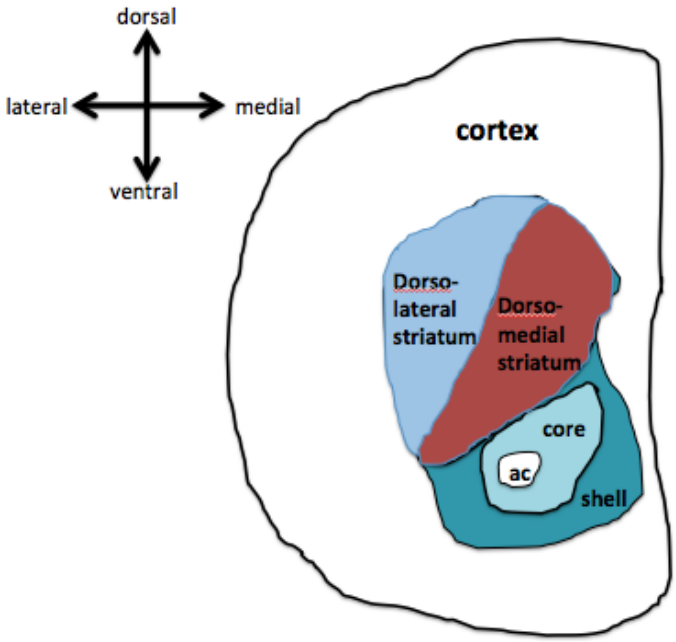

Figure 1: Map of the Extended Striatum.

A coronal section of one hemisphere of the extended striatum is shown above. The dorsal striatum is involved in motor coordination. The nucleus accumbens core and shell are involved in reward. Adapted from (Voorn et al. 2004).

Figure 2: Coronal and Sagittal Illustrations of Corticostriatal inputs.

Using a color coordinate system, we have illustrated the locations of cortical neurons and the location of their projections within the striatum. Data on cell body and terminal field locations were extracted from studies of projections into the extended striatum (Britt et al. 2012; Brown, Smith, and Goldbloom 1998; McGeorge and Faull 1989; Phillipson and Griffiths 1985; Sesack et al. 1989; Wall et al. 2013). We made a series of coronal (Figure 2A) and sagittal (Figure 2B) sections and color-coded the striatal complex in blocks according to the following color scheme: low red shade indicates a medial position and high red shade indicates a lateral position; low green shade indicates a ventral position and high green shade indicates a dorsal position; and low blue shade indicates a caudal position and high blue shade indicates a frontal position. We then indicated on coronal and sagittal sections with ovals showing location of cell bodies color-coded to have the same colors as their projection targets in the striatal complex. In the sagittal sections representing rat brains, the number in the lower right corner indicates mm lateral from the midline. In the coronal sections, the number in the lower right corner indicates mm in front of the interaural line (Wallace, LJ, unpublished).

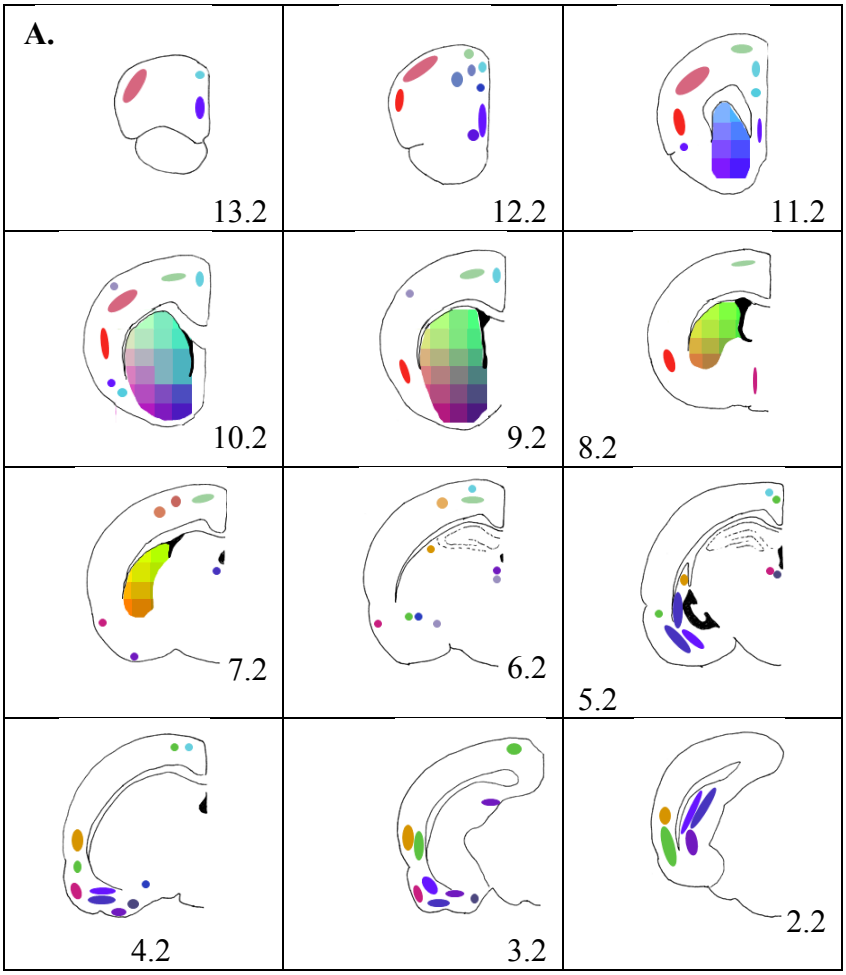

Continued

Figure 2: Coronal and Sagittal Illustrations of Corticostriatal Inputs.

Figure 2 (Continued): Coronal and Sagittal Illustrations of Corticostriatal Inputs.

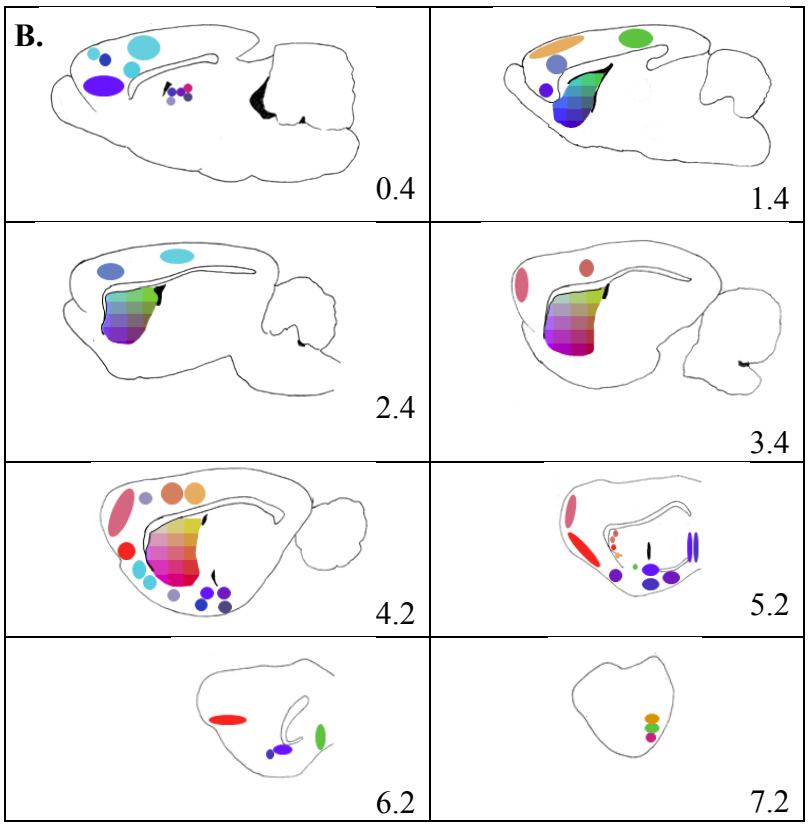

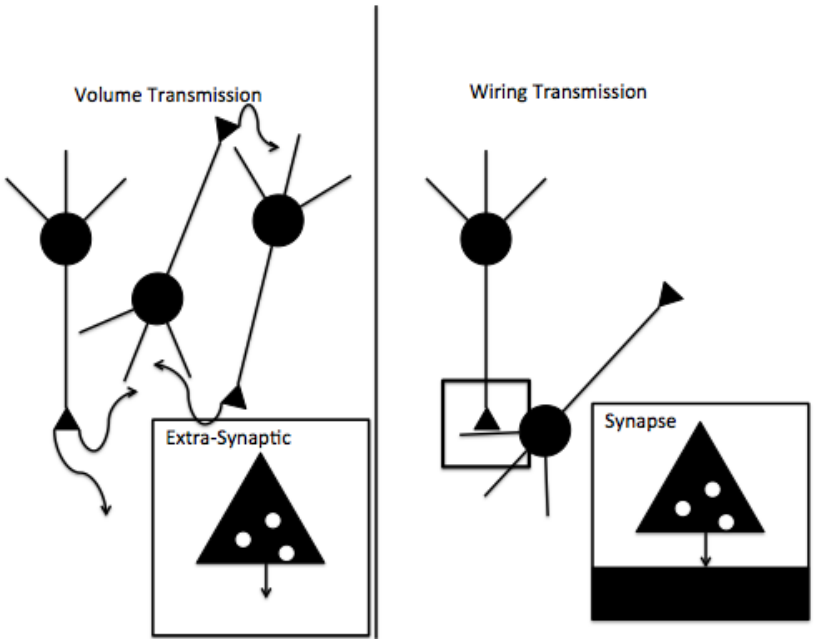

Figure 3: Volume Transmission vs. Wiring Transmission.

This figure illustrates the differences between volume transmission, in which the neurotransmitter has the ability to diffuse within three-dimensional space and bind receptors on multiple neurons in the vicinity, and wiring transmission, in which a defined structure facilitates neurotransmission. Adapted from (Agnati et al. 1995).

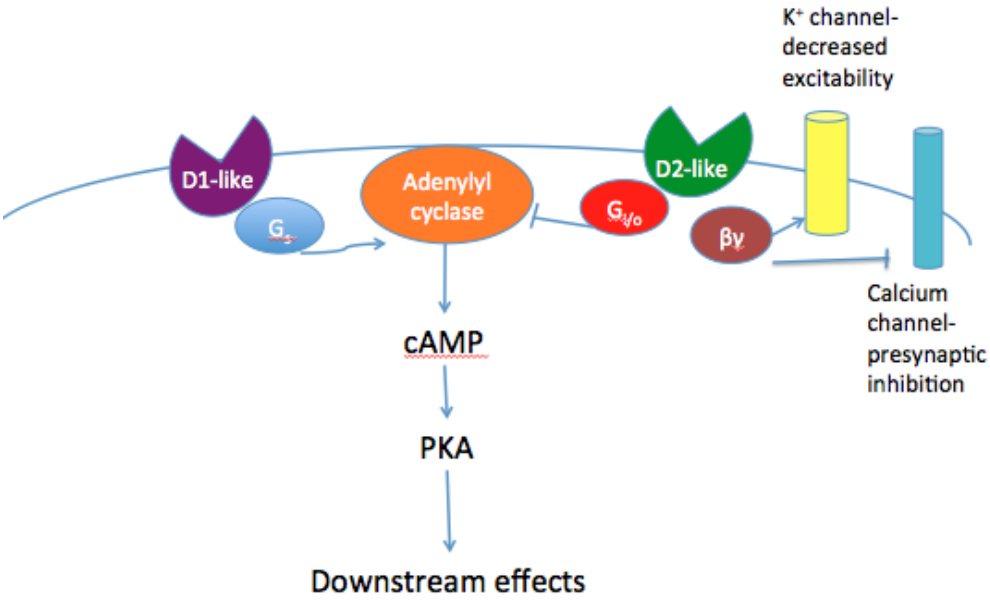

Figure 4: Dopamine Receptor Signaling Pathways.

Two types of dopamine receptors exist: the D1-like receptors and the D2-like receptors. D1-like receptors are are coupled to $G\alpha_{olf}$ or $G\alpha_{s}$, which activates adenylyl cyclase, which leads to the production of cyclic AMP and activation of protein kinase A. This has downstream effects that ultimately lead to increased excitability in the cell and contributes to synaptic plasticity. The D2-like receptors are coupled to $G\alpha_{i/o}$, which inhibits adenylyl cyclase/cyclic AMP/PKA pathway, thus preventing the downstream effects of protein kinase A activation. The D2-like receptors can also decrease the excitability of potassium channels or block calcium channels and cause presynaptic inhibition via the βγ subunit. Adapted from (Savica and Benarroch 2014).

Chapter 2: Computational Modeling of Striatal Extracellular Dopamine Kinetics Suggests Low Probability of Neurotransmitter Release

2.1. Introduction

Dopamine signaling in the striatum and nucleus accumbens communicates novelty and saliency of the current environmental input and is involved in the learned formation of appropriate responses. Dopamine neurons from the ventral tegmental area (VTA) innervate the nucleus accumbens (ventral striatum), while dopamine neurons from the substantia nigra pars compacta (SNc) innervate the dorsal striatum. The number of dopaminergic cell bodies in VTA and SNc is small, about 20,000-30,000 in mice and 40,000-45,000 in rats (Björklund and Dunnett 2007); however, the axonal projections in the expanded striatum ramify extensively, forming dense, intricate axonal arborizations (Gauthier et al. 1999; Matsuda et al. 2009; Prensa and Parent 2001). The axonal tree from one neuron can influence up to 5.7% of striatal volume (Matsuda et al., 2009). Dopaminergic axons have varicosities (dopamine release sites) distributed along their axons within the expanded striatum, making an estimated 500,000 varicosities per neuron (Andén et al. 1966). Therefore, each dopaminergic neuron has the potential to exert a large influence in the striatum. Most (60-70%) of striatal dopaminergic varicosities are not associated with synaptic specialization (Descarries et al. 1996). This ultrastructural

observation coupled with amperometric experiments (Garris and Wightman 1994) suggest that dopamine signaling occurs through volume transmission. Thus, the neurotransmitter molecules can diffuse and affect receptors within a few micrometers of the release site. Dopamine is retrieved from the extracellular signaling compartment via the dopamine transporter (DAT) (Gether et al. 2006). Dopaminergic neurons fire intrinsically at about 1-5 Hz (Bunney, Aghajanian, and Roth 1973; Koeltzow et al. 1998), suggesting that a baseline dopaminergic tone is important to striatal function.

Neuronal communication occurs when an action potential depolarizes a terminal membrane. This opens voltage gated calcium channels, which allows influx of calcium that interacts with storage vesicle membranes to stimulate the release of neurotransmitter (Catterall 2011). Control of timing and physical location of release is crucial to proper signaling. Release of a neurotransmitter is thought to be primarily controlled through the firing rate (frequency pattern of action potentials) of the neuron. However, several parameters at the axon terminal are capable of modulating the coupling of action potential to release of neurotransmitter. For example, activation of autoreceptors located on nerve terminals (Ford 2014) or activation of cannabinoid receptors on glutamatergic and GABAergic nerve terminals (Katona and Freund 2012) often decreases total neurotransmitter release. It is also possible that an action potential might not propagate throughout all of the axonal arborizations (Bucher and Goaillard 2011).

Recent evidence suggests that dopamine secretion is not characterized by each action potential being associated with a high probability of full exocytotic release. In one study, measurement of dopamine released from cultured dopaminergic cells suggested that transient small synaptic vesicle fusion pores form, releasing about 25% of a vesicle's

contents during each opening (Staal, Mosharov, and Sulzer 2004) In another study, dopamine storage vesicles were visualized using a false fluorescent neurotransmitter. The data suggested that 0.03 - 0.21% of dopamine synaptic vesicles fused in each stimulus, varying as a function of stimulation frequency (Gubernator et al. 2009). Previous simulation models performed in our lab also suggest that only a fraction of each vesicle is released during trains of electrical stimulation (Wallace and Hughes 2008).

The first goal of the current study is to estimate the likelihood of full exocytotic dopamine release associated with each firing event under baseline conditions. This was done using a computer simulation model of an extracellular compartment associated with a dopaminergic varicosity. This model was then used to evaluate the relationships between dopamine release rate, DAT kinetics, and dopamine levels and compare model outputs to published data for striatal dopamine content, extracellular levels of dopamine measured by no-net-flux microdialysis, and DAT kinetics. Under baseline conditions, the results suggest that the amount of dopamine release occurring with each firing event is a small fraction of the contents of a single vesicle per varicosity. The second goal is to estimate the fraction of total stored dopamine released during a highly stimulated condition. This was done using the same model system to simulate published measurements of extracellular dopamine following electrical stimulation of striatal slices *in vitro*. The results suggest the amount of dopamine release induced by a single electrical stimulation may be as large as the contents of two vesicles per varicosity.

2.2. Materials and Methods

2.2.1. Quantitative Parameters Relative to Dopamine Varicosities and Dopamine Transporter

The computer simulation model requires quantitative details describing dopamine varicosities and DAT kinetics. A summary of gross tissue level parameter values derived from published data is provided in Table 1. In the original publications, data are reported in a variety of different units (molar, pmol/mg protein, mg/gram wet weight, etc.). To facilitate comparisons, all data were converted to molar using conversion factors of 0.151 mg protein/mg tissue, 0.084 mg membrane protein/mg tissue, tissue density of 1 g/mL, and molar mass of dopamine of 153 g/mole. Values for DAT V_{max} vary substantially between different experimental paradigms. We chose to use the values from in vivo experiments in which V_{max} was determined from rate of decline of dopamine after supramaximal stimulation of the medial forebrain bundle. Values for DAT K_m also vary substantially between different experimental paradigms. Values determined from rate of uptake of dopamine into transfected cells form one cluster, and those determined from rate of uptake of dopamine into brain tissue form another cluster. The transfected cell paradigm suffers from the disadvantage of not being neuronal tissue but has the advantage of being an intact system. The brain tissue paradigm suffers from the disadvantage of being a broken cell preparation (cell homogenates) or of being perturbed by the insertion of an electrode but has the advantage of being a neuronal system. Not

knowing which system most accurately resembles intact, undisturbed brain; we elected to examine effects using both values.

Our computations and simulation models examined parameters associated with a single varicosity containing a single release site. Therefore, gross tissue values were converted to numbers associated with the average for a single varicosity (assumes that all sites are identical) (Table 2). Some of our computations and simulation models compared dorsal striatum, nucleus accumbens core, and nucleus accumbens shell. However, data comparing varicosity density, dopamine levels, and DAT levels in nucleus accumbens core and shell are not abundant. The data that are available strongly support the concept that varicosity density, dopamine level, and DAT density are lower in nucleus accumbens than in dorsal striatum and that there is a gradient in these parameters from dorsal striatum to nucleus accumbens core to nucleus accumbens shell (Calipari et al. 2012; Cragg 2003; Mennicken et al. 1992). We chose to keep vesicle dopamine content and number of vesicles in a varicosity constant throughout the entire extended striatal complex, using the values calculated for dorsal striatum in both nucleus accumbens core and shell regions. We then calculated varicosity density and dopamine levels required to provide these numbers and noted they were in the ranges reported for nucleus accumbens. DAT catalytic rate was determined by dividing V_{max} by DAT density. As this value was similar in striatum and nucleus accumbens, an average value was applied to all regions. To determine dopamine-DAT binding rate constants, we used MCell simulations of dopamine uptake assays *in vitro*. The association rate constant was varied (with dissociation rate constant set to 0) to find a value that produced a K_m value from simulation data equal to each of the average K_m values we averaged from published data.

The dissociation rate constant was arbitrarily chosen. Because it is about $1/20^{th}$ the value of the transport rate, it has no impact on any of the results.

2.2.2. Simulation Model

Simulations of extracellular space associated with a dopaminergic varicosity were accomplished using MCell (Monte Carlo Cell), a stochastic simulation program that uses Monte Carlo algorithms to estimate molecule movement and reactions in three-dimensional space (J. R. Stiles et al. 1996; J. Stiles and Bartol 2001; Kerr et al. 2008). The model has three sets of parameters. One is a morphology representing extracellular space through which dopamine can diffuse. Two models of extracellular space were evaluated. One was spherical with volume of $2.1x10^{-15}$ L (radius 0.79 μm) for the dorsal striatum, $3x10^{-15}$ L (radius 0.89 μm) for the nucleus accumbens core and $7.7x10^{-15}$ L (radius 1.22 μm) for the nucleus accumbens shell model. The second model was a cylinder with volume of $2.1x10^{-15}$ L (radius 0.65 μm, height 1.58 μm) for the dorsal striatum, $3x10^{-15}$ L (radius 0.73 μm, height 1.78 μm) for the nucleus accumbens core and $7.7x10^{-15}$ L (radius 1.0 μm, height 2.44 μm) for the nucleus accumbens shell model. The second set of parameters characterized dopamine secretion into extracellular space. Dopamine was released from a point source on the surface of the spherical model and from a point source in the center of the end of the cylinder model. The third set of parameters characterizes dopamine removal by DAT. For the cylindrical model, DAT was arranged in a band of 0.75 microns width beginning 0.5 microns from the release site (Figure 5). For the cylindrical model, DAT was arranged in a band of 0.75 microns width

beginning at 0.5 microns from the end of the cylinder containing the release site. In MCell, transport is modeled as a binding reaction followed by a transport step:

$$DA + DAT \leftrightarrows DADAT \rightarrow DA\_TRANS + DAT$$

DADAT represents the bound DA·DAT complex. The second reaction simulates dopamine transport with a recycling of the transporter (DADAT), where DA_TRANS represents transported dopamine. Forward rate constants for the first reaction were either $5x10^6$ or $1.3x10^8$ per molar per second (see Table 2), reverse rate was 0.5 per second, and rate constant for the second reaction was 9 per second.

For simulations of baseline level of dopamine, values for parameters were input into the model, and a pulse of dopamine was released every 0.2 seconds (simulating 5 Hz firing rate) or 1 second (simulating 1 Hz firing rate). The simulation was run for sufficient iterations to represent 30 seconds time, which produced a steady state level of extracellular dopamine. For simulations of effects of a single electrical pulse in brain slices, values for parameters were input into the model, and a pulse of dopamine was released at the beginning of the simulation. The simulation was run for sufficient iterations to represent 2-3 seconds.

2.3. Results

2.3.1. Models Assuming Release of Contents of a Single Vesicle

We first evaluated the hypothesis that each action potential releases the contents of one vesicle from each varicosity with each pulse. Using our computational model

simulating extracellular space surrounding a dopaminergic varicosity, the average level of extracellular dopamine was calculated using four different sets of conditions: firing rate of 1 and 5 Hz paired with a K_{on} of $5x10^6$ or $1.3x10^8$ M^{-1} sec^{-1}. The simulation baseline dopamine ranged from 50 nM to micromolar levels (Table 3).

Published data from no-net-flux micro-dialysis experiments in awake rodents report average baseline levels of dopamine in the low nano-molar range: average of 9.5 nM in rat dorsal striatum (Bianco et al. 2008; Castner, Xiao, and Becker 1993; Chen, Lai, and Pan 1997; Glick et al. 1994; S. R. Jones et al. 1998; Martin-Fardon et al. 1997; Sam and Justice 1996; A. D. Smith, Olson, and Justice 1992), 5.9 nM in mouse dorsal striatum (He and Shippenberg 2000; Hewett et al. 2010; Käenmäki et al. 2010), 4.5 nM in rat nucleus accumbens (Crippens, Camp, and Robinson 1993; Glick et al. 1994; Kalivas and Duffy 1993; Parsons and Justice 1992; Parsons, Smith, and Justice 1991a; A. D. Smith and Weiss 1999), and 4.8 nM in mouse nucleus accumbens (Käenmäki et al. 2010; Zapata and Shippenberg 2002). Thus, the model output is large compared to the experimental data. This suggests that the hypothesis that contents of one vesicle are released from each varicosity at each firing event is wrong, suggesting release rate is much smaller than hypothesized.

We also evaluated the hypothesis that each action potential releases the contents of one vesicle from each varicosity with each pulse from a slightly different point of view. If contents of a single dopaminergic storage vesicle are released every 0.2 seconds (5 Hz firing rate) and recaptured all at once, the recapture event would have to occur at 0.001 seconds in order to produce an average extracellular dopamine concentration of 10 nM. This increases to 0.005 seconds at a 1 Hz firing rate. We then explored in our MCell

model conditions that would support such a rapid clearance. Increasing the rate constant for dopamine binding to DAT to the point where binding is diffusion limited failed to produce such rapid clearance. This observation suggests that release rate is much smaller than hypothesized.

2.3.2. Models Estimating Dopamine Basal Release Rate

The premise of this set of experiments is that the basal dopamine release rate can be estimated using computer simulation studies if the average baseline dopamine level, dopamine neuron firing rate, extracellular morphology and DAT kinetics are known. Using our simulation model, we determined the number of dopamine molecules released at each release event to produce an average extracellular dopamine level in our simulation output equal to that reported in no-net flux dialysis experiments. The results show a range from 2-400 molecules depending on the brain region, firing rate employed and K_{on} rate. This amounts to 0.1-21% of the estimated content of a vesicle. Parameter values for simulations and corresponding dopamine release rates are shown in Tables 4 and 5. The release rate was the same for both the spherical and cylindrical morphologies. Since our estimated number of dopamine molecules in a vesicle is 1,900, the simulation results suggest that less than 25% of the contents of a vesicle is released at each firing event. For dorsal striatum, we also ran simulations in which the entire contents of one vesicle were released every N action potentials, where 1/N is the percent of vesicle contents released in Tables IV and V. The average extracellular dopamine in these simulations was the same as that shown in Tables IV and V. For example, the

extracellular dopamine levels were 8 and 39 nM for 1and 5 Hz firing rates using the slow on-rate kinetics and a 1% release probability.

2.3.3. Models estimating dopamine release under stimulated condition

This study was done to estimate dopamine release under conditions usually associated with a high rate of neurotransmitter secretion in order to estimate the fraction of stored dopamine released. We chose to simulate published experiments in which extracellular dopamine is measured using amperometric techniques following a single electrical pulse near a recording electrode in slices *in vitro*. The average peak dopamine concentration from such experiments was 1.74 μM for dorsal striatum, 1.13 μM for accumbens core, and 0.45 μM for accumbens shell. The number of dopamine molecules needed to provide these concentrations is 2,089, a number slightly larger than the contents of one vesicle.

Published data for the effects of electrical stimulation of slices on extracellular dopamine levels monitor rate of decrease of dopamine after the stimulation pulse. Such data provided a reference to which we could compare our simulation model to validate that the parameters we used for estimating baseline dopamine levels are reasonable. For one set of simulations, total DAT per varicosity was fixed at 2,500, and the V_{max} per transporter, k_{on} binding rate parameters, and number of molecules released were varied until model output provided a good fit to published data for dorsal striatum (Fig. 6), nucleus accumbens core (Fig. 7), and nucleus accumbens shell (Fig. 8). Good matches to experimental data were obtained with V_{max} values of 9-10 dopamine molecules/sec, k_{on} of

1-2x10^6 $M^{-1}sec^{-1}$, and 3,100 dopamine molecules released. The V_{max} from these simulations was close to the value we calculated from published data (Table 2), and the k_{on} value close to the lower affinity value calculated from published data (Table 2). For a second set of simulations, we fixed the k_{on} to 1.3x10^8 $M^{-1}sec^{-1}$, the value associated with the higher affinity value calculated from published data (Table 2), and varied V_{max} value, number of available transporters, and number of dopamine molecules released. Good matches to experimental data were obtained with 330-375 transporters, 3,100 dopamine molecules released and V_{max} value of 9-10 dopamine molecules/sec. These results suggest that a large range of sets of on rate and available transporter pairs produces output that fits the published experimental data.

2.4. Discussion

The first goal of the current study is to estimate the likelihood of full exocytotic dopamine release associated with each firing event under baseline conditions. Our simulation results using a variety of kinetic and firing rate parameters always showed a basal release rate of less than 25% of the contents of a single vesicle. The second goal is to estimate the amount of dopamine release during a highly stimulated condition. Simulation results suggest that the contents of up to 2 vesicles are released under these conditions. The conclusion of our paper is that dopamine release probability at any particular varicosity is low. This suggests that factors capable of increasing release probability could have a powerful effect on sculpting phasic dopamine signals.

2.4.1. Considerations relative to the simulation model

The model, in essence, consists of three components: dopamine release, DAT, and morphology. Of these, the parameter that deviates most from reality is morphology. The ideal model would utilize an accurate morphology associated with a dopamine release site. Ultrastructural studies suggest the extracellular morphology is best approximated by a network of tubes with an average diameter of 35 nm (Thorne and Nicholson 2006). Given the extracellular volume of 2.1 μm^3 associated with each varicosity in the dorsal striatum, the network would have a total length of 2180 μm. Within this network, DAT would be located in clusters somewhat close to the dopamine release site. A number of "tubes" would be branching away from the release site, some from locations between the release site and DAT and others distal to the cluster of DAT. Accurately modeling such a complicated morphology requires extensive ultrastructural studies on extracellular space in the striatum and substantial computational power. We chose to utilize simpler models for our study. In our model, we used two morphologies: a sphere and a cylinder. Our comparison of these two morphologies showed that morphology had little, if any, impact on our results (Tables 4 and 5). In an additional evaluation of morphology, we reduced the size of the extracellular space to one-third the original volume. This would evaluate the possibility that dopamine might not diffuse into spaces farther from the release site. This simulation yielded identical results (data not shown) to those reported in Table 4 and 5. We found the reason for this lack of impact of geometry on the results is that dopamine diffusion rate is much faster than the rate of dopamine binding to DAT. Based on this, we believe our conclusion is valid in spite of limitations of using a simplified morphology.

For DAT kinetics, we tested multiple values for both the association rate and turnover rate. Under all conditions tested, at most 25% of a single vesicle was required to match baseline extracellular dopamine as measured by no-net-flux dialysis. The conclusion that dopamine release probability at any particular varicosity is low was consistently observed under multiple kinetic conditions. The evaluation done with the faster on rate and 2,800 DAT would be close to maximum rate at which dopamine could possibly be removed as this on rate approaches the value at which binding would be diffusion limited. Several studies show that DAT transitions between a plasma membrane location and an intracellular location (Melikian 2004), suggesting that fewer DAT are available for actually transporting dopamine than used in our simulation model. Thus, our simulations using all of the DAT available for transport are biased towards higher levels of dopamine release, which provides additional support to the conclusion that dopamine release probability is low.

In our analysis of electrically stimulated dopamine release in brain slices, the estimate of release of contents of approximately two vesicles necessary for our model to match published data were independent of dopamine transporter kinetics (Figs. 6-8). Two extremes of possible kinetics were used in these studies: maximum number of available transporters paired with a slower on-rate for dopamine binding to DAT and maximum on-rate for dopamine binding to DAT paired with fewer available transporters. As binding data for the transporter does not distinguish between surface and internalized protein; we cannot be certain how many transporters are present and capable of moving dopamine at any given time. Each model, regardless of the kinetic parameters, required the release of contents of about two vesicles of dopamine per varicosity to match the

voltammetry data. The maximum extracellular dopamine concentration in these experiments was in the ballpark of 1 μM, a level approximately 100-fold higher than the estimated baseline dopamine level in vivo. Extrapolating from this comparison suggests that about 2% of the contents of a vesicle in each varicosity is released with each firing event under baseline in vivo conditions, further supporting our conclusion that dopamine release probability is low.

The strength of our conclusion also depends on the validity of the data we used for extracellular dopamine levels. For example, if the 5-10 nM level reported for no-net-flux dialysis underestimates the true concentration of extracellular dopamine, then our simulation model also underestimates the rate of dopamine release. While no-net-flux dialysis data for baseline levels of extracellular dopamine are very consistent, some other methods have provided higher values. For example, a drop of several hundred nanomolar in extracellular dopamine levels (measured using amperometry technique) was observed after administration of kynurenate (Kulagina, Zigmond, and Michael 2001). However, other studies using amperometry have not provided support for higher levels of basal extracellular dopamine. For example, a study directly examining baseline extracellular dopamine using fast scan cyclic voltammetry *in vivo* in awake animals provided robust data for an average extracellular dopamine level of 20-30 nM in nucleus accumbens (Owesson-White et al. 2012). Another argument for low levels of baseline extracellular dopamine derives from studies of effect of activation of dopamine D2 receptors on electrically stimulated dopamine release from striatum and nucleus accumbens in slices. Such studies consistently document that saturation of D2 receptors blocks dopamine release (Bello et al. 2011; Benoit-Marand, Borrelli, and Gonon 2001; Kennedy, Jones,

and Wightman 1992). This suggests that baseline dopamine levels must be sufficiently low that D2 receptors are not activated.

In addition to our modeling data, some experimental data have been consistent with the concept that only a small fraction of dopamine molecules in a single storage vesicle is released under baseline conditions. For example, measurement of dopamine released from cultured dopaminergic cells suggested that transient small synaptic vesicle fusion pores form, releasing about 25% of a vesicle's contents during each opening (Staal, Mosharov, and Sulzer 2004). In another study, dopamine storage vesicles were visualized using a false fluorescent neurotransmitter. The data suggested that 0.03 - 0.21% of dopamine synaptic vesicles fused in each stimulus, varying as a function of stimulation frequency (Gubernator et al. 2009). These data support our conclusion.

2.4.2. Implications of the results

From a mathematical perspective, a low probability of dopamine release can be accomplished through more than one mechanism. These include each firing event stimulating full exocytotic release of a single vesicle at a fraction of varicosities, kiss and run mechanism resulting in partial release of contents of a single vesicle at each varicosity, kiss and run mechanism resulting in partial release of contents of a single vesicle from some fraction of total varicosities, and release of dopamine from a non-vesicular pool. Data shown in this paper are from simulation models compatible with the condition that a small percent of the contents of every vesicle is released at each firing event. We also ran simulation models of the condition that the entire contents of a vesicle

are released at a small percent of firing events. The results yielded average baseline dopamine levels in the low nano-molar range. Thus, we cannot conclude from our simulation models which mechanism is functional in the brain.

From a biochemical perspective, several mechanisms could produce a low probability of dopamine release. One possibility is the existence of silent dopaminergic neurons that are not actively secreting neurotransmitter under baseline conditions. Some electrophysiological studies suggest that about half of dopaminergic neurons in the nucleus accumbens are not active in a normal, quiescent animal (Grace et al. 2007), while other studies suggest all dopaminergic neurons are tonically active (Dai and Tepper 1998). Another possibility is that all neurons are active but that action potentials do not propagate throughout the extensive axonal trees. Dopaminergic fibers are thin and unmyelinated, characteristics consistent with lesser action potential propagation capabilities (Pissadaki and Bolam 2013). At this point, we are not aware of studies measuring signal propagation in multiple branches of dopaminergic neurons. A third possibility is that release machinery is not responsive to depolarization under baseline conditions because of a low density of voltage-gated calcium channels. One could then hypothesize that the presence of signals acting at the release site to induce calcium influx could modulate the effects of dopamine neuron firing. One potential signal is activation of nicotinic acetylcholine receptors. Binding and functional data suggest that nearly every dopaminergic varicosity contains a nicotinic acetylcholine receptor (I. W. Jones, Bolam, and Wonnacott 2001). Activation of such receptors might further depolarize the membrane above the level induced by an action potential, allowing for dopamine release. Studies employing nicotinic agonists and antagonists have shown varying effects on

dopamine release. However, a study using optogenetics to study the effect of cholinergic interneuron activation clearly documents that activation of a population of cholinergic interneurons elicits dopamine release *in vivo* in the absence of any other stimulus. This dopamine release was nicotinic receptor dependent and frequency independent (Threlfell et al. 2012).

A very low baseline dopamine signal coupled with the ability to sculpt local dopamine release at the terminal level has interesting implications relative to the function of the extended striatal complex. The extended striatal complex receives inputs from across the entire volume of the cerebral cortex in a topographical manner modified by function such that cortical areas controlling different modalities of a behavior project to the same striatal area (Voorn et al. 2004). Thus, the global dopamine signal might indicate the saliency and novelty of current sensory information, while local signals provide a sculpted phasic dopamine response corresponding to the particular behavior or emotion where learning/behavioral change needs to occur. Thus, the global firing dopamine signal set by the firing rate/pattern sets a tone on top of which local signals drive specific behaviors. This might be a component of the mechanisms used to fine tune behaviors to maximize well-being.

In summary, dopamine signaling in the striatum and nucleus accumbens communicates novelty and saliency of the current environmental input and is involved in learned formation of appropriate responses. The tonic, or baseline, dopamine signal results from a regular firing of dopamine neurons at approximately 1-5 Hz. The conclusion of our paper is that at these baseline conditions dopamine release probability

at any particular varicosity is very low. This suggests that factors capable of increasing release probability could have a powerful effect on sculpting phasic dopamine signals.

2.5. Acknowledgements

This research was originally published in Synapse.

Rooney, Katherine E. and Lane J. Wallace. 2015. "Computational Modeling of Extracellular Dopamine Kinetics Suggests Low Probability of Neurotransmitter Release." *Synapse* 69: 515-525.

Table 1. Parameter values derived from biochemical data

Parameter	Value
Dopamine level (striatum)	79.2 μM [a]
Dopamine level (accumbens)	50.9 μM [b]
Dopamine varicosity density (striatum)	$1x10^{+8}/mm^3$ [c]
Dopamine varicosity density (accumbens)	$2\text{-}6x10^{+7}/mm^3$ [d]
Dopamine transporter level (striatum)	0.47 μM [e]
Dopamine transporter level (accumbens)	0.21 μM [f]
Dopamine transporter Vmax (striatum)	4.08 μM/sec [g]
Dopamine transporter Vmax (accumbens)	2.14 μM/sec [h]
Dopamine transporter Km (transfected cells)	2.17 μM [i]
Dopamine transporter Km (tissue prep)	0.2 μM [J]

[a] Derived from (Bardullas, Giordano, and Rodríguez 2011; Abekawa et al. 2001; Buu 1989; Cartmell et al. 2000; Gao and Dluzen 2001; Miller, Shore, and Clarke 1980; Ponzio et al. 1984; Takahashi et al. 1997; Sharp, Zetterström, and Ungerstedt 1986; Vezina et al. 1992; Yu, Kuo, and Cherng 2001; Yuan et al. 2001)

[b] Derived from (Bardullas, Giordano, and Rodríguez 2011; Cartmell et al. 2000; Fitoussi, Dellu-Hagedorn, and De Deurwaerdère 2013; Sharp, Zetterström, and Ungerstedt 1986; Vezina et al. 1992; Westerink and Korf 1976)

[c] Derived from (Doucet, Descarries, and Garcia 1986)

[d] Derived from (Doucet, Descarries, and Garcia 1986; Zhou et al. 2006)

[e] Derived from (Boja et al. 1995; Bonnet et al. 1986; Chen, Lai, and Pan 1997; Dubocovich and Zahniser 1985; Erikson, Jones, and Beard 2000; Garreau et al. 1997; Hooks, Juncos, et al. 1994; Janowsky et al. 1986; Marshall et al. 1990; Moll et al. 2000; Nakayama, Koyama, and Yamashita 1993; Rothman et al. 1994)

[f] Derived from (Bonnet et al. 1986; Erikson, Jones, and Beard 2000; Hooks, Juncos, et al. 1994; Janowsky et al. 1986; Marshall et al. 1990)

[g] Derived from (Garris and Wightman 1994; May and Wightman 1989; Wu et al. 2001)

[h] Derived from (Garris and Wightman 1994; May and Wightman 1989; Wu et al. 2001)

[i] Derived from (Carneiro et al. 2002; Chang et al. 2001; Eshleman et al. 1995; Itokawa et al. 2000; Kitayama et al. 1992; Lee et al. 1996; Lin and Uhl 2002; C. J. Loland, Norregaard, and Gether 1999; Claus Juul Loland et al. 2002; Lin and Uhl 2005)

[j] Derived from (Horn 1990; Marshall et al. 1990; Wu et al. 2001; Harris and Baldessarini 1973; Near, Bigelow, and Wightman 1988; Rothman et al. 2001; S. H. Snyder and Coyle 1969)

Table 2. Parameter values associated with a single varicosity.

Parameter	Value
Number of dopamine molecules per varicosity	475,000
Number of vesicles per varicosity	250
Number of dopamine molecules per vesicle	1,900
Extracellular volume associated with a release site (dorsal striatum)	$2x10^{-15}$ liter
Extracellular volume associated with a release site (accumbens core)	$3.1x10^{-15}$ liter
Extracellular volume associated with a release site (accumbens shell)	$7.7x10^{-15}$ liter
Number of DAT associated with a release site	2,800
DAT catalytic rate	9 /sec
DAT-DA binding on-rate (transfected cells)	$5x10^{+6}$ $M^{-1}sec^{-1}$
DAT-DA binding on-rate (tissue prep)	$1.3x10^{+8}$ $M^{-1}sec^{-1}$
DAT-DA binding off-rate	0.5 sec^{-1}
Dopamine diffusion rate	$4x10^{-6}$ cm^2/sec [a]

[a] Derived from (Land et al. 1984; Rice and Cragg 2008; Schönfuss et al. 2001)

Table 3. Extracellular dopamine levels with full vesicle release

Firing Rate	Dopamine Level	
	$K_{on}=5x10^{6}$ M^{-1} sec^{-1}	$K_{on}=1.3x10^{8}$ M^{-1} sec^{-1}
1 Hz	770 nM	50 nM
5 Hz	Continually increasing	300 nM

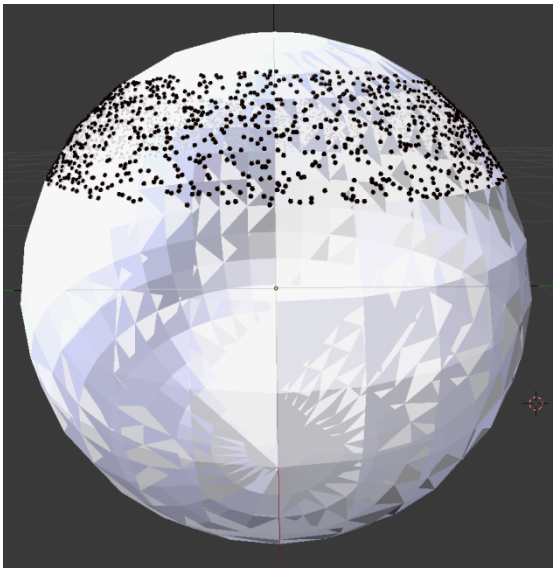

Figure 5: Visualization of the location of DAT on the spherical model of extracellular space associated with a dopaminergic varicosity.

The sphere has a diameter of 0.79 μm, and dopamine is released from a point source at the top of the sphere. Black dots represent DAT molecules, of which there are 2,500 in this model.

Table 4. Estimated rate of basal dopamine release in simulation models[1].

Region	Concentration[2]	Firing Rate	Release Rate[3]
Dorsal Striatum	8 nM	1 Hz	100
	8 nM	5 Hz	20
Nucleus Accumbens Core	4 nM	1 Hz	50
	4 nM	5 Hz	10
Nucleus Accumbens Shell	4 nM	1 Hz	50
	4 nM	5 Hz	10

[1] Simulations used a spherical morphology, 2,800 total DAT molecules with a transport rate of 9 dopamine per second and an on-rate of dopamine binding to DAT of $5x10^6$ M^{-1} sec^{-1}.

[2]average dopamine concentration from the simulation output

[3]release rate is number of dopamine molecules released per firing event to produce the average extracellular dopamine concentration listed.

Table 5. Estimated rate of basal dopamine release in simulation models[1].

Region	Concentration[2]	Firing Rate	Release Rate[3]
Dorsal Striatum	9 nM	1 Hz	400
	9 nM	5 Hz	100
Nucleus Accumbens Core	4 nM	1 Hz	175
	4 nM	5 Hz	40
Nucleus Accumbens Shell	4 nM	1 Hz	200
	5 nM	5 Hz	50

[1] Simulations used a spherical morphology, 2,800 total DAT molecules with a transport rate of 9 dopamine per second and an on-rate of dopamine binding to DAT of 1.3×10^8 M^{-1} sec^{-1}.

[2]average dopamine concentration from the simulation output

[3]release rate is number of dopamine molecules released per firing event to produce the average extracellular dopamine concentration listed.

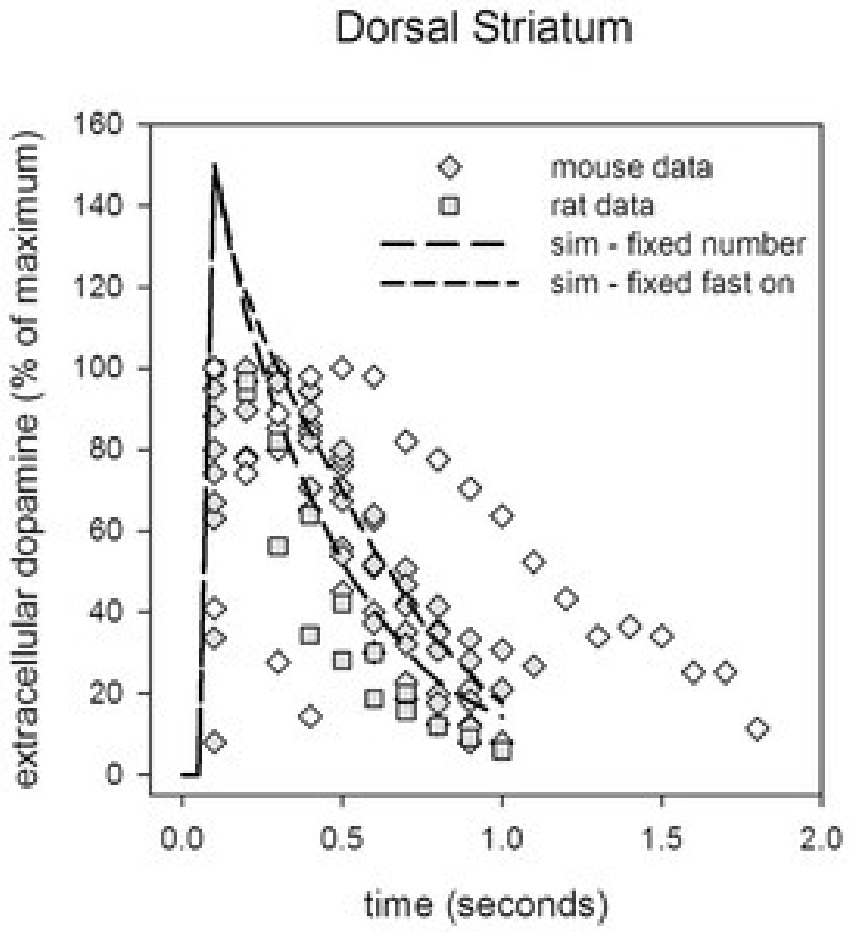

Figure 6: Simulation model output compared to published data for which rate of dopamine disappearance was measured as a function of time after electrical stimulation in dorsal striatum in brain slices *in vitro*.

Simulation parameter values for sim-fix number were 2,500 transporters $k_{on}=1.5x10^6$ $M^{-1}sec^{-1}$, Vmax = 10 dopamine molecules/sec, and 3,100 dopamine molecules released. Simulation parameter values for sim-fast on were 300 transporters $k_{on}=1.3x10^8$ $M^{-1}sec^{-1}$, Vmax = 10 dopamine molecules/sec, and 3,100 dopamine molecules released. The 100% value = 1.735 μM. Published data are from (Anzalone et al. 2012; Bello et al. 2011; Birbeck, Khalid, and Mathews 2014; Hnasko et al. 2010; S. R. Jones et al. 1998; S. R. Jones et al. 1999; Y Schmitz et al. 2001; L. Zhang et al. 2009; Perez et al. 2010). We noted that two sets of experimental data differed substantially from the majority, and these are indicated by open symbols.

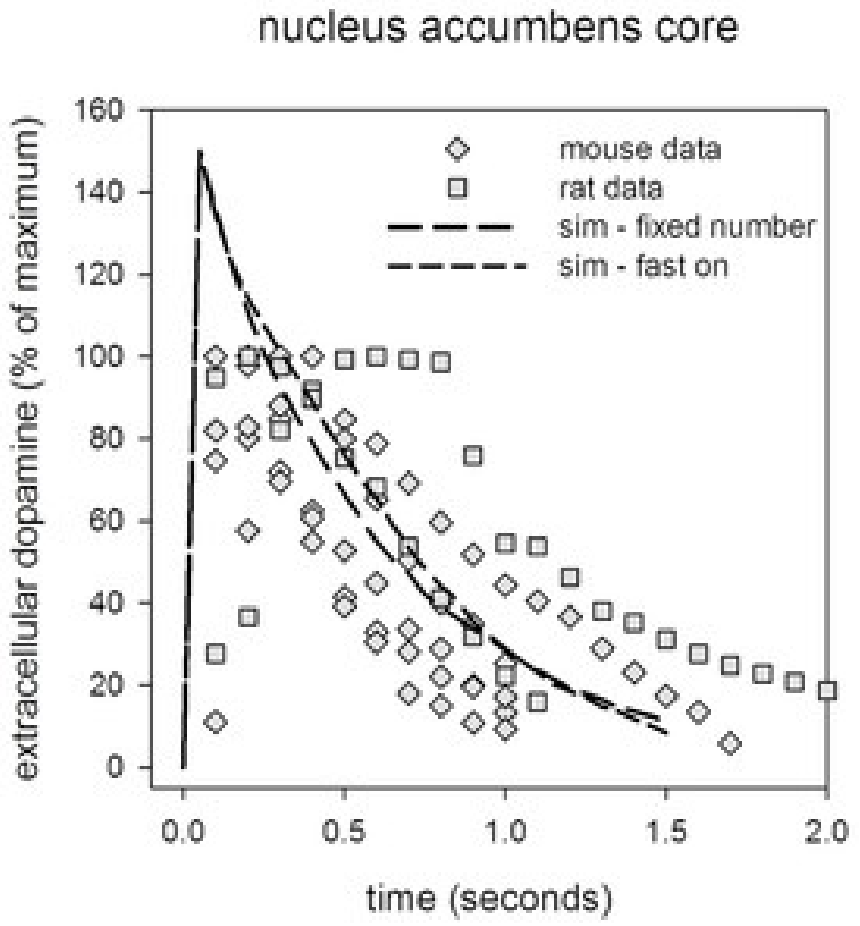

Figure 7: Simulation model output compared to published data for which rate of dopamine disappearance was measured as a function of time after electrical stimulation in nucleus accumbens core in brain slices *in vitro*.

Simulation parameter values for sim–fix number were 2,500 transporters $k_{on}=1.75x10^{6}$ $M^{-1}sec^{-1}$, Vmax = 9 dopamine molecules/sec, and 3,100 dopamine molecules released. Simulation parameter values for sim–fast on were 300 transporters $k_{on}=1.3x10^{8}$ $M^{-1}sec^{-1}$, Vmax = 9 dopamine molecules/sec, and 3,100 dopamine molecules released. The 100% value = 1.126 µM. Published data are from (Ferris et al. 2012; Ferris et al. 2011; Mateo et al. 2004; Siciliano et al. 2014; Yorgason et al. 2014; L. Zhang et al. 2009).

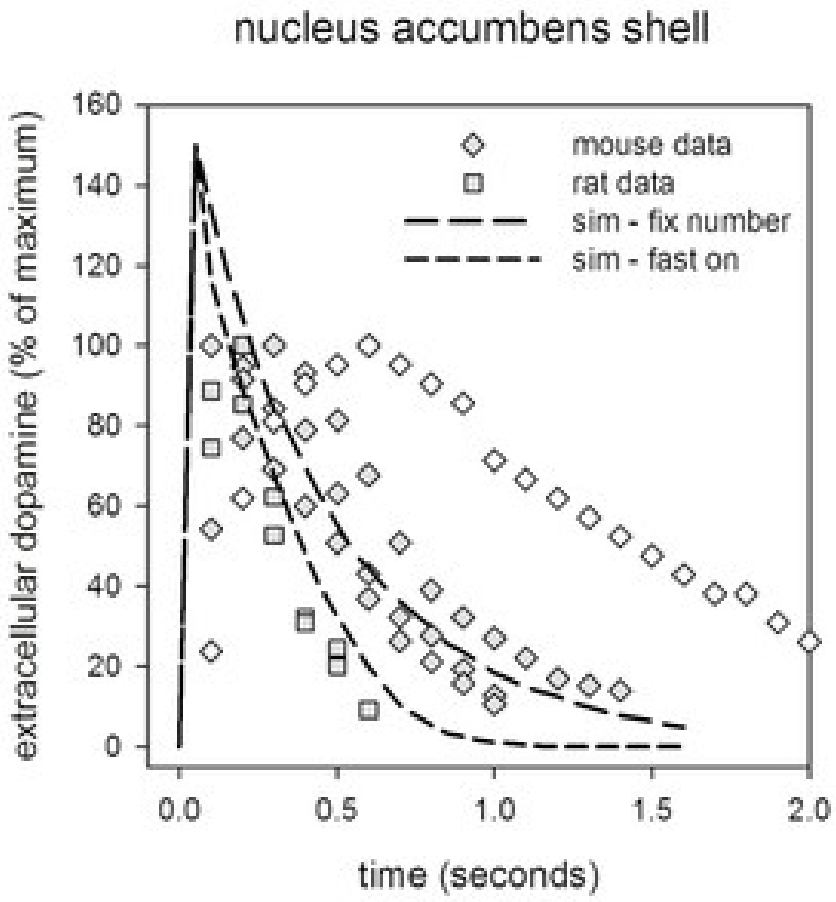

Figure 8: Simulation model output compared to published data for which rate of dopamine disappearance was measured as a function of time after electrical stimulation in nucleus accumbens shell in brain slices i*n vitro*.

Simulation parameter values for sim–fix number were 2,500 transporters, $k_{on}=2x10^6$ $M^{-1}sec^{-1}$, Vmax = 9 dopamine molecules/sec, and 3,100 dopamine molecules released. Simulation parameter values for sim–fast on were 375 transporters, $k_{on}=1.3x10^8$ $M^{-1}sec^{-1}$, Vmax = 9 dopamine molecules/sec, and 3,100 dopamine molecules released. The 100% value = 0.453 μM. Published data are from (Adrover, Shin, and Alvarez 2014; Fawaz et al. 2009; Mateo et al. 2004; Patyal, Woo, and Borgland 2012; Perez et al. 2010; L. Zhang et al. 2009). We noted that one set of experimental data differed substantially from the majority, and this is indicated by open symbols.

Chapter 3: Quantitative View of the Striatal Complex

3.1. Introduction

The extended striatum, consisting of regions called dorsal striatum, nucleus accumbens core, nucleus accumbens shell, and possibly olfactory tubercle, plays a major role in learning, motivation, and development of habits. The individual components of the striatal complex have been extensively studied. A number of review articles have been published, focusing on various parameters such as functions regulated by the striatal complex, cell types found within the complex, connections into and out from the complex, electrophysiological perspectives, and molecules located within the complex. One perspective that has not been reviewed is quantitative details of number of varicosities and receptors; therefore, this review provides a quantitative picture of these aspects of the striatal complex. This information is useful for making inferences about signaling and functional regulation.

3.1.2. Striatal Neuron Subtypes

In this review, we begin with a brief overview of the cell types present in the striatal brain region. The most abundant neurons of the striatum, the medium spiny

neuron (MSN), comprise 90-95% of total neurons in this region (Graveland and Difiglia 1985; Gerfen and Wilson 1996). The name derives from the moderate density of spines on their dendritic processes. MSNs send projections along two distinct pathways. One projection, known as the direct pathway, sends fibers to the globus pallidus interna/substantia nigra pars reticulata, and neurons comprising this pathway express dopamine D1 receptors. The indirect pathway sends projections to the globus pallidus externa, and neurons in this pathway express dopamine D2 receptors. There is only a 5-15% overlap of expression of D1/D2 receptors in adult MSNs, thus allowing for a distinct segregation of the two pathways (Cerovic et al. 2013). MSNs utilize GABA and several peptides as neurotransmitters. As the MSN are the only outputs from the striatal complex, the computational integration that occurs in this brain region is entirely expressed in their firing pattern. The MSNs are intrinsically quiet (Wilson and Kawaguchi 1996); therefore, their activity pattern is determined by glutamatergic inputs and subsequent modification within dendritic structures of the elicited depolarizing signals.

In addition to axons projecting out of the striatum, all MSNs have 5-10 collateral axons synapsing within the striatum (Wilson and Groves 1980). On average, these collaterals, which branch extensively, are between 200 and 500 μm long when measured in the rat nucleus accumbens shell (van Dongen et al. 2008). The collaterals target the majority of MSNs and tonically active (cholinergic) interneurons (Chuhma et al. 2011).

The other 5% of neurons present in the striatum consist of interneurons: four classes of GABAergic interneurons as well as cholinergic interneurons. Cholinergic interneurons account for 1-2% of total neurons in this brain region. Axons of cholinergic interneurons in the striatum branch profusely (Contant et al. 1996), and it is not clear

what proportion of branches are dendrites and are axons. Cholinergic interneurons are tonically active (Bennett and Wilson 1999), providing a constant basal level of acetylcholine in the extracellular environment. As the only other cholinergic innervation into the striatum is a very small tract from the pedunculopontine nucleus (Dautan et al. 2014), the vast majority of cholinergic synapses arise from the interneurons.

The remaining interneurons are GABAergic in nature and are divided into four subclasses based on their electrophysiological properties. The subclasses are the fast spiking GABAergic interneurons, the low threshold spiking interneurons, the calretinin positive GABAergic interneurons (Tepper and Bolam 2004), and tyrosine hydroxylase positive GABAergic interneurons (Ibáñez-Sandoval et al. 2010). The fast spiking neurons, which are also characterized by their expression of parvalbumin, are thought to make up about 0.7% of the total neurons in the rat striatum (Luk and Sadikot 2001) and are electrotonically coupled via gap junctions (Kita, Kosaka, and Heizmann 1990). The fast spiking interneurons receive a glutamatergic input from the cortex as well as GABAergic input from MSN axon collaterals and a cholinergic input (Tepper and Bolam 2004). The low threshold spiking interneurons express neuropeptide Y, somatostatin and nitric oxide synthase (Y. Smith and Parent 1986). These neurons account for about 0.8% of neurons in the rodent striatum (Rymar et al. 2004) and have the least dense axonal arborization (Kawaguchi 1993). The calretinin neurons account for about 0.8% of neurons in rodent striatum (Rymar et al. 2004) and are relatively sparse in the caudal areas of the striatum (Bennett and Bolam 1993). There are currently no electrophysiological data for these cells, so their profile is not known. Finally, the tyrosine hydroxylase GABAergic interneurons are further divided into four subclasses

based on their electrophysiological profiles. They were first described in 1987 in the primate (Dubach et al. 1987) and since then have been described in other species such as rats (Meredith et al. 1999), mice (Mao et al. 2001; Petroske et al. 2001) and humans (Porritt et al. 2000; Petroske et al. 2001; Cossette, Lecomte, and Parent 2005). Even though these neurons contain tyrosine hydroxylase, they lack the aromatic L-amino acid decarboxylase, dopamine transporter, VMAT2 and dopamine and do not release dopamine when stimulated (Xenias et al. 2015).

3.2. Striatal Inputs/neuronal pathways

All areas of the striatal complex appear to have three sets of glutamatergic inputs that can activate striatal output neurons. One input is from the cerebral cortex, with ventral areas of the striatal complex receiving input from anterior portions of the cortex and dorsal portions of the striatum receiving input from posterior aspects of the cortex. A second input is from amygdala. The third input is from thalamus for dorsal regions of striatal complex and from ventral hippocampus for ventral regions of the striatal complex. Dopaminergic neurons in the ventral tegmental area (VTA) and substantia nigra pars compacta (SNc) also send inputs to the nucleus accumbens and dorsal striatum, respectively. A small GABAergic/ enkephalinergic input originates from the external globus pallidus (Mallet et al. 2012) as well as a small GABAergic pathway from VTA to accumbens (Van Bockstaele and Pickel 1995).

Statistically speaking, these inputs most likely synapse on MSNs. These neurons have a large, densely branching dendritic tree. Typically, 3-6 parent dendrites on average

emanate from the cell body of each medium spiny neuron (Kincaid, Zheng, and Wilson 1998). These primary dendrites split approximately 20 μm from the cell body into secondary and tertiary branches. In the rat nucleus accumbens the dendrites extend up to 750 μm from the cell body (Meredith et al. 1992), and the average total length of the dendrites for the shell and core is 1,453 μm and 2,425 μm, respectively. The extensive length of the dendrites suggests that each neuron possesses a large number of inputs.

Varicosities/release elements can be counted in various histological and electron microscopic studies. Specific markers are sometimes used to associate varicosities/release sites with various neurotransmitter systems. For glutamate, three different markers have been used. Since the vast majority of glutamate synapses form at spine heads, the number/density of dendritic spines serves as an index of glutamatergic inputs. The VGlut1 and VGlut2 transporter proteins also serve as markers of glutamatergic inputs. In the striatal complex, these markers segregate, with VGlut1 localized to inputs from cortical areas and VGlut2 localized to inputs from subcortical areas (R. T. Fremeau et al. 2001; Robert T. Fremeau et al. 2004). The VGAT transporter protein serves as a marker for GABAergic inputs, the ChAT enzyme involved in the synthesis of acetylcholine serves as a marker for cholinergic inputs, the TH enzyme involved in catecholamine synthesis and the DAT transporter serve as markers for dopaminergic inputs, and the SERT transporter serves as a marker for serotonin inputs. We are not aware of good markers for opioid and other peptide neurotransmitters. We collated data from several different laboratories using a variety of techniques to count varicosities and inputs into Table 6. The fact that the number of glutamatergic inputs closely matches the spine

density and that the total number of inputs determined from counting total varicosities and the sum of specialized components are close suggests that estimates are reliable.

Since the medium spiny neurons account for more than 90% of the neurons in the striatum and their large dendritic trees suggest many inputs, statistically assigning inputs to associate with medium spiny neurons should be relatively accurate. This is done by dividing the density of varicosities/release sites by the density of cells in the striatum, 80,000 per mm^3 (Antipova et al. 2013; Oorschot 1996; Humphries, Wood, and Gurney 2010; Zheng and Wilson 2002), which is a close approximation of the density of medium spiny neurons in the striatum. Table 6 summarizes our findings.

The large number of inputs per neuron (12,500) suggests that each neuron in the striatum functions as a major integration center to provide a single output. The sheer number of inputs per neuron implies that no single input is sufficiently privileged to be able to initiate an axon potential. Thus, induction of an action potential likely requires simultaneous activation of many glutamatergic inputs. The vast array of inhibitory GABA inputs and modulatory acetylcholine and dopamine inputs provides the anatomical substrate for a substantial number of patterns of modulation. About half of the inputs to each neuron are glutamatergic in nature. Of these, about 60% originate from the cortex and 40% from subcortical areas. While we speculate that normally the generation of action potentials requires activation of inputs from all three glutamatergic pathways, each pathway has sufficient connectivity to drive action potentials when maximally stimulated (Britt et al. 2012). The large branching dendritic tree with many inputs may provide substantial computational power, as well. It is possible that dendritic branches each serve as a computational unit. A recent paper measured the changes in spine density

during learning and found that new spines were localized to a single dendritic branch (Yang et al. 2014).

Another interesting observation from these data is that the number of serotonin varicosities is on the order of 100-fold lower than the levels of any other input. If serotonin is to have any functional impact on medium spiny neurons, the inputs would have to be located on or very close to the cell body. A very likely alternative is that the serotonin inputs preferentially innervate one of the classes of interneurons.

Although the striatum is considered to be a dopaminergic area, the dopaminergic inputs only account for about 10% of the total inputs to a medium spiny neuron. In referring to the dopamine system, the striatum is dopaminergic in that it contains far more dopamine than other brain regions. Thus, the term "dopaminergic" refers to comparisons of amount of dopamine between brain areas rather than to a comparison of amount of dopamine with other neurotransmitters in the striatal region. Relative to the latter, a comparison of dopamine and acetylcholine is interesting. Tissue levels of dopamine in the striatum are about 80 μM (Miller, Shore, and Clarke 1980; Ponzio et al. 1984; Sharp, Zetterström, and Ungerstedt 1986; Buu 1989; Vezina et al. 1992; Takahashi et al. 1997; Cartmell et al. 2000; Abekawa et al. 2001; Gao and Dluzen 2001; Yu, Kuo, and Cherng 2001; Yuan et al. 2001; Bardullas, Giordano, and Rodríguez 2011), which is only slightly larger than the average tissue acetylcholine concentration of 53 μM (Carta et al. 2006; Euvrard et al. 1977). In contrast, the comparative amounts of release sites shows the opposite order, number of cholinergic release sites is double that of dopaminergic release sites. In comparing another parameter, each cholinergic interneuron in the striatum has, on average, 500,000 axon varicosities (Contant et al. 1996), and each dopamine neuron

has, on average, 500,000 varicosities per neuron in the striatum (Andén et al. 1966). This suggests that there is double the number of cholinergic interneurons to dopamine neurons innervating the striatum.

The varicosities described in Table 6 include both synaptic and non-synaptic inputs, which influences how each neurotransmitter signals within the striatum. Glutamate and GABA inputs are predominantly synaptic, which means these neurotransmitters signal within a defined synapse. The signaling molecules are confined to the synapse, which is typically ensheathed by glial cells and is only about 20 nanometers wide (Zuber et al. 2005). Glutamate and GABA are the main excitatory and inhibitory signals in the central nervous system. These neurotransmitters activate ion channels on the postsynaptic cell and can depolarize or hyperpolarize the cell membrane. Dopamine and acetylcholine, however, signal via an extrasynaptic mechanism, and a majority of the inputs do not form defined synapses within the striatum. These neurotransmitters signal via a mechanism known as volume transmission, in which they can diffuse a few microns from the release site and influence the membrane potential and ionotropic receptors via G-protein coupled receptors and second messenger systems in a "neighborhood" around the release sites.

3.3. Receptors in Striatum

In order for neuronal communication to occur, receptors must be present to receive the signal from the varicosities and synapses. The majority of receptors involved in neuronal communication in the striatum fall into two classes, ion channels or G

protein-coupled receptors. Ion channels act as a pore that, when activated, allows for the flow of ions through the membrane and can either depolarize or hyperpolarize the membrane. G protein-coupled receptors, when activated, initiate a signaling cascade within the cell that may indirectly alter the potential of a segment of neuronal membrane or the gating properties of the ion channels. Glutamate, GABA, and acetylcholine activate the ion channel receptors known to be in the striatum. The modulatory G protein-coupled receptors for which we found data in the striatum include acetylcholine, dopamine, opioid peptides, and endogenous cannabinoids. Table 7 shows binding data for receptors present in the striatum.

The most abundant receptor is CB1. This is interesting given that the endogenous cannabinoid molecules are not stored but are made on demand. Muscarinic receptors are a close second. Dopamine receptor density is about half of the muscarinic receptor density, reinforcing the observation that the striatum is a dopaminergic region only on the basis of comparison to other brain regions. The low density of nicotinic acetylcholine receptors is interesting given that it is likely that every dopamine varicosity contains a nicotinic acetylcholine receptor. The data in figure 10 show the number of receptors divided by the number of varicosities containing the neurotransmitter that activates each receptor.

Numbers of receptor subtypes provide useful and interesting information, but location of the receptors is crucial for understanding their functional roles. Various histochemical and electron microscopic techniques have been used to provide information on receptor protein location. Table 8 summarizes these data. Every dopaminergic and glutamatergic nerve terminal have been shown to express nicotinic

acetylcholine receptors (R. D. Schwartz, Lehmann, and Kellar 1984; Livingstone et al. 2009). Regarding muscarinic receptors, the M1 subtype is found on all medium spiny neurons. M2 receptors are found on glutamate terminals and on at least some cholinergic terminals, where they function to decrease release of glutamate and acetylcholine, respectively. M4 receptors are located on approximately two thirds of medium spiny neurons (Alcantara et al. 2001; Liste, Bernard, and Bloch 2002; Lobo 2009; Harrison, Tissot, and Wiley 1996).

One interesting item from this table is that dopamine D1 receptors are located only on MSN, and only on about 52% of them. A caveat associated with this observation is that receptors might be located elsewhere but at a level below detection limit. In spite of that caveat, it is clear that D1 receptors have a very restricted localization with regards to cell type. Another interesting item is that nicotinic acetylcholine receptors are found only on dopamine, glutamate, and serotonin axons/terminals and never on dendrites/cell bodies. In addition, AMPA receptors are located on glutamate and dopamine terminals as well as on dendrites. Ion-gating receptors on axons/terminals are most likely causing a depolarizing signal that participates in release of neurotransmitter. Thus, these ion-gating receptors provide a biochemical mechanism for amplifying the effects of an action potential when it reaches the terminal.

Another technique for determining which cell type produces a receptor is mRNA expression. These data identify which cell types produce the mRNA necessary for a particular protein but do not determine the subcellular location of the receptors, such as dendrites, cell bodies, axons or terminals. These data do not necessarily identify a protein as being in the striatum. For example, if the receptors are expressed on the axons of

medium spiny neurons, they may not be located in the striatum and thus would not need to be included in this review. Nonetheless, we have collected all data we can and organized it into Table 9. Medium spiny neurons produce mRNA for a majority of the receptors found within the striatum based on the data we collected. The interneurons in the striatum, however, seem to only produce mRNA for a subset of the receptors, based on the literature we reviewed. For example, cholinergic interneurons have been found to produce mRNA for metabotropic glutamate receptors and $GABA_B$ receptors, but not D2 receptors. GABAergic interneurons produce mRNA for $GABA_B$ receptor subunits and cannabinoid receptors. The combination of potential low abundance of mRNA coupled with the low abundance of interneurons likely produces the situation where some mRNA species may be missed. This would explain why the interneurons have been shown to express more receptor proteins (Table 8) than mRNA (Table 9).

3.3.1. The Serotonergic System

During our investigation, we uncovered interesting quantitative details relative to the serotonergic inputs to the striatum. The serotonergic inputs to the striatum account for less than 1% of the inputs present in the striatum. When we quantified the number of serotonin receptors, however, we found that there are over 2800 serotonin receptors for every input. This is the largest receptor to neurotransmitter input ratio we calculated, and suggests the serotonin input could have a powerful influence within the striatum. Because the number of inputs is low but the number of receptors is high, we hypothesize that,

instead of being evenly distributed, the serotonergic input is specific to one subtype of neuron.

3.4. Dopamine Neighborhood

As we are specifically interested in dopamine signaling in the striatum, we organized a set of quantitative details as they pertain to dopamine. Assuming dopamine signals in volume/neighborhood fashion, we asked the question of what other signaling elements are present in the neighborhood of a single varicosity based on statistical averages. Some dopamine receptors are located on axon terminals/varicosities, and the data presented earlier on varicosity density could be directly used to estimate type and number of varicosities likely containing presynaptic receptors. Other dopamine receptors are located on dendrites. We reason that in order for these to have an effective modulatory function, these receptors on dendrites are likely found in close apposition to varicosities. Thus, identification of varicosities/terminals in the vicinity of a single dopamine release site provides an estimate of the potential modulatory functions of dopamine D1 receptors. Figure 11 illustrates the varicosities/release sites found in the neighborhood of a single dopamine release site.

Relative to D1 receptors, the vast majority, if not all, are located on elements of about 52% of MSN. MSN elements in the vicinity of a dopamine release site can include dendrites and axon terminals from the collateral axon tree. However, it is usually assumed that the bulk of the D1 receptors are on dendrites. Based on the data in Table 7, there are, on average, 220 dopamine D1 receptors within the neighborhood of a single

release site. We are not aware of any data suggesting whether these D1 receptors are randomly distributed along dendrites or specifically clustered in apposition to various varicosities/terminals. Activation of D1 receptors stimulates protein kinase A mediated protein phosphorylation. If D1 receptors are randomly distributed along the dendrites, then a substantial phosphorylation modification might occur that could markedly alter computational activity in the dendritic tree. On the other hand, if the D1 receptors are clustered in apposition to varicosities/terminals, then data from Figure 11 suggests that these receptors could be located where they might modulate post-synaptic inputs from about 5 glutamatergic, 2 GABAergic, and 2 cholinergic inputs where more than 20 D1 receptors, on average, are available to modulate each input. If D1 receptors are clustered, it is possible that activated protein kinase A might be very intense in strategic locations.

D2 receptors are located on about 48% of the MSNs, glutamate terminals, cholinergic interneurons and axons, as well as on dopaminergic varicosities. Based on the data in Table 7, there are, on average, 64 dopamine D2 receptors within the neighborhood of a single release site. It is estimated that about 20% of the D2 receptors are located on dopaminergic axons/varicosities and 70% are located on medium spiny neurons (Anzalone et al. 2012). This means, within the volume associated with one dopamine release site, 45 D2 receptors are located on medium spiny neurons, 13 D2 receptors on dopamine terminals, and 6 D2 receptors located on other elements. This small number of D2 receptors on MSN suggests either that receptors are strategically located where a localized signal could substantially modify current flow or that a substantial post-D2 receptor amplification mechanism must exist in order for D2 receptor activation to modulate the computational activity of the MSN dendritic tree. It is not clear what this

might be since there is not a known enzyme stimulation associated with D2 receptors. Perhaps each activated receptor can in turn activate a substantial number of G-coupled proteins, which then can act on a substantial number of protein substrates. An alternate hypothesis is that the D2 receptors are preferentially located on the neuron where they would have maximum impact.

In the case of D2 receptors on axon terminals, the small number, estimated at 13 for dopamine terminals and 6 for other axon terminals, suggests a highly localized function within the small volume of these elements. Thus, receptor amplification is likely not needed. An estimate of number of dopamine transporter (made by dividing B_{max} from binding studies by varicosity density) is about 2,500. It is not intuitively obvious why the number of proteins available to remove dopamine from signaling space is so much larger than the number of receptors.

3.5. Caveats

For all of the data we have used statistical averages and distributed everything equally, which may not actually be representative of the striatum. Likely, certain inputs preferentially innervate different neuron subtypes, and all receptors may not be evenly distributed across cells. For the purposes of this review, however, we wanted to be complete and to provide a general quantitative description of the striatum as a whole.

3.6. Conclusion

In conclusion, our quantitative review has revealed that each neuron within the striatum receives over 12,500 individual inputs. This suggests that integration must occur within each cell, and it is likely that none of the inputs are privileged. The dopamine system in the striatum accounts for a minority of the elements, but the receptors are present on a majority of the cells and inputs, suggesting it has a broad influence on the overall function and output of the striatum.

Table 6: Quantitative details of axons present in striatum

Neurotransmitter	Cell Body	Density	# per Neuron
Total	All	10E+08	12,500 [a]
Glutamatergic	All	---	5,000 [b]
	All		4,300 [c]
	Cortex	2.3E+08	2,900 [d]
	Sub cortex	1.1E+08	1,400 [d]
GABA	All	1.9E+08	2,400 [e]
ACh	Interneuron	2E+08	2,500 [f]
DA	VTA/SN	1E+08	1,300 [g]
Serotonin	Dorsal Raphe	3.2E+06	40 [h]

[a] density varicosities (Oorschot 1996)/ density of neurons (80,000 neurons/mm^3 - see text)
[b] spine density of 2.5 spines spines/μm (Shen et al. 2008) times a total dendrite length of about 2,000 μm (Meredith et al. 1992)
[c] sum of averages of cortex and subcortex
[d] average density of VGluT1 or VGluT2 (Wouterlood et al. 2012; Y. Zhang et al. 2013)/density of neurons
[e] average density of VGAT (Wouterlood et al. 2012)/ density of neurons
[f] (Contant et al. 1996)/density of neurons
[g] (Doucet, Descarries, and Garcia 1986)/ density of neurons
[h] (Soghomonian, Doucet, and Descarries 1987; Soghomonian, Descarries, and Watkins 1989)/density of neurons

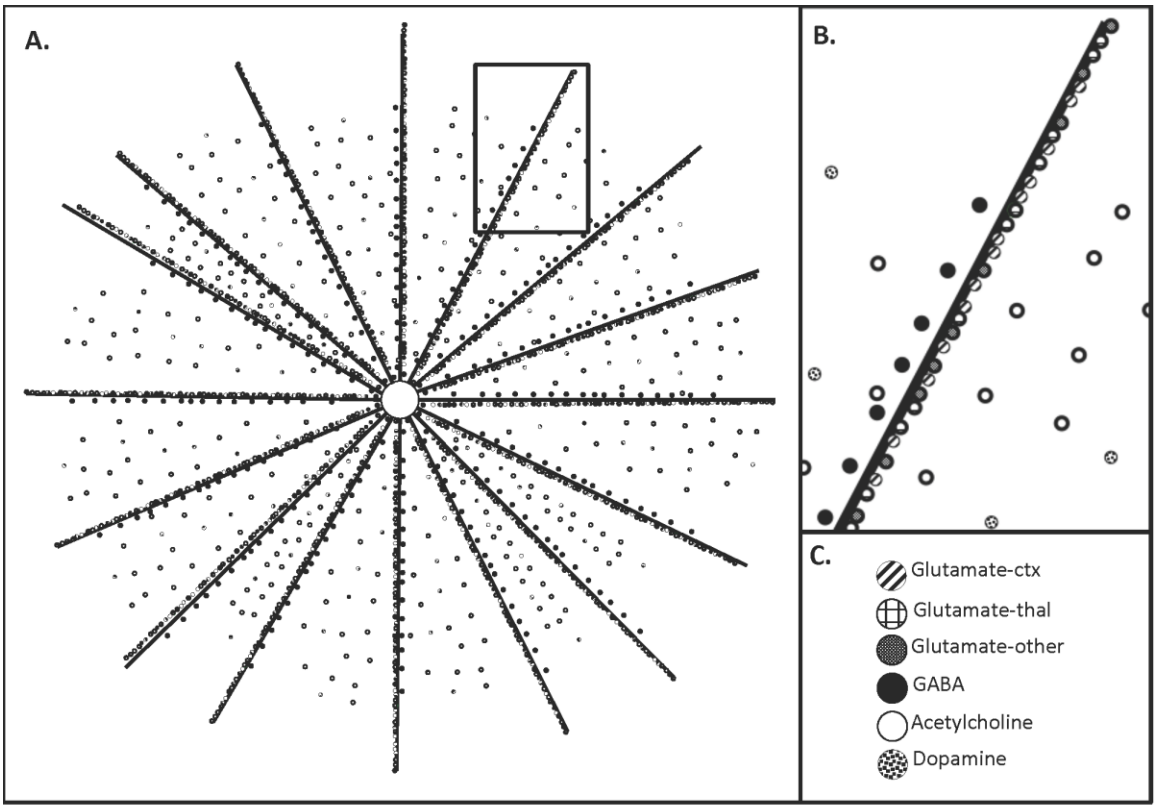

Figure 9: Visualization of inputs to a single medium spiny neuron.

(A) This illustration shows the massive number of inputs (only $1/10^{th}$ are actually shown) a single neuron receives in the striatum. Glutamatergic and GABAergic inputs are shown in this figure to directly synapse on dendritic branches of the neuron, while the modulatory neurotransmitters acetylcholine and dopamine have inputs scattered between the dendrites, as a majority of these inputs do not form direct synapses. (B) Magnification of a single dendrite segment identified by the box in (A). Each input type is labeled as shown in (C).

Table 7: Receptor density in the striatum.

Receptor	Average B_{max} in fmol/mg total protein
Cannabinoid	1075 [a]
Nonselective muscarinic	1042 [b]
M1	427 [c]
M2	180 [d]
AMPA	838 [e]
Nonselective dopaminergic	562 [f]
D1	435 [g]
D2	127 [h]
Nonselective opioid	330 [i]
Mu-opioid	120 [j]
Delta-opioid	152 [k]
Kappa-opioid	58 [l]
Serotonin	170 [m]
Adenosine	157 [n]
Adrenergic	48 [o]
Nicotinic	19 [p]

[a] Derived from (Romero et al. 1995; Bidaut-Russell, Devane, and Howlett 1990)
[b] Derived from (Gilbert, Hanley, and Iversen 1979; Nonaka and Moroji 1984)
[c] Derived from (Watson, Yamamura, and Roeske 1983; Araujo, Lapchak, and Quirion 1991; Lapchak et al. 1989b; Mendes de Freitas et al. 2005)
[d] Derived from (Lapchak et al. 1989b)
[e] Derived from (Kustova et al. 1997; Kürschner et al. 1998)
[f] Sum of averages for D1 and D2 receptors
[g] Derived from (Hyttel 1987; Mendes de Freitas et al. 2005)
[h] Derived from (Murrin and Zeng 1986; Walters and Carr 1988; Hyttel 1987)
[i] Sum of averages for mu, delta and kappa opioid receptors
[j] Derived from (Bhargava, Gulati, and Ramarao 1989; Maher, Selley, and Childers 2000; Wewers et al. 1999; Fadda et al. 1992)
[k] Derived from (Varona et al. 2003; Cadet and Rothman 1986; Vathy, Rimanóczy, and Slamberová 2000; Fadda et al. 1992)
[l] Derived from (Tempel and Zukin 1987)
[m] Derived from (Samanin et al. 1980; Mendes de Freitas et al. 2005; Hyttel 1987)
[n] Derived from (Halimi et al. 2000; Ferre et al. 1991; Cunha et al. 1996)
[o] Derived from (Walters and Carr 1988)
[p] Derived from (Lapchak et al. 1989a; Wigestrand et al. 2011; Speth et al. 1977)

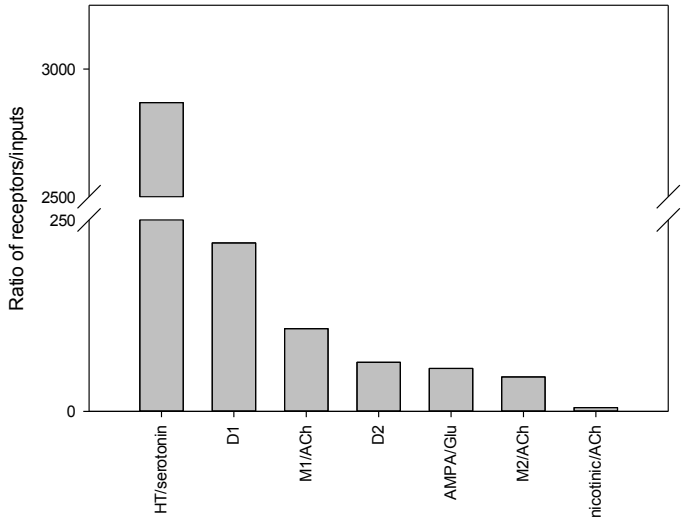

Figure 10: Ratio of receptor density to inputs in the striatum.

The data presented illustrates the ratio of density of receptors for each neurotransmitter system, calculated from B_{max} data in Table 7, to the density of inputs calculated from Table 6.

Table 8: Receptor protein expression on striatal elements

	Medium spiny neurons	Cholinergic inter-neurons	GABAergic inter-neurons	Glutamate inputs	Dopamine inputs	Cholinergic axons	GABAergic axons	5-HT axons
D1 receptor [a]	✓							
D2 receptor [b]	✓	✓		✓	✓	✓		
Muscarinic receptors [c]	✓	✓				✓		
Nicotinic receptors [d]				✓	✓			✓
mGluRs [e]	✓	✓		✓			✓	
AMPA receptors [f]	✓	✓	✓	✓	✓			
NMDA receptors [g]	✓							
Kainate receptors [h]	✓	✓	✓					
$GABA_A$ receptors [i]	✓	✓	✓				✓	
$GABA_B$ R1 subunit [j]	✓	✓	✓	✓				
$GABA_B$ R2 subunit [k]				✓	✓			
Adenosine receptors [l]	✓			✓				
Cannabinoid receptors [m]	✓		✓	✓				

[a] (Strange 1993)
[b] (Strange 1993; J. C. Schwartz et al. 1998; Tarazi and Baldessarini 1999)
[c] (Alcantara et al. 2001; Liste, Bernard, and Bloch 2002; Lobo 2009; Harrison, Tissot, and Wiley 1996)
[d] (Livingstone et al. 2009; R. D. Schwartz, Lehmann, and Kellar 1984)
[e] (Bonsi et al. 2007)
[f] (Kwok et al. 1997; Stefani et al. 1998; Tarazi and Baldessarini 1999)
[g] (Tarazi and Baldessarini 1999)
[h] (Stefani et al. 1998; Tarazi and Baldessarini 1999)
[i] (Caruncho, Liste, and Labandeira-García 1996; Fritschy and Mohler 1995; Fujiyama et al. 2000; Härtig et al. 1995; Waldvogel et al. 1997)
[j] (Lacey et al. 2005; Yung, Ng, and Wong 1999)
[k] (Durkin et al. 1999; Ng and Yung 2001)
[l] (Lobo 2009; Xie, Ramkumar, and Toth 2007)
[m] (Cerovic et al. 2013; Oude Ophuis et al. 2014; Pisani et al. 2011)

Table 9: Receptor mRNA expression on striatal elements

	Medium spiny neurons	Cholinergic inter-neurons	GABA-ergic inter-neurons
D1 receptor [a]	✓		
D2 receptor [b]	✓		
Muscarinic receptors [c]	✓		
mGluRs [d]	✓	✓	
$GABA_A$ receptors [e]	✓	✓	✓
$GABA_B$ R1 subunit [f]	✓	✓	✓
$GABA_B$ R2 subunit [g]			
5-HT receptors [h]	✓		
Adenosine receptors [i]	✓		
Opioid receptors [j]	✓		
Cannabinoid receptors [k]	✓		✓

[a] (Strange 1993)
[b] (Strange 1993; J. C. Schwartz et al. 1998; Tarazi and Baldessarini 1999)
[c] (Alcantara et al. 2001; Liste, Bernard, and Bloch 2002; Lobo 2009; Harrison, Tissot, and Wiley 1996)
[d] (Bonsi et al. 2007)
[e] (Caruncho, Liste, and Labandeira-García 1996; Fritschy and Mohler 1995; Fujiyama et al. 2000; Härtig et al. 1995; Waldvogel et al. 1997)
[f] (Lacey et al. 2005; Yung, Ng, and Wong 1999)
[g] (Durkin et al. 1999; Ng and Yung 2001)
[h] (Furay et al. 2011)
[i] (Lobo 2009; Xie, Ramkumar, and Toth 2007)
[j] (Oude Ophuis et al. 2014)
[k] (Cerovic et al. 2013; Oude Ophuis et al. 2014; Pisani et al. 2011)

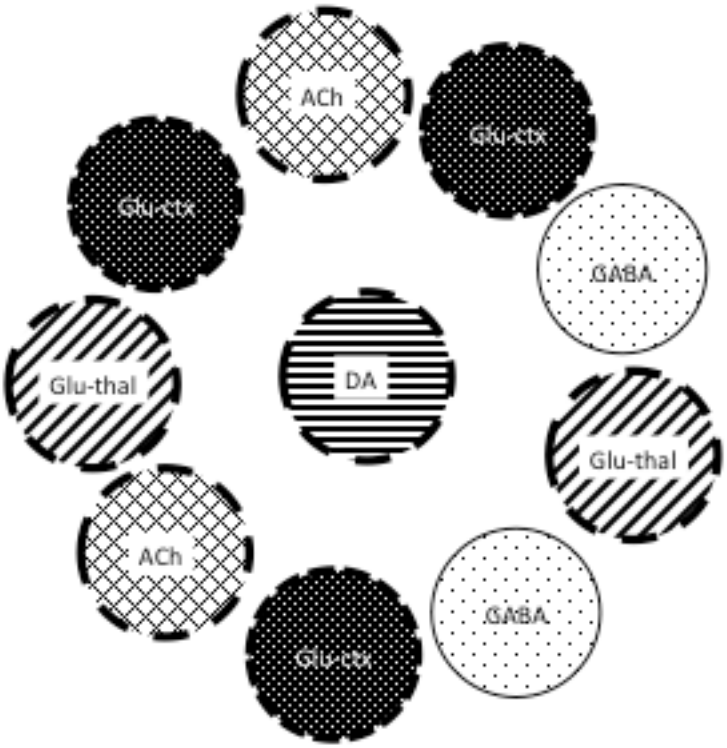

Figure 11: Varicosities and D2 receptors in the neighborhood of a single dopamine release site.

For every one dopamine varicosity, there are 3 glutamate inputs from the cortex, 2 glutamate inputs from the thalamus/amygdala, 2 cholinergic inputs and 2 GABA inputs. 8 of the 10 inputs associated with one dopamine input express dopamine D2 receptors, as indicated by the dashed border around each input in the illustration.

Chapter 4: Computational Modeling of Dopamine Receptor Occupation in the Neighborhood of Single Dopamine Release Site

4.1. Introduction

Dopamine signaling in the striatum and nucleus accumbens communicates novelty and saliency of the current environmental input and is involved in the learned formation of appropriate responses. Dopamine released in the extended striatum activates G-protein coupled receptors on multiple cells and axons in the area. The main two classes are dopamine D1 like receptors, which are coupled to a $G\alpha_s$ protein and stimulate adenylate cyclase, and D2 like receptors, which are coupled to a $G\alpha_i$ protein and inhibit cyclic AMP production, as well as modulate calcium and potassium channels (Beaulieu and Gainetdinov 2011). Dopamine D1 receptors are primarily expressed on 52% of the medium spiny neurons in the striatum (Cerovic et al. 2013). Dopamine D2 receptors are located on the other half of medium spiny neurons, as well as on cholinergic interneurons in the striatum. Dopamine D2 receptors are expressed on dopamine axons, glutamatergic axons, and cholinergic axons in the striatum and function as autoreceptors, as well.

The number of dopaminergic cell bodies in VTA and SNc is small, about 20,000-30,000 in mice and 40,000-45,000 in rats (Bjorklund and Dunnett, 2007); however, the axonal projections in the expanded striatum ramify extensively, forming dense, intricate

axonal arborizations (Gauthier et al., 1999; Matsuda et al., 2009; Prensa and Parent, 2001). The axonal tree from one neuron can influence up to 5.7% of striatal volume (Matsuda et al., 2009). Dopaminergic axons have varicosities (dopamine release sites) distributed along their axons within the expanded striatum, making an estimated 500,000 varicosities per neuron (Anden et al., 1966). Most (60-70%) of striatal dopaminergic varicosities are not associated with synaptic specialization (Descarries et al., 1996). This ultrastructural observation coupled with voltammetry experiments (Garris and Wightman, 1994) suggest that dopamine signaling occurs through volume transmission. Thus, the neurotransmitter molecules can diffuse and affect receptors within a few micrometers of the release site. Recently, using a computer model, we showed that dopamine release probability in the rodent striatum is low. How this affects dopamine receptor occupancy, however, was not investigated.

Multiple studies show that dopamine receptors are activated in the striatum and influence overall behavior. For example, du Hoffmann et al., recently showed that local blockade of either D1 or D2 receptors in rat nucleus accumbens inhibits the excitation of neurons in the striatum evoked by reward predictive cues during a sucrose reward task. Injection of the antagonists also increased the latency to reward seeking in the rodents (Hoffmann and Nicola 2014). Our group has determined the release rate of dopamine from a single varicosity was low using a computer model under both baseline conditions and after a large electrical stimulus (Chapter 2). This, paired with the information we have also gathered on the quantitative details of receptors in the striatum (Chapter 3), allowed us to create a model of receptor occupation within the volume associated with one dopamine release site in the rodent striatum.

The first goal of the current study is to estimate dopamine D1 and D2 receptor occupation under baseline conditions, utilizing either partial vesicle release or low release probability. This was done using both simple and complex computer simulation models of an extracellular compartment associated with a dopaminergic varicosity. These models were then used to evaluate the relationship between dopamine release rate and uptake, complexity of the simulation space, and receptor occupation. Receptor binding kinetics were pre-determined by matching the model output to published data on receptor binding affinities. Under baseline conditions, the results suggest that the low affinity D1 receptors remain unbound, while about 50% of the high affinity D2 receptors are bound to dopamine, on average. The second goal of this study was to evaluate D1 and D2 receptor occupation during simulations of a phasic burst. The results suggest that a short burst has very little effect on receptor occupation, suggesting the main purpose for the burst is not to increase receptor occupation. The third goal of the present study is to determine what the release probability needs to be in order to occupy a majority of the D1 receptors. Our model suggests this is dependent on the DAT kinetics and complexity of the model space.

4.2. Materials and Methods

4.2.1. Quantitative Parameters related to Dopamine Varicosities and Dopamine Receptors

The computer simulation model requires quantitative details describing dopamine varicosities, dopamine receptor details and DAT kinetics. A summary of gross tissue

level parameter values derived from published data is provided in Table 10. In the original publications, data are reported in a variety of different units (molar, pmol/mg protein, mg/gram wet weight, etc.). To facilitate comparisons, all data were converted to molar using conversion factors of 0.151 mg protein/mg tissue, 0.084 mg membrane protein/mg tissue, tissue density of 1 g/mL, and molar mass of dopamine of 153 g/mole. As reported previously (Chapter 2), values for DAT V_{max} vary substantially between different experimental paradigms. For these models, we again elected to run our models using both values for the transporter K_m.

Our computations and simulation models examined parameters associated with a single varicosity containing a single release site. Therefore, gross tissue values were converted to numbers associated with the average for a single varicosity (assumes that all sites are identical; Table 11). We determined the dopamine-DAT binding rate constants as described previously. To determine dopamine receptor binding rate constants, we used MCell simulations of dopamine binding assays *in vitro*. The association rate constant was varied to find a value that produced a K_m value from simulation data equal to each of the average K_m values we averaged from published data. The dissociation rate constant of 0.4 per second was chosen based on the value used by Dreyer et al (Jakob Kisbye Dreyer and Hounsgaard 2013).

4.2.2. Simple Simulation Model

Simulations of extracellular space associated with a dopaminergic varicosity were accomplished using MCell (Monte Carlo Cell), a stochastic simulation program that

uses Monte Carlo algorithms to estimate molecule movement and reactions in three-dimensional space (J. R. Stiles et al. 1996; J. Stiles and Bartol 2001; Kerr et al. 2008). The model has five sets of parameters. One is a morphology representing extracellular space through which dopamine can diffuse. For these models we used a sphere with volume of 2.1×10^{-15} L (radius 0.79 μm) for the dorsal striatum. The second set of parameters characterized dopamine secretion into extracellular space. Dopamine was released from a point source on the surface of the model. The third set of parameters characterizes dopamine removal by DAT. The molecules were arranged in a band of 0.75 microns width beginning 0.5 microns from the release site. In MCell, transport is modeled as a binding reaction followed by a transport step:

$$DA + DAT \leftrightarrows DADAT \rightarrow DA\_TRANS + DAT$$

DADAT represents the bound DA·DAT complex. The second reaction simulates dopamine transport with a recycling of the transporter (DADAT), where DA_TRANS represents transported dopamine. Forward rate constants for the first reaction were either 5×10^{6} or 1.3×10^{8} per molar per second (see Table 11), reverse rate was 0.5 per second, and rate constant for the second reaction was 9 per second. The fourth set of parameters characterizes dopamine binding to the dopamine D1 receptors. The receptors were clustered on the surface of the model directly across from the release site and the binding was modeled as a single, reversible reaction:

$$DA + D1 \leftrightarrows DAD1$$

DAD1 represents the bound DA·D1 receptor complex. Forward rate constant was 5×10^{5} $M^{-1}sec^{-1}$ and the reverse rate constant was 0.4 per second. The fifth set of parameters characterizes dopamine binding to the dopamine D2 receptors. The receptors were placed

in distinct clusters on surface of the model in three different areas to represent dopamine autoreceptors, D2 receptors on medium spiny neurons and D2 receptors on other varicosities. The binding was modeled as a single, reversible reaction:

$$DA + D2 \leftrightarrows DAD2$$

DAD2 represents the bound DA·D2 receptor complex. Forward rate constant was 8.2×10^{7} $M^{-1}sec^{-1}$ and the reverse rate constant was 0.4 per second.

4.2.3. Complex Simulation Model

The striatum is a complex area filled with axonal fibers, blood vessels, neurons, and glial cells. This means a simple sphere is not the most accurate representation of the extracellular space in the striatum. To better simulate this space, we used MCell to also build a complex model of the space associated with one release site. This model consists of the same five parameters sets as described above for the simple simulation model, with additional parameters incorporated into the model space. The complex model consisted of an outer sphere with a volume of 1×10^{-14} L (radius of 1.36 μm). The space is filled with 6 icospheres, each with a volume of 1.25×10^{-15} L (radius of 0.67 μm). Together, these icospheres add to a total of 7.5×10^{-15} L, leaving about 2.8×10^{-15} L of free space in the model, which we consider to be the extracellular space. The dopamine molecules are released from a point source in the center of the outer sphere. The transporters are surrounding this point source, and the dopamine D1 and D2 receptors are clustered to distinct areas across the icospheres (Figure 12). The dopamine D2 receptors that represent autoreceptors on the dopamine varicosities are approximately 0.2 μm from the

release site. Receptors that represent D2 receptors located on medium spiny neurons are located 0.45 μm to 1.35 μm from the release site, and D2 receptors located on other varicosities are approximately 1.36 μm from the release site. D1 receptors located on medium spiny neurons are located 0.45 μm to 1.35 μm from the release site as well.

4.2.4. Modeling dopamine release

To model tonic dopamine release, we utilized two methods: constant partial vesicle release and intermittent full vesicle release. For simulations of baseline dopamine release using constant partial vesicle release, values for parameters were input into the model and a pre-determined portion of single dopamine vesicle was released every 0.2 seconds (simulating 5 Hz firing rate). The simulation was run for sufficient iterations to produce a steady state level of extracellular dopamine. For simulations of an intermittent full vesicle release, the release rate was set to 5 Hz with a release probability of 1%. When a release event occurred, one full vesicle (1900 dopamine molecules) would be released.

To model a phasic burst of dopamine, we utilized the constant partial vesicle release method only. A pre-determined portion of single dopamine vesicle was released every 0.2 seconds (simulating 5 Hz firing rate) and then a random 3 pulse, 20 Hz firing event would occur sometime within the model. Each pulse of the phasic burst released the same pre-determined portion of the dopamine vesicle that is used for the 5 Hz baseline-firing events.

To model an increase in release probability, the release rate was set to 5 Hz with a variable release probability. When a release event occurred, one full vesicle (1900 dopamine molecules) would be released.

4.3. Results

4.3.1. Modeling receptor occupation with baseline dopamine release

Previously, we determined the release rate necessary to maintain an extracellular dopamine concentration in the dorsal striatum of 10 nM (Chapter 2). We expanded on these data to determine what percent of receptors are occupied and if morphological location of receptors influences the occupancy in a complex simulation model.

The data in Tables 12 and 13 shows that, for both the slow and fast DAT kinetics, dopamine D1 receptor occupation is negligible while D2 receptor occupation varies between 7-67% depending on the parameters tested. In the constant partial vesicle release model the D2 receptor occupancy was much higher (45-63%) than in the intermittent full release (11-21%) model. In addition to a difference in average occupancy, there was a difference between the release models in the time course of occupancy. With constant partial vesicle release, there is a nearly constant level of D2 receptor occupancy. With the intermittent full release model, full occupancy occurred very briefly after a release event. However, dopamine release events were so sparse that the average occupancy was small (Figure 13). Finally, dopamine receptor occupancy did not differ substantially between the simple and complex model spaces.

4.3.2. Modeling receptor occupation in the presence of phasic dopamine burst firing

Since dopamine neurons in the substantia nigra and ventral tegmental area are known to exhibit phasic firing events lasting up to 200 milliseconds when the subject is introduced to something novel (Heien and Wightman 2006), we modeled a single 3-pulse burst at 20 Hz on top of a tonic, 5 Hz firing rate. The model output showed a brief doubling of the extracellular dopamine content, but there was no change in dopamine D1 or dopamine D2 receptor occupation (Figure 14).

4.3.3. Modeling receptor occupation in the presence of an increased release probability

Since D1 receptors must be occupied to produce D1 receptor mediated behaviors, we sought to determine the conditions in which significant receptor occupancy would occur. We did this by increasing the release probability for the intermittent full release model. The simulation suggests that, for fast DAT kinetic parameters, the release probability would need to be increased to 30% to activate about 80% of the dopamine D1 receptors in the simple model. However, with slow DAT kinetics only around a 20% occupation of D1 receptors occurred with a 30% release probability (Tables 14 and 15).

The simulations further showed that as release probability increases, dopamine D1 receptor occupation is dependent on the complexity of the simulation space. Thus receptors 0.79 μm from the release site show 77% occupancy while those at 1.35 μm show 25% occupancy. This suggests that the location of the D1 receptor determines its

signaling capability. We did not see this dependency at baseline levels of dopamine, but the extracellular dopamine concentrations at baseline are much lower than the K_d value of the D1 receptor (10 nM vs. 1 μM). This suggests that large bursts of dopamine release may preferentially activate the D1 receptors closest to the release site. The location dependency was not seen with the dopamine D2 receptors, but these receptors have a much higher affinity for dopamine (10 nM), and are almost fully saturated before substantial D1 receptor occupation occurs.

4.4. Discussion

The first goal of the current study is to estimate dopamine D1 and D2 receptor occupation under baseline conditions, utilizing either constant partial vesicle release or intermittent full vesicle release. Under baseline conditions, the results suggest that the low affinity D1 receptors remain unoccupied, while about 50% of the high affinity D2 receptors are occupied, on average. The second goal of this study was to evaluate D1 and D2 receptor occupation during simulations of a phasic burst. The results suggest that a short burst has very little effect on receptor occupation, suggesting the main purpose for the burst is not to increase receptor occupation. The third goal of the present study is to determine what the release probability in the intermittent full release model needs to be in order to activate a majority of the D1 receptors. With higher release probability, D1 receptor occupancy is markedly dependent on receptor location within the model and DAT kinetics. For example, a 30% release probability activates over 80% of D1 receptors in the simple model with fast DAT kinetics. The same release probability and DAT

kinetics only activates about 25% of the D1 receptors in the complex model. Furthermore, with slow DAT kinetics, only about 20% of D1 receptors were occupied in either model. This suggests that D1 receptor occupation is dependent on DAT kinetics and the complexity of the model space.

4.4.1. Considerations relative to the simulation model

The model, in essence, consists of 4 components: dopamine release, DAT, dopamine receptors, and morphology. For this study, we utilized two different types of morphology, a simple sphere and a complex sphere. The ideal model would utilize an accurate morphology with the proper placement of all receptors and transporters relative to the release site. We have no data as to the exact location of receptors relative to a release site, but we do have data on components within the striatum that express these receptors. To best model the morphology in the striatum, we placed the receptors in distinct clusters throughout the model to represent the components on which they might be located.

In the simple model, we placed the receptors in clusters along the face of the sphere. Ultrastructural studies suggest the extracellular morphology is best approximated by a network of tubes with an average diameter of 35 nm (Thorne and Nicholson 2006). We have shown previously that our simple model is a valid model for a dopamine release site in the striatum because the dopamine diffusion rate is much faster than the rate of dopamine binding to DAT (Chapter 2).

We also created a more complex modeling space to better represent the true morphology. In this model, we placed solid spheres within our model sphere to act as components within the striatum and create crevices and tunnels for the dopamine to diffuse through. The receptors were placed in clusters on distinct "components" to represent their placement throughout the striatum. There was no difference between the two models with a low dopamine release probability; however, as we increased the dopamine release probability, we found that morphology does have an impact on dopamine receptor occupation.

For dopamine receptor binding, we used binding data published in the literature and created models of receptor binding studies to determine the association and dissociation rates of binding. The binding rates we used, however, were determined from published studies in which the system was at equilibrium. The conditions we tested in this study did not necessarily create an environment in which the system was at equilibrium, which may have impacted our results. Our model is meant to simulate the average varicosity based on conditions and parameters that are already known, though, so constants determined from equilibrium binding are the most applicable parameters to use in this study.

For dopamine D2 receptor binding, we found data for two different K_d values (10 nM and 40 nM) as well as multiple studies on the existence of a short and long form of D2 receptors. There is also evidence that D2 receptors that function as autoreceptors are different from D2 receptors found on medium spiny neurons (Giros et al. 1989; Monsma et al. 1989; Usiello et al. 2000). These studies, however, do not point to any overall differences in receptor binding between the two different D2 receptor forms. We modeled

receptor binding for the two different K_d values and found little difference because the K_d values are very similar and both very close to baseline extracellular dopamine levels measured via no net flux microdialysis (10 nM) (Bianco et al. 2008; Castner, Xiao, and Becker 1993; Chen, Lai, and Pan 1997). We decided to use only the 10 nM K_d value for our modeling studies, which bias our results to higher levels of occupation. This gives us a maximum level of occupation for all parameters we tested.

To our knowledge, there is one other group that has published similar receptor occupation simulation results using their own computer model (Jakob K. Dreyer et al. 2010). Using a mathematical model, Dreyer et al. obtained similar receptor occupation results to our MCell simulation output; however, their data on receptor occupation during phasic bursts differs. There are a few key differences between our two models, though. First, their simulation space was much larger than ours (15,000 μm^3 vs. 2.1 μm^3). The larger simulation space included a maximum of 100 release sites, while our model contains only one release site. Both simulation models used the same K_d values for both D1 and D2 receptors. The biggest difference between both models is the dopamine release parameters. Dreyer et al. released dopamine tonically to obtain an average extracellular dopamine concentration of 37 nM. During phasic bursts, their extracellular dopamine concentration increased to 100-300 nM depending on the number of bursts. This is 3-fold higher than our baseline of 10 nM and more than 2-fold higher than our burst concentration. Given all these differences, however, Dreyer's model still produced similar receptor occupation levels in their tonic model (3.5% D1 receptors bound, 75% D2 receptors bound) to our model (1% D1 receptors bound, 50% D2 receptors bound).

Both models reinforce the idea that dopamine D1 receptor occupation is low, and a large increase in extracellular dopamine is required to activate these receptors.

4.4.2. Implications of the results

Under baseline conditions, a little over half of the dopamine D2 receptors are occupied, on average, with a constant partial vesicle dopamine release mechanism. If this model is an accurate representation of the striatum, this implies significant D2 signaling under baseline conditions that could be either increased or decreased in response to changing levels of extracellular dopamine. The observations that D2 receptor antagonists increase extracellular dopamine levels and that D2 receptor agonists produce behavioral effects are consistent with this hypothesis (Beaulieu and Gainetdinov 2011). With the intermittent full vesicle release model, very short bursts of full D2 receptor occupancy occur infrequently with the result that average receptor occupancy is only about 10%. This implies a paradigm in which signaling is conveyed by frequency of pulses rather than average extracellular concentration.

Less than 1% of the dopamine D1 receptors are occupied under baseline conditions within all DAT kinetic and morphological paradigms tested. This implies no D1 mediated signaling under baseline conditions.

Dopamine neurons are also known to fire in phasic bursts when the subject is introduced to a novel stimulus (Heien and Wightman 2006). We modeled a 3 pulse, 20 Hz phasic burst randomly interspersed amongst tonic 5 Hz firing and found that the burst had no impact on overall receptor occupation. Our model shows a brief doubling of the

extracellular dopamine concentration but no increase in receptor occupation. Under the pulse conditions used, the increase in dopamine is so transient that the kinetics of receptor binding are not fast enough to register the concentration change. The small increase in extracellular dopamine we modeled agrees with multiple published studies. Floresco et al. used in vivo microdialysis to look at the DA concentration in rat nucleus accumbens. Stimulation of the pedunculopontine tegmental nucleus, a region that sends glutamatergic and cholinergic inputs to dopamine cell bodies in the VTA, did not produce any observable increase in extracellular dopamine. An increase in extracellular dopamine concentration was only observed after inhibition of DAT in the nucleus accumbens (Floresco et al. 2003). Another group used voltammetry to look at dopamine release in rat nucleus accumbens after exposure to a 50 kHz ultrasonic vocalization from rats, which they believe induces phasic dopamine firing. They saw a 5 nM increase in the extracellular dopamine transient via voltammetry after only this frequency, which matches our data (Willuhn et al. 2014). Another group looked at dopamine release via voltammetry in rats performing a lever press/sucrose reward paradigm and their data shows that the DA increases are only in the 5-10 nM range as well (Wassum, Ostlund, and Maidment 2012).

It is possible that a burst occurs to prime the terminals with an influx of calcium from the rapid arrival of action potentials. This priming could then increase the release probability for the following release event. For the phasic bursts, we only released the same number of dopamine molecules in our model as we do for each action potential under tonic firing.

It is also possible that signals acting at the level of the terminal, such as activation of presynaptic nicotinic receptors, coupled with the phasic burst, increase the release rate enough to increase receptor occupation. Binding and functional data suggest that nearly every dopaminergic varicosity contains a nicotinic acetylcholine receptor (I. W. Jones, Bolam, and Wonnacott 2001). Activation of such receptors might further depolarize the membrane above the level induced by an action potential, allowing for dopamine release. Studies employing nicotinic agonists and antagonists have shown varying effects on dopamine release. However, a study using optogenetics to study the effect of cholinergic interneuron activation clearly documents that activation of a population of cholinergic interneurons elicits dopamine release *in vivo* in the absence of any other stimulus. This dopamine release was nicotinic receptor dependent and frequency independent (Threlfell et al. 2012).

To model the hypothetical influence of nicotinic receptors, we used our model and increased the dopamine release probability until a majority of the dopamine D1 receptors were occupied. To reach a >80% occupation of the D1 receptors in the simple model, we had to increase the release probability to 30%. When we increased the release probability in the complex model, however, we only saw about a 25% occupation of D1 receptors. This was dependent on the DAT kinetics. These data suggests that location of the receptors and the complexity of the space has an impact on the probability of the receptors being activated. These results suggest that dopamine signaling is dependent on release probability, DAT kinetics, receptor location, and factors that increase release probability.

Our model is meant to provide a global, average simulation of dopamine neurotransmission based on published data. The data and results provided here are not meant to provide exact numbers for all parameters involved, but rather provide evidence that support overall concepts. Based on our model, we hypothesize that local signals, such as presynaptic nicotinic receptors, act to increase dopamine release probability to enhance signaling within distinct neighborhoods. The striatum receives thousands of inputs as discussed in chapter 3, and local signals acting at the dopamine terminal would allow for the signaling of specific behaviors that do not require large, global increases in dopamine. This would allow for distinct signaling through the various regions of the striatum and lead to different outputs depending on the signal.

In conclusion, under baseline dopamine release conditions, only about half of the dopamine D2 receptors within the sphere of a single release site are activated. This does not change after a phasic burst. The only way to activate D1 receptors is to increase the dopamine release probability to 30% or higher. Signals that act at the terminal, such as nicotinic receptors, may have the capability of increasing dopamine release probability to levels that activate D1 receptors. The D1 receptor occupation is dependent on the location of the receptors with regards to the release site as well as the DAT kinetics. This suggests that multiple factors are vital to dopamine signaling.

Table 10: Parameter values derived from biochemical data for rodent dorsal striatum

Parameter	Value
Dopamine level	79.2 μM [a]
Dopamine varicosity density	$1x10^{+8}/mm^3$ [b]
Dopamine transporter level	0.47 μM [c]
Dopamine transporter V_{max}	4.08 μM/sec [d]
Dopamine transporter K_m (transfected cells)	2.17 μM [e]
Dopamine transporter K_m (tissue prep)	0.2 μM [f]
Dopamine D1 receptor level	0.01 μM [g]
Dopamine D1 receptor K_d	1 μM [h]
Dopamine D2 receptor level	0.04 μM [i]
Dopamine D2 receptor K_d	10 nM [J]

[a] Derived from (Abekawa et al., 2001; Bardullas et al., 2011; Buu, 1989; Cartmell et al., 2000; Gao and Dluzen, 2001; Miller et al., 1980; Ponzio et al., 1984; Sharp et al., 1986; Takahashi et al., 1997; Vezina et al., 1992; Yu et al., 2001; Yuan et al., 2001)

[b] Derived from (Doucet et al., 1986)

[c] Derived from (Boja et al., 1995; Bonnet et al., 1986; Chen et al., 1997a; Dubocovich and Zahniser, 1985; Erikson et al., 2000; Garreau et al., 1997; Hooks et al., 1994; Janowsky et al., 1986; Marshall et al., 1990; Moll et al., 2000; Nakayama et al., 1993; Rothman et al., 1994)

[d] Derived from (Garris and Wightman, 1994; May and Wightman, 1989; Wu et al., 2001)

[e] Derived from (Carneiro et al., 2002; Chang et al., 2001; Eshleman et al., 1995; Itokawa et al., 2000; Kitayama et al., 1992; Lee et al., 1996; Lin and Uhl, 2002; Lin and Uhl, 2005; Loland et al., 1999; Loland et al., 2002; Melikian and Buckley, 1999; Norregaard et al., 1998; Norregaard et al., 2000; Yatin et al., 2002)

[f] Derived from (Harris and Baldessarinig, 1973; Horn, 1990; Marshall et al., 1990; Near et al., 1988; Rothman et al., 2001; Snyder and Coyle, 1969; Wu et al., 2001)

[g] (Hyttel 1987; Mendes de Freitas et al. 2005)

[h] (Jakob Kisbye Dreyer and Hounsgaard 2013; Rice and Cragg 2008)

[i] (Hyttel 1987; Murrin and Zeng 1986; Walters and Carr 1988)

[j] (Jakob Kisbye Dreyer and Hounsgaard 2013; Rice and Cragg 2008)

Table 11: Parameter values associated with a single varicosity.

Parameter	Value
Number of dopamine molecules per varicosity	475,000
Number of vesicles per varicosity	250
Number of dopamine molecules per vesicle	1,900
Extracellular volume surrounding a release site (dorsal striatum)	$2x10^{-15}$ liter
Number of DAT associated with a release site	2,800
DAT catalytic rate	9 /sec
DAT-DA binding on-rate (transfected cells)	$5x10^{+6}$ $M^{-1}sec^{-1}$
DAT-DA binding on-rate (tissue prep)	$1.3x10^{+8}$ $M^{-1}sec^{-1}$
DAT-DA binding off-rate	0.5 sec^{-1}
D1-DA binding on-rate	$5x10^{5}$ $M^{-1}sec^{-1}$
D1-DA binding off-rate	0.4 sec^{-1}
D1 receptor number	220
D2-DA binding on-rate	$8.2x10^{7}$ $M^{-1}sec^{-1}$
D2-DA binding off-rate	0.4 sec^{-1}
D2 receptors located on medium spiny neurons	45 [b]
D2 receptors located on dopamine terminals	13 [b]
D2 receptors located on other varicosities	6 [b]
Dopamine diffusion rate	$4x10^{-6}$ cm^2/sec [a]

[a] Derived from (Land et al., 1984; Rice and Cragg, 2008; Schonfuss et al., 2001)
[b] D2 receptor distribution derived from (Anzalone et al. 2012)

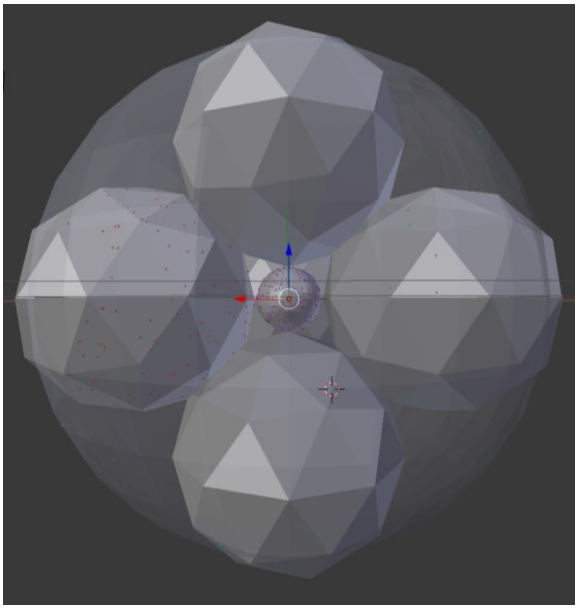

Figure 12: Complex model simulation space.

Dopamine is released from the center sphere. Six icospheres (2 not pictured) act to provide barriers to the free diffusion of dopamine as well as provide a surface for dopamine D1 and D2 receptors to reside.

Table 12: Estimated rate of basal dopamine release at 5 Hz in dorsal striatum simulation models[1].

Model	Concentration[1]	Release Rate[2]	% D1 occupied	% D2 on MSN occupied	% D2 on DA terminals occupied	% D2 on other terminals occupied
Simple-Constant partial vesicle release	8 nM	20	0.6	54.2	63.1	46.7
Complex-Constant partial vesicle release	9 nM	20	0.7	45.1	44.8	66.7
Simple-intermittent full vesicle release	12 nM	1900	1.3	20.4	20.8	16.7
Complex-intermittent full vesicle release	7 nM	1900	0.5	11.9	11.5	15

[1] Simulations used a simple or complex morphology, 5 Hz firing rate, 2,800 total DAT molecules with a transport rate of 9 dopamine per second and an on-rate of dopamine binding to DAT of $5x10^6$ M^{-1} sec^{-1}. Intermittent full vesicle release models had a release probability of 1%.

[2]average dopamine concentration from the simulation output

[3]release rate is number of dopamine molecules released per firing event to produce the average extracellular dopamine concentration listed.

Table 13: Estimated rate of basal dopamine release at 5 Hz in dorsal striatum simulation models[1].

Model	Concentration[1]	Release Rate[2]	% D1 occupied	% D2 on MSN occupied	% D2 on DA terminals occupied	% D2 on other terminals occupied
Simple-Constant partial vesicle release	9 nM	50	0.7	56.9	59.2	60.0
Complex-Constant partial vesicle release	10 nM	50	0.8	44.0	56.2	45.0
Simple-intermittent full vesicle release	14 nM	1900	1.4	12.2	15.4	18.3
Complex-intermittent full vesicle release	12 nM	1900	0.5	6.9	10.0	8.3

[1] Simulations used a simple or complex morphology, 300 total DAT molecules with a transport rate of 9 dopamine per second and an on-rate of dopamine binding to DAT of 1.3×10^{8} M^{-1} sec^{-1}. Intermittent full vesicle release models had a release probability of 1%.

[2]average dopamine concentration from the simulation output

[3]release rate is number of dopamine molecules released per firing event to produce the average extracellular dopamine concentration listed.

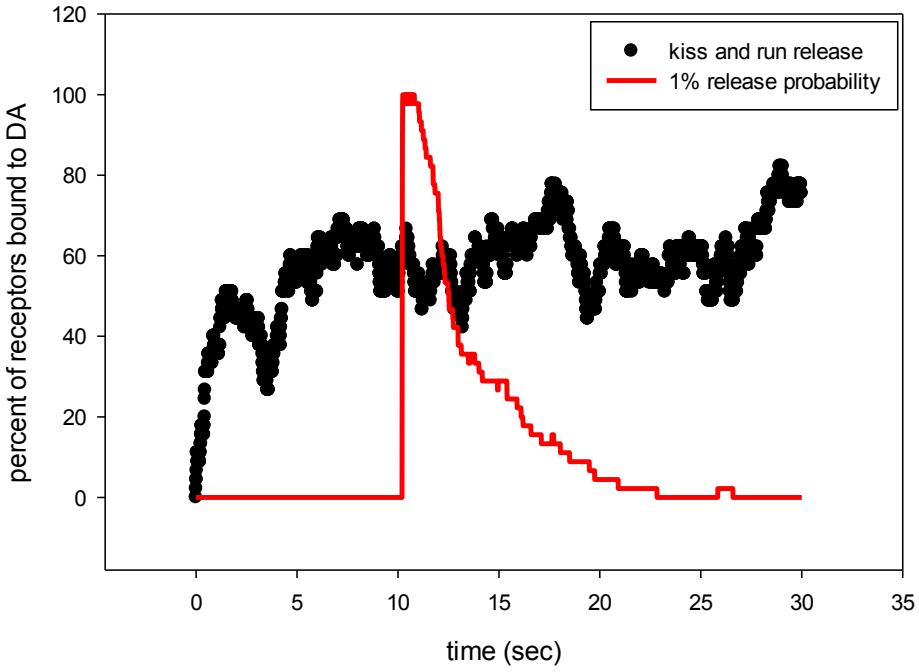

Figure 13: Dopamine D2 receptor occupation with a constant partial vesicle release model versus an intermittent full vesicle release model.

Simulation of dopamine D2 receptor occupation using the simple model and fast DAT kinetics. Red line indicates D2 receptor occupation when one dopamine vesicle (1900 molecules) is released using an intermittent full vesicle release model with a 1% release probability across 30 seconds of simulated data. Black dots represent D2 receptor occupation under a constant partial vesicle release simulation of 50 dopamine molecules per pulse at a 5 Hz firing rate for 30 seconds of simulated data. DAT kinetics were as follows: 300 dopamine transporters, V_{max}=9 dopamine/second, K_{on} rate for dopamine binding to DAT= $1.3x10^{8}$ M^{-1} sec^{-1}.

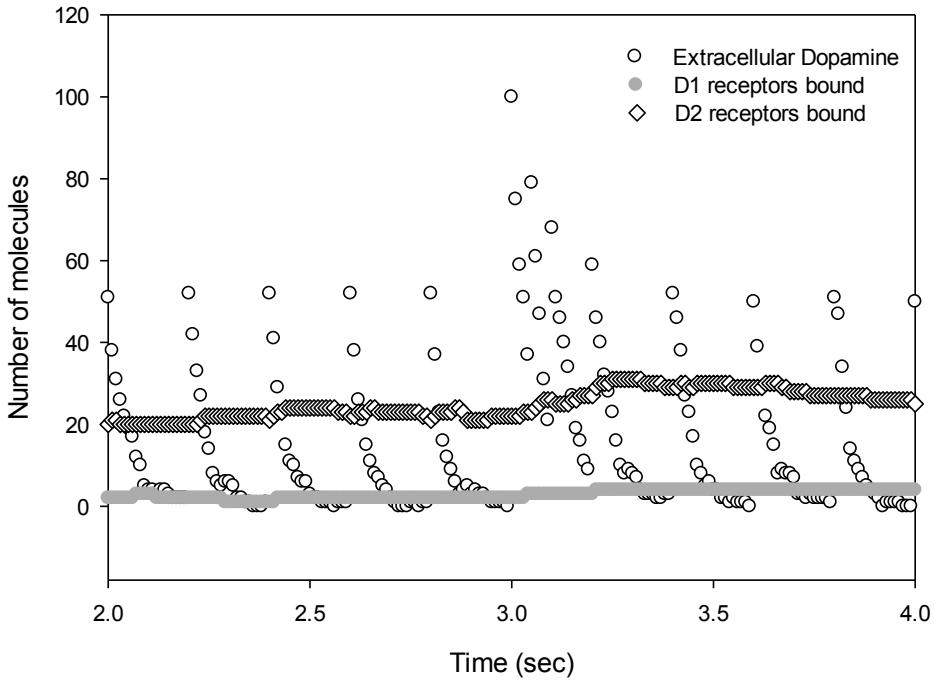

Figure 14: Dopamine receptor occupation compared to extracellular dopamine content after a 3 pulse phasic burst.

The number of extracellular dopamine molecules are indicated by the open circle. No observable increase in D1 (gray circle) or D2 (open diamond) receptor occupation is seen. For this simulation the simple model and fast DAT kinetics were used. Simulation consisted of a tonic, 5 Hz firing rate using constant partial vesicle release of 50 dopamine molecules per pulse with one 3 pulse, 20 Hz phasic burst occurring at 3 seconds. DAT kinetics were as follows: 300 dopamine transporters, V_{max}=9 dopamine/second, K_{on} rate for dopamine binding to DAT= $1.3x10^{8}$ M^{-1} sec^{-1}.

Table 14: Estimated extent of receptor occupation with a 30% release probability-slow DAT[1].

Model	Concentration[1]	Release Rate[2]	% D1 occupied	% D2 on MSN occupied	% D2 on DA terminals occupied	% D2 on other terminals occupied
Simple	0.25 μM	1900	21.6	85.6	84.6	83.3
Complex	0.5 μM	1900	22.1	80.0	92.3	78.3

[1] Simulations used a simple or complex morphology, 5 Hz firing rate, 2,800 total DAT molecules with a transport rate of 9 dopamine per second and an on-rate of dopamine binding to DAT of $5x10^6$ M^{-1} sec^{-1}.
[1]average dopamine concentration from the simulation output
[2]release rate is number of dopamine molecules released per firing event to produce the average extracellular dopamine concentration listed.

Table 15: Estimated rate of receptor occupation with a 30% release probability-fast DAT[1].

Model	Concentration[1]	Release Rate[2]	% D1 occupied	% D2 on MSN occupied	% D2 on DA terminals occupied	% D2 on other terminals occupied
Simple	6.6 µM	1900	77.2	95.6	94.6	95.0
Complex	1.0 µM	1900	24.8	73.3	88.5	68.3

[1] Simulations used a simple or complex morphology, 300 total DAT molecules with a transport rate of 9 dopamine per second and an on-rate of dopamine binding to DAT of 1.3×10^8 M^{-1} sec^{-1}.
[1]average dopamine concentration from the simulation output
[2]release rate is number of dopamine molecules released per firing event to produce the average extracellular dopamine concentration listed.

Chapter 5: Computational Modeling of Dopamine Receptor Occupation in the Neighborhood of Single Dopamine Release Site in the Presence of Cocaine and Amphetamine

5.1. Introduction

The dopamine neurons of the ventral tegmental area are one component of the reward pathway in the brain, which reinforces behavior that is necessary for survival such as eating, drinking and sex. When an unanticipated reward is presented, dopamine signaling increases. This increase modulates circuits involved in memory and behavior, which ensures that these behaviors are repeated. Addicting drugs hijack this pathway and increase the extracellular levels of dopamine by increasing firing rate, increasing the amount of dopamine released or through non-exocytotic mechanisms. Whenever the addicting drug is present, it causes an increase in extracellular dopamine, which reinforces use of the drug (Hyman, Malenka, and Nestler 2006). Long-term use causes a change in the circuits of the brain, which eventually causes the user to become dependent on the drug.

Amphetamine and cocaine are both powerful stimulants that have addicting properties. In most studies it is believed that the drugs' ability to increase extracellular dopamine in the extended striatum is required for the hyperactivity and rewarding

properties of these chemicals (Bozarth and Wise 1986; Koob and Bloom 1988; Kuhar, Ritz, and Boja 1991). Although both of these drugs increase extracellular dopamine, they do so in different ways. Cocaine blocks the reuptake of dopamine, leading to an accumulation of the neurotransmitter in the extracellular space, whereas amphetamine produces its effects by promoting release of dopamine from non-vesicular pools as well as by blocking reuptake of the neurotransmitter (Fischer and Cho 1979). The difference in mechanism leads to a much larger increase in extracellular dopamine by amphetamine as compared to by cocaine.

This difference in amount of increase in extracellular dopamine may have mechanistic relevance in that some effects of cocaine are not attenuated by dopamine receptor blockers while all effects of amphetamine are. For example, in the presence of dopamine receptor antagonists, cocaine-induced hyper-locomotion is reduced, whereas conditioned place preference is unaffected (Kaddis, Uretsky, and Wallace 1995; Spyraki, Fibiger, and Phillips 1982a). Unlike cocaine, the presence of dopamine receptor antagonists reduce both amphetamine induced hyper-locomotion as well as place preference (Mackey and van der Kooy 1985; McGregor and Roberts 1993; Spyraki, Fibiger, and Phillips 1982b). This suggests that dopamine receptor occupation may be differentially affected between the two psychostimulants.

The goal of this study is to determine how the increase in extracellular dopamine in the presence of cocaine or amphetamine alters dopamine receptor occupation. This was done using computer simulation models of an extracellular compartment associated with a dopaminergic varicosity. These models were then used to evaluate the relationship between dopamine release rate, uptake and receptor binding, all in the presence of

increasing concentrations of cocaine or 2 mg/kg amphetamine. Simulation results suggest that the highest cocaine dose tested increases dopamine D2 receptor occupation by about 30%, whereas it only increases dopamine D1 receptor occupation by about 4%. 2 mg/kg amphetamine increases dopamine D1 receptor occupation to 13% in the simple model, but only to about 6% in the complex model. D2 receptors are almost fully saturated (~97%) in the presence of 2 mg/kg amphetamine in the simple model, but only about 70% are bound in the complex model. The conclusion of our paper is that micromolar concentrations of cocaine in the striatum significantly increase dopamine D2 receptor occupation, but have a lesser effect on D1 receptor occupation. The presence of 2 mg/kg amphetamine causes a larger increase in extracellular dopamine than cocaine, which leads to a higher percentage of D1 receptors bound.

5.2. Materials and Methods

5.2.1. Quantitative parameters related to dopamine varicosities and dopamine receptors

The computer simulation model requires quantitative details describing dopamine varicosities, dopamine receptor details and DAT kinetics. A summary of gross tissue level parameter values derived from published data is provided in Table 16. In the original publications, data are reported in a variety of different units (molar, pmol/mg protein, mg/gram wet weight, etc.). To facilitate comparisons, all data were converted to molar using conversion factors of 0.151 mg protein/mg tissue, 0.084 mg membrane protein/mg tissue, tissue density of 1 g/mL, and molar mass of dopamine of 153 g/mole.

As reported previously, (Chapter 2) values for DAT V_{max} vary substantially between different experimental paradigms. For these models, we elected to run our models using only the fast DAT kinetics.

Our computations and simulation models examined parameters associated with a single varicosity containing a single release site. Therefore, gross tissue values were converted to numbers associated with the average for a single varicosity (assumes that all sites are identical) (Table 17). We determined the dopamine-DAT binding rate constants as described previously. Briefly, to determine the constants we used MCell simulations of dopamine binding assays *in vitro*. The association rate constant was varied to find a value that produced a K_m value from simulation data equal to each of the average K_m values we averaged from published data. The dissociation rate constant of 0.4 per second was chosen based on the value used by Dreyer et al (Jakob Kisbye Dreyer and Hounsgaard 2013).

5.2.2. Simple simulation model

Simulations of extracellular space associated with a dopaminergic varicosity were accomplished using MCell (Monte Carlo Cell), a stochastic simulation program that uses Monte Carlo algorithms to estimate molecule movement and reactions in three-dimensional space (J. R. Stiles et al. 1996; J. Stiles and Bartol 2001; Kerr et al. 2008). The model has five sets of parameters. One is a morphology representing extracellular space through which dopamine can diffuse. For these models we used a sphere with volume of 2.1×10^{-15} L (radius 0.79 μm) for the dorsal striatum. The second set of

parameters characterized dopamine secretion into extracellular space. Dopamine was released from a point source on the surface of the model. The third set of parameters characterizes dopamine removal by DAT. The molecules were arranged in a band of 0.75 microns width beginning 0.5 microns from the release site. In MCell, transport is modeled as a binding reaction followed by a transport step:

$$DA + DAT \leftrightarrows DADAT \rightarrow DA\_TRANS + DAT$$

DADAT represents the bound DA·DAT complex. The second reaction simulates dopamine transport with a recycling of the transporter (DADAT), where DA_TRANS represents transported dopamine. The forward rate constant for the first reaction was 1.3×10^8 per molar per second (see Table 17), reverse rate was 0.5 per second, and rate constant for the second reaction was 9 per second. The fourth set of parameters characterizes dopamine binding to the dopamine D1 receptors. The receptors were clustered on the surface of the model directly across from the release site and the binding was modeled as a single, reversible reaction:

$$DA + D1 \leftrightarrows DAD1$$

DAD1 represents the bound DA·D1 receptor complex. Forward rate constant was 5×10^5 $M^{-1}sec^{-1}$ and the reverse rate constant was 0.4 per second. The fifth set of parameters characterizes dopamine binding to the dopamine D2 receptors. The receptors were placed in distinct clusters on surface of the model in three different areas to represent dopamine autoreceptors, D2 receptors on medium spiny neurons and D2 receptors on other varicosities. The binding was modeled as a single, reversible reaction:

$$DA + D2 \leftrightarrows DAD2$$

DAD2 represents the bound DA·D2 receptor complex. Forward rate constant was $8.2x10^{7}$ $M^{-1}sec^{-1}$ and the reverse rate constant was 0.4 per second.

For the purposes of this model, we released dopamine at a rate of 5 Hz with partial vesicle release for each firing event. Using published data, we determined the brain concentration of cocaine for increasing i.p. injections of cocaine (5-25 mg/kg) by utilizing the best fit line in Figure 16. Release conditions for amphetamine were determined previously by our lab to match published data on brain dopamine and amphetamine concentrations after administration of 2 mg/kg amphetamine in rodents.

5.2.3. Complex Simulation Model

The striatum is a complex area filled with axonal fibers, blood vessels, neurons, and glial cells. This means a simple sphere is not the most accurate representation of the extracellular space in the striatum. To better simulate this space, we used MCell to also build a complex model of the space associated with one release site. This model consists of the same five parameters sets as described above for the simple simulation model, with additional parameters incorporated into the model space. The complex model consisted of an outer sphere with a volume of $1x10^{-14}$ L (radius of 1.36 μm). The space is filled with 6 icospheres, each with a volume of $1.25x10^{-15}$ L (radius of 0.67 μm). Together, these icospheres add to a total of $7.5x10^{-15}$ L, leaving about $2.8x10^{-15}$ L of free space in the model, which we consider to be the extracellular space. The dopamine molecules are released from a point source in the center of the outer sphere. The transporters are surrounding this point source, and the dopamine D1 and D2 receptors are clustered to

distinct areas across the icospheres (Figure 12). The dopamine D2 receptors that represent autoreceptors on the dopamine varicosities are approximately 0.2 μm from the release site. Receptors that represent D2 receptors located on medium spiny neurons are located 0.45 μm to 1.35 μm from the release site, and D2 receptors located on other varicosities are approximately 1.36 μm from the release site. D1 receptors located on medium spiny neurons are located 0.45 μm to 1.35 μm from the release site as well.

5.2.4. Cocaine model parameters

In order to model the effect of cocaine on the extracellular concentration of dopamine, we first had to determine the correct kinetic parameters for cocaine binding to DAT. In order to do this, we modeled an *in vitro* receptor-binding assay. The association and dissociation rate constants were varied to find a set of values that produced a K_m value from simulation data equal to each of the average K_m values we averaged from published data. In MCell, we modeled cocaine binding to DAT as a binding reaction:

$$COC + DAT \leftrightarrows COCDAT$$

COCDAT represents the bound cocaine•DAT complex. This reversible binding equation has a forward rate constant of 1.3×10^6 M^{-1} sec^{-1} and a reverse rate of 3 per second.

5.2.5. Amphetamine model parameters

Previously our lab has determined the ideal parameters to best model the increase in extracellular dopamine in the presence of amphetamine. To best model the effects of

amphetamine, we had to alter our dopamine release parameters as well as use transporter kinetics similar to the slow DAT kinetics we determined previously. Dopamine was released at 5 Hz, with each action potential releasing 21 dopamine molecules into the extracellular space with an initial release of 240 dopamine molecules to achieve steady state in the model within the 10-second model timespan. In MCell, we modeled amphetamine binding to DAT as a binding reaction:

$$AMPH + DAT \leftrightarrows AMPHDAT$$

AMPHDAT represents the bound amphetamine•DAT complex. This reversible binding equation has a forward rate constant of $2x10^6$ M^{-1} sec^{-1} and a reverse rate of 0.5 per second. 16800 amphetamine molecules were released into the extracellular space at the start of the simulation to represent 2 mg/kg amphetamine. A non-DAT removal mechanism was also included in this model to account for all other dopamine removal processes such as diffusion or uptake into glial cells. All parameters used for the amphetamine model are listed in Table 18.

5.3. Results

5.3.1. Modeling striatal extracellular dopamine in presence of increasing doses of cocaine

We first used published data to confirm the accuracy of our model. Data from multiple sources that measured the striatal extracellular dopamine concentration in response to cocaine administration was pooled and graphed. As the cocaine concentration

increases, there is a linear increase in extracellular dopamine concentration (Figure 15). We also pooled published data on the measured brain concentration of cocaine for multiple doses of cocaine. This also showed a linear relationship with the dose of cocaine administered (Figure 16). In our computer simulation, we used a best-fit line to determine the cocaine concentration in the brain for a given dose (Table 19) and then determined the extracellular dopamine concentration. Our model values are shown with the published data in Figure 15.

5.3.2. Modeling dopamine receptor occupancy in presence of increasing doses of cocaine

Cocaine binds to the dopamine transporter, leading to an increase in extracellular dopamine. This study was done to determine how the cocaine-induced increase in extracellular dopamine alters dopamine receptor occupancy. We found that the presence of increasing concentrations of cocaine increases dopamine D2 receptor occupancy from a control of about 50% to near full occupancy (Figure 17). We also found that for all doses tested, cocaine only slightly increases dopamine D1 receptor occupancy, going from approximately 1% occupation in controls to a maximum of about 5% of receptors occupied at the highest concentration of cocaine (25 mg/kg, Figure 18). We achieved similar occupancy results for the 5 and 10 mg/kg doses in the complex model (1.5% D1 bound, 50-70% D2 bound).

5.3.3. Modeling dopamine receptor occupancy in presence of 2 mg/kg amphetamine

Amphetamine also affects the dopamine transporter and causes an increase in extracellular dopamine. Published studies suggest amphetamine causes a much larger increase in extracellular dopamine than cocaine (De Souza Silva et al. 1997). We sought to model how this larger increase in extracellular dopamine influences receptor occupation. We used both the simple and complex model to study the impact of 2 mg/kg amphetamine on dopamine receptor occupation. We found that, in the simple model, 2 mg/kg amphetamine increased dopamine D1 receptor occupation to 13% and D2 receptor occupation to about 97%. When we ran the same parameters in the complex model, however, our average extracellular dopamine concentration was lower (0.1 μM vs. 0.22 μM). The lower extracellular dopamine concentration resulted in lower levels of dopamine receptor occupancy (Figure 19).

5.4. Discussion

Cocaine and amphetamine are both addicting drugs that increase the extracellular concentration of dopamine in the striatum by interacting with the dopamine transporter. The goal of this study is to determine how the increase in extracellular dopamine in the presence of the drugs alters dopamine receptor occupation. This was done using a simple computer simulation model of an extracellular compartment associated with a dopaminergic varicosity. Simulation results suggest that the highest cocaine dose tested increases dopamine D2 receptor occupation by about 30% from a baseline of about 50%,

whereas it only increases dopamine D1 receptor occupation to 4%. 2 mg/kg amphetamine increases dopamine D1 receptor occupation to 13% in the simple model, but only to about 6% in the complex model. D2 receptors are almost fully saturated (~97%) in the presence of 2 mg/kg amphetamine in the simple model, but only about 70% are bound in the complex model. The conclusion of our paper is that micromolar concentrations of cocaine and amphetamine in the striatum significantly increase dopamine D2 receptor occupation, but have a lesser effect on D1 receptor occupation.

5.4.1. Considerations relative to the simulation model

The model, in essence, consists of six components: dopamine release, DAT, D1 receptor binding, D2 receptor binding, drug binding and morphology. Of these, the parameter that deviates most from reality is morphology. A simple sphere does not accurately represent the extracellular space in the striatum, as it is simpler than the network of tubes thought to create the extracellular space (Thorne and Nicholson 2006). Therefore, we also used a complex simulation space to determine receptor occupation in the presence of 5 and 10 mg/kg cocaine as well as 2 mg/kg amphetamine. The conclusions are the same for both models even though the details are slightly different. Receptor occupation was lower overall in the complex model compared to the simple model. We believe the results achieved with our simple model are suggestive of the maximum receptor occupation in the presence of increasing concentrations of cocaine, which provides support of our conclusion that cocaine does not greatly increase dopamine D1 receptor occupation, whereas amphetamine has a slightly larger effect.

For DAT kinetics, different parameter values were used in the cocaine and amphetamine simulations. For the cocaine simulation, the fast rate of onset for DAT was used because this parameter achieves similar increases in extracellular dopamine in the presence of cocaine to the published data. No combination of kinetic parameters could be found to achieve similar results with the slow DAT kinetic parameters used in previous studies. In contrast to cocaine, amphetamine has effects other than inhibition of dopamine transporter. These additional effects alter rate of dopamine secretion. A separate project determined a set of parameters for which the simulation output matches published data. This set of parameters involved the slow DAT kinetics. The important factor relative to receptor occupation is level of extracellular dopamine. Thus, it appears that resolution of the problem of which set of DAT kinetics apply in the brain will have no effect on the conclusions relative to receptor occupancy.

5.4.2. Implication of results

Regarding D2 receptors, the simulations suggest that, even under low probability release conditions, increases in extracellular dopamine elicited by cocaine or amphetamine are sufficient to occupy all D2 receptors. In contrast, D1 receptors remain largely unoccupied. However, we know they must become occupied because behavioral studies show that the presence of dopamine antagonists in the nucleus accumbens reduce cocaine-induced locomotion (Maldonado et al. 1993; McGregor and Roberts 1993; Kaddis, Uretsky, and Wallace 1995), as well as the locomotor and place preference effects of amphetamine (Mackey and van der Kooy 1985; Mithani et al. 1986; Spyraki,

Fibiger, and Phillips 1982b). These data suggest that D1 receptors are activated in the presence of stimulants. We hypothesize that local signals acting at the terminal that have the ability to increase dopamine release probability, coupled with the effects psychostimulants have on extracellular dopamine concentration, work synergistically to increase dopamine D1 receptor binding. In the presence of these drugs, low-powered local signals that increase dopamine release are enhanced and may activate D1 receptor pathways that normally would not be activated in the absence of the drug. Another possibility is that signals acting at the level of the D1 receptor have the capability to move D1 receptors into a high affinity state, which would then increase D1 receptor activation. It is not clear if factors that can influence the interaction between the G-protein and receptor exist, or if receptors are able to switch between high and low affinity states easily. However, assuming signals exist that can change the affinity state of dopamine D1 receptors, these signals would be able to alter dopamine D1 receptor activation. Either of these conditions could have the potential to increase dopamine D1 receptor binding to a level that would explain the behavioral effects of dopamine receptor antagonists in the presence of cocaine and amphetamine.

Cocaine may also be exerting its behavioral effects through non-dopaminergic receptors as well. Recently, experiments have shown that cocaine also targets the sigma-1 receptor. This receptor is expressed in the brain and in various peripheral tissues. The exact function of the sigma-1 receptor remains to be elucidated, but it has been shown to modulate the function of dopamine, acetylcholine, NMDA and opioid receptors (Narayanan et al. 2011). The natural ligand for the sigma-1 receptors has yet to be elucidated as well, but some believe neurosteroids are able to bind this receptor (Cobos et

al. 2008). Sigma receptor antagonists and sigma-1 receptor knockdown reduces cocaine-induced locomotor hyperactivity and blocks induction and expression of cocaine-induced conditioned place preference in rodents (Robson et al. 2012). Other evidence also suggests that the glutamate plays a role in the addicting properties of psychostimulants. When the AMPA receptor antagonist DNQX is administered prior to cocaine administration, it attenuates the acquisition of conditioned place preference (Kaddis, Uretsky, and Wallace 1995). This suggests that cocaine exerts its effects through multiple pathways and the dopamine system is only one of the pathways involved.

In conclusion, our model shows that at the highest concentrations of cocaine tested, dopamine D2 receptor occupation increased by 30% from a baseline of about 50%, whereas D1 receptor occupation only increased to about 4% total. Amphetamine had a greater effect on dopamine D1 receptor occupation than cocaine, but still only increased D1 receptor binding to about 13%. Based on our previous studies, we believe that the cocaine and amphetamine induced increase in extracellular dopamine, coupled with local signals that increase dopamine release probability or dopamine receptor affinity, enhance the strength of the dopamine signal in the striatum, explaining the behavioral effects of the drugs.

Table 16: Parameter values derived from biochemical data for rodent dorsal striatum.

Parameter	Value
Dopamine level	79.2 μM [a]
Dopamine varicosity density	$1x10^{+8}/mm^3$ [b]
Dopamine transporter level	0.47 μM [c]
Dopamine transporter V_{max}	4.08 μM/sec [d]
Dopamine transporter K_m (transfected cells)	2.17 μM [e]
Dopamine transporter K_m (tissue prep)	0.2 μM [f]
Dopamine D1 receptor level	0.01 μM [g]
Dopamine D1 receptor K_d	1 μM [h]
Dopamine D2 receptor level	0.04 μM [i]
Dopamine D2 receptor K_d	10 nM [j]
Cocaine-DAT K_d	0.5 μM [k]
Amphetamine-DAT K_d	0.2 μM[l]

[a] Derived from (Abekawa et al., 2001; Bardullas et al., 2011; Buu, 1989; Cartmell et al., 2000; Gao and Dluzen, 2001; Miller et al., 1980; Ponzio et al., 1984; Sharp et al., 1986; Takahashi et al., 1997; Vezina et al., 1992; Yu et al., 2001; Yuan et al., 2001)

[b] Derived from (Doucet et al., 1986)

[c] Derived from (Boja et al., 1995; Bonnet et al., 1986; Chen et al., 1997a; Dubocovich and Zahniser, 1985; Erikson et al., 2000; Garreau et al., 1997; Hooks et al., 1994; Janowsky et al., 1986; Marshall et al., 1990; Moll et al., 2000; Nakayama et al., 1993; Rothman et al., 1994)

[d] Derived from (Garris and Wightman, 1994; May and Wightman, 1989; Wu et al., 2001)

[e] Derived from (Carneiro et al., 2002; Chang et al., 2001; Eshleman et al., 1995; Itokawa et al., 2000; Kitayama et al., 1992; Lee et al., 1996; Lin and Uhl, 2002; Lin and Uhl, 2005; Loland et al., 1999; Loland et al., 2002; Melikian and Buckley, 1999; Norregaard et al., 1998; Norregaard et al., 2000; Yatin et al., 2002)

[f] Derived from (Harris and Baldessarinig, 1973; Horn, 1990; Marshall et al., 1990; Near et al., 1988; Rothman et al., 2001; Snyder and Coyle, 1969; Wu et al., 2001)

[g] (Hyttel 1987; Mendes de Freitas et al. 2005)

[h] (Jakob Kisbye Dreyer and Hounsgaard 2013; Rice and Cragg 2008)

[i] (Hyttel 1987; Murrin and Zeng 1986; Walters and Carr 1988)

[j] (Jakob Kisbye Dreyer and Hounsgaard 2013; Rice and Cragg 2008)

[k] (Han and Gu 2006; Hearn et al. 1991)

[l] (Harris and Baldessarini 1973; Rothman et al. 2001)

Table 17: Parameter values associated with a single varicosity for cocaine model.

Parameter	Value
Number of dopamine molecules per varicosity	475,000
Number of vesicles per varicosity	250
Number of dopamine molecules per vesicle	1,900
Extracellular volume surrounding a release site (dorsal striatum)	$2x10^{-15}$ liter
Number of DAT associated with a release site	300
DAT catalytic rate	9 /sec
DAT-DA binding on-rate	$1.3x10^{+8}$ $M^{-1}sec^{-1}$
DAT-DA binding off-rate	0.5 sec^{-1}
D1-DA binding on-rate	$5x10^{5}$ $M^{-1}sec^{-1}$
D1-DA binding off-rate	0.4 sec^{-1}
D1 receptor number	220
D2-DA binding on-rate	$8.2x10^{7}$ $M^{-1}sec^{-1}$
D2-DA binding off-rate	0.4 sec^{-1}
Cocaine-DAT binding on-rate	$1.3x10^{6}$ $M^{-1}sec^{-1}$
Cocaine-DAT binding off-rate	3 sec^{-1}
D2 receptors located on medium spiny neurons	45 [b]
D2 receptors located on dopamine terminals	13 [b]
D2 receptors located on other varicosities	6 [b]
Dopamine diffusion rate	$4x10^{-6}$ cm^2/sec [a]

[a] Derived from (Land et al., 1984; Rice and Cragg, 2008; Schonfuss et al., 2001)
[b] D2 receptor distribution derived from (Anzalone et al. 2012)

Table 18. Parameter values associated with a single varicosity for amphetamine model.

Parameter	Value
Extracellular volume associated with a release site (dorsal striatum)	$2x10^{-15}$ liter
Number of DAT associated with a release site	2,500
DAT catalytic rate	5 /sec
DAT-DA binding on-rate	$1x10^{+6}$ $M^{-1}sec^{-1}$
DAT-DA binding off-rate	0.5 sec^{-1}
D1-DA binding on-rate	$5x10^{5}$ $M^{-1}sec^{-1}$
D1-DA binding off-rate	0.4 sec^{-1}
D1 receptor number	220
D2-DA binding on-rate	$8.2x10^{7}$ $M^{-1}sec^{-1}$
D2-DA binding off-rate	0.4 sec^{-1}
Amphetamine-DAT binding on-rate	$2x10^{6}$ $M^{-1}sec^{-1}$
Amphetamine-DAT binding off-rate	0.5 sec^{-1}
Non-DAT binding on-rate	$1.3x10^{3}$ $M^{-1}sec^{-1}$
Non-DAT binding off-rate	0.002 sec^{-1}
Non-DAT catalytic rate	0.005 /sec
D2 receptors located on medium spiny neurons	45 [b]
D2 receptors located on dopamine terminals	13 [b]
D2 receptors located on other varicosities	6 [b]
Dopamine diffusion rate	$4x10^{-6}$ cm^2/sec [a]
Amphetamine diffusion rate	$4x10^{-6}$ cm^2/sec [a]

[a] Derived from (Land et al., 1984; Rice and Cragg, 2008; Schonfuss et al., 2001)

Table 19: Brain concentrations of cocaine and corresponding i.p. injection dose.

Cocaine dose (i.p. injection; mg/kg)	Cocaine brain concentration[a] (μM)
5	1.65
10	4.41
15	7.16
20	9.91
25	12.67

[a] Brain concentrations were determined using the best-fit line to the data in Figure 16.

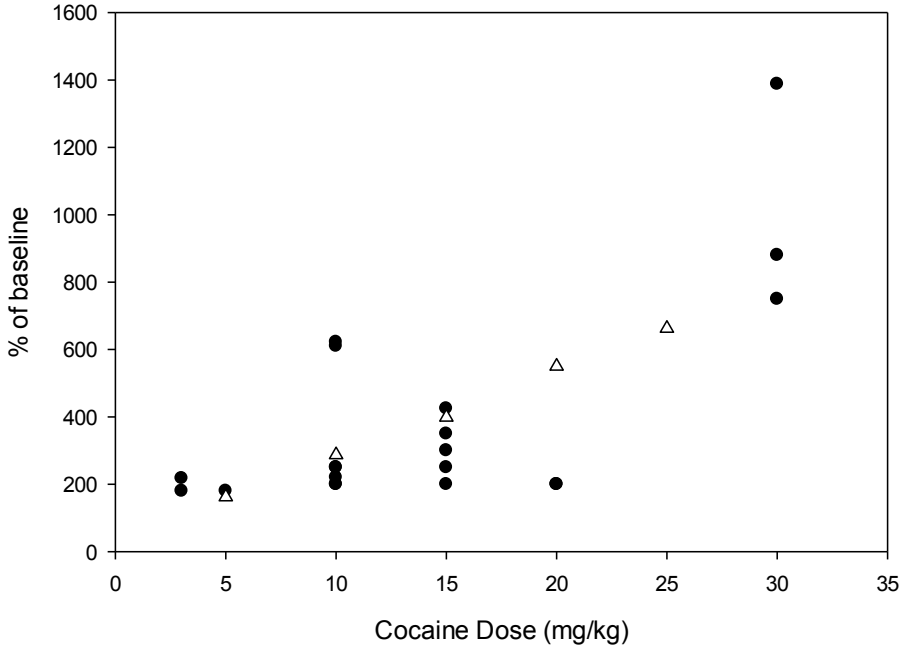

Figure 15: Striatal dopamine concentration vs. i.p. cocaine dose.

Published data of measured increases in striatal extracellular dopamine is shown plotted against increasing doses of cocaine (•). Computer simulations were then used to model the relationship between cocaine dose and percent increase in striatal extracellular dopamine (△). Published data are from (Camp, Browman, and Robinson 1994; Church, Justice, and Byrd 1987; Coury et al. 1992; Hooks, Duffy, et al. 1994; Inada, Polk, Jin, et al. 1992; Inada, Polk, Purser, et al. 1992; Kalivas and Duffy 1993; Maisonneuve and Kreek 1994; Nicolaysen, Pan, and Justice Jr. 1988; Rossetti et al. 1991).

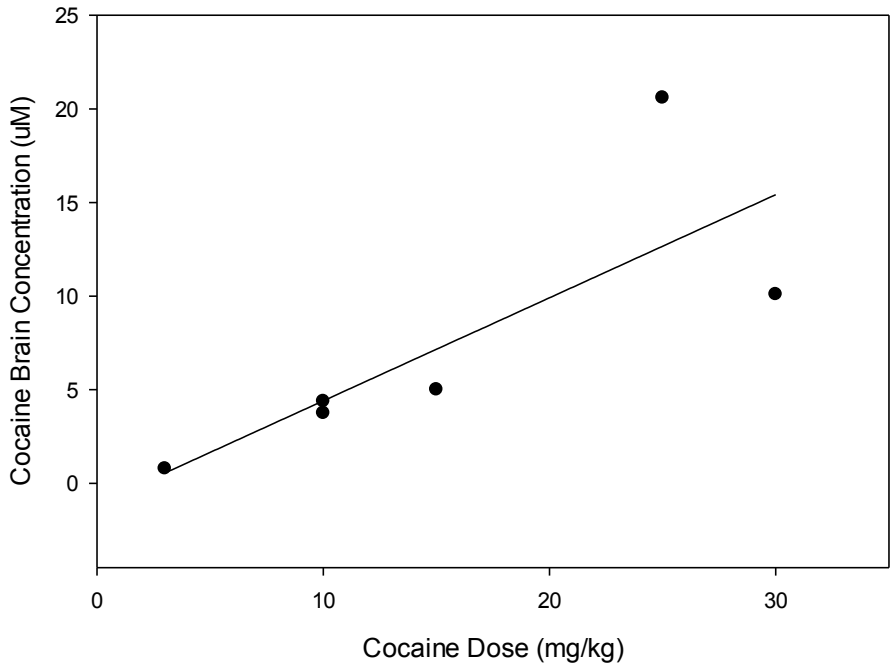

Figure 16: Concentration of cocaine in rodent brain vs. i.p. cocaine dose.

Published data from (Benuck, Lajtha, and Reith 1987; Camp, Browman, and Robinson 1994; Cass and Gerhardt 1994; Maisonneuve and Kreek 1994; Nicolaysen, Pan, and Justice Jr. 1988; Reith, Benuck, and Lajtha 1987).

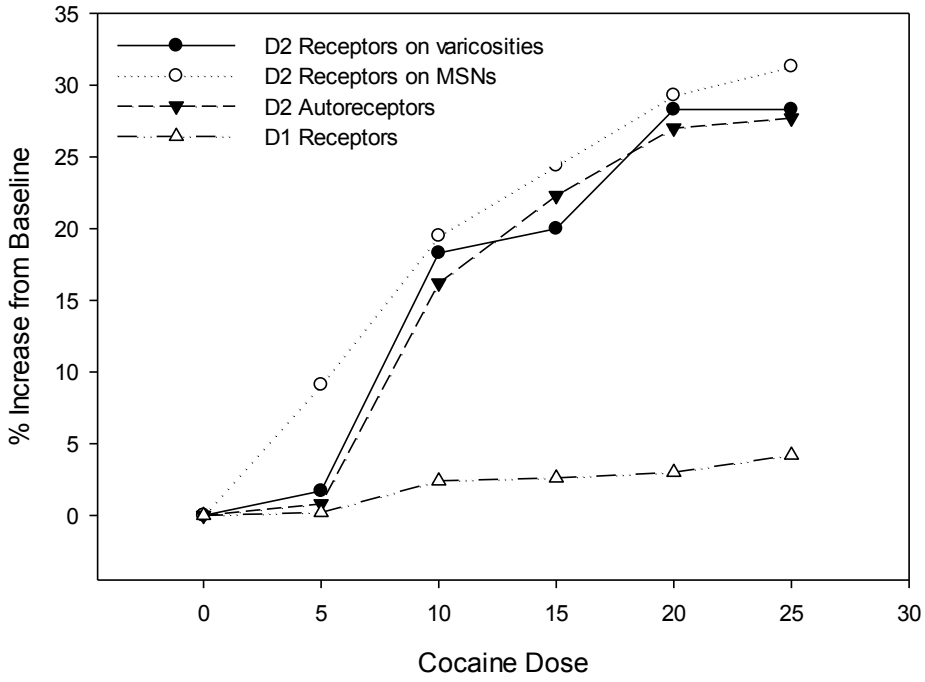

Figure 17: Dopamine D1 and D2 receptor occupation in the presence of increasing concentrations of cocaine.

The number of dopamine D2 receptors occupied for all three subsets of D2 receptors (solid triangles: D2 autoreceptors on dopamine varicosities; solid circles: D2 receptors on other varicosities; open circles: D2 receptors on medium spiny neurons) increases by about 30% across all cocaine doses tested. The number of dopamine D1 receptors (open triangles) occupied, however, only increases by about 4% across all cocaine doses tested.

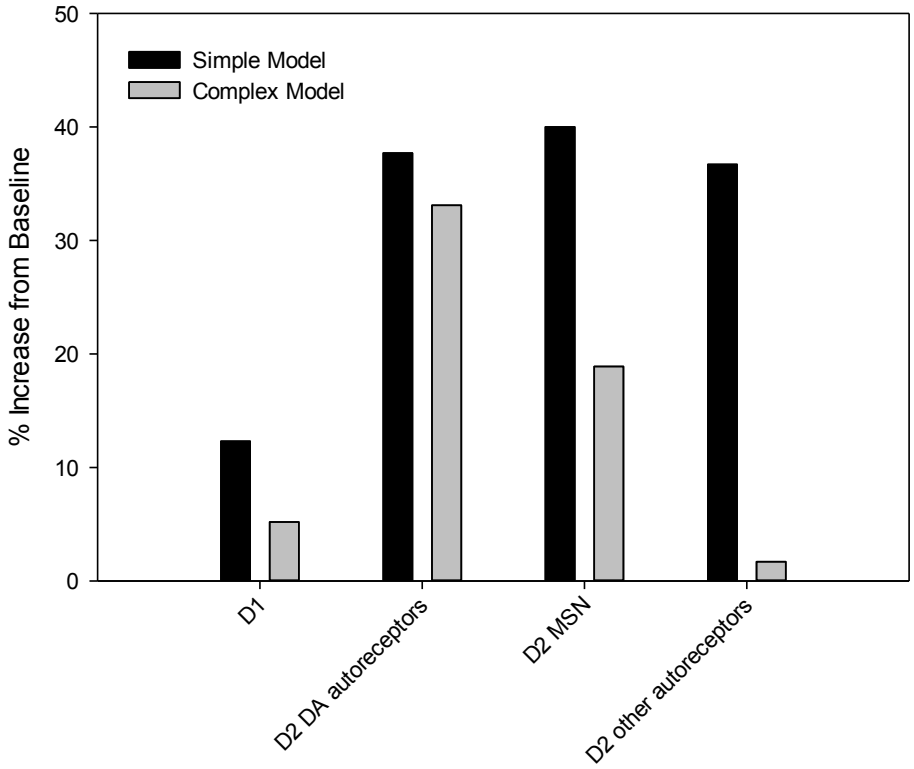

Figure 18: Dopamine receptor occupation in the presence of 2 mg/kg amphetamine.

In the presence of 2 mg/kg amphetamine, dopamine D1 and D2 receptor occupation increases in both the simple and complex models. D1 receptor occupation increases to a maximum of 13% above baseline, whereas D2 receptor occupation increases to a maximum of 40% above baseline.

Chapter 6: Significance and Future Perspectives

6.1. Summary and significance of dissertation research

Dopamine is a highly studied neurotransmitter that is important in movement, motivation, reward, learning, attention and memory. It is also implicated in multiple disease states such as addiction, Parkinson's disease, schizophrenia and others. Dopamine neurons exist in distinct nuclei. Two of these nuclei, located in the substantia nigra and ventral tegmental area, innervate the extended striatum. Dopamine communicates via volume transmission throughout the striatal complex. It acts as a modulatory neurotransmitter by activating G-protein coupled receptors, which modify a neuron's response through multiple signaling pathways. Because dopamine is modulatory instead of excitatory or inhibitory, it is more difficult to study its effects on target neurons because there is no easily measured response, such as a direct change in membrane potential. While much research has been done on global effects of dopamine, little has focused on the individual dopamine release sites. Much of the prominent view of dopamine signaling is inferred from studying other neurotransmitter systems, such as glutamate or the neuromuscular junction. Both morphological and biophysical data suggest that dopamine signals differently from these highly studied neurotransmitters,

suggesting that extrapolating what we know about how they operate to the dopamine system may not be accurate. Our lab has been utilizing various computer models of dopamine signaling to evaluate potential answers to questions on dopamine signaling that remain unanswered. One advantage of computer models is the ability to integrate all of the players involved in regulating dopamine signaling to create a big picture of dopamine signaling at the level of release site and receptors in its vicinity.

The medium spiny neuron is the only output neuron in the striatum. On average, each neuron receives over 10,000 inputs, of which about half are glutamate. These neurons are quiescent in their baseline state. In order to generate an action potential to code an output message, glutamate inputs need to be active to depolarize dendrites. Currents from the depolarization events must then travel from initiation site to the axon hillock (Figure 19). The current dissipates at varying rates depending on the diameter of the dendrite and the leakiness of the membrane. Currents from various depolarization events sum as their paths combine. When the depolarization at the axon hillock reaches threshold, an axon potential is initiated. Thus, the pattern of action potentials is a function of the number of active glutamate inputs and the leakiness of dendritic membranes. Dopamine terminals present in the striatum serve a modulatory role. As dopamine receptors are located both at the signal initiation sites and in several locations throughout the dendritic tree, where leakiness can be regulated, dopamine has substantial potential for modulating the output code of the medium spiny neurons.

The first step in dopamine's modulation of medium spiny neuron output is release of dopamine from axon varicosities into signal space/compartment. Our results suggest that the probability of release of the dopamine contents of a single vesicle induced by

each firing event is low. In our opinion, the most parsimonious explanation is that the contents of one vesicle are released from a few percent of the varicosities in the dendritic tree of any given dopamine neuron. Furthermore, our data suggest that the burst-firing pattern of dopamine neurons observed in *in vivo* experiments has minimal impact by itself on the level of extracellular dopamine. Other simulations suggest that under baseline conditions about half of dopamine D2 receptors are occupied while negligible numbers of D1 receptors are occupied. We interpret these findings as meaning that an important component of dopamine signaling is the regulation of probability of vesicular release of dopamine. We hypothesize that the low probability of vesicular release throughout the vast axonal tree provides a baseline on top of which very localized signals are generated. This could be accomplished by increasing action potential conductance in the axonal tree or by increasing amount of calcium entering varicosities with each action potential. Regarding the latter, nicotinic acetylcholine receptors are expressed on dopamine terminals, and activation of these is capable under certain conditions of driving dopamine release even in the absence of an action potential (Threlfell et al 2012). Thus, localized cholinergic signals could be involved in sculpting dopamine signals.

Dopamine in extracellular space acts on receptors to influence medium spiny neuron output code. This can be accomplished by regulating amount of glutamate release or regulating amount of leakiness of medium spiny neuron dendrites. Dopamine has the potential to reduce glutamate release via activation of dopamine D2 receptors located on glutamate terminals, which would reduce the depolarizing currents in the medium spiny neurons. Dopamine also has the ability to modulate the output of the striatum via actions within the medium spiny neuron itself. Dopamine D2 receptors are expressed on half of

medium spiny neurons. One potential mechanism by which these receptors alter leakiness is through activation of inwardly rectifying potassium channels. A second potential mechanism that would impact strength of glutamate signals would be inhibition of protein kinase A-mediated phosphorylation of AMPA and NMDA receptors. Dopamine D1 receptors are expressed on the other half of the output neurons. A potential mechanism by which they can influence excitatory inputs is through activation of protein kinase A-mediated phosphorylation of AMPA receptors (Snyder et al. 2000). This modification amplifies the AMPA current and enhances the glutamate signal, making it more likely that the neuron will depolarize beyond its threshold. Therefore, depending on which receptors are activated, dopamine has the ability to either enhance the depolarization of the medium spiny neurons or diminish it.

The effects of D1 receptors on phosphorylation of AMPA receptors has been shown *in vivo*, however, our model suggests that D1 receptors remain unoccupied in most dopamine release conditions. One potential explanation as to how these receptors become activated is that a local signal, acting at the receptor, has the ability to shift the D1 receptors into a high affinity state. Richfield et al. determined that about 80% of the D1 receptor exist in the low affinity state with a K_d around 1 μM (Richfield, Penney, and Young 1989). The remaining 20% high affinity D1 receptors had a K_d value between 10-50 nM (Richfield, Penney, and Young 1989; May 1992). There are two theories to describe the affinity state of a G protein-coupled receptor. First, there is a theory that the G protein and receptor form a stable interaction regardless of binding state of the receptor. This interaction leads to a high affinity for the receptor, and, when bound to an agonist, the G protein activates effector proteins without dissociating from the receptor

(Hein and Bünemann 2009; Qin et al. 2011). The second theory is the collision-coupling model, in which the G protein and receptor are uncoupled and move freely throughout the cell membrane. When the receptor binds an agonist, it has a higher affinity for a G-protein, which then binds, activates and dissociates to activate effector proteins (Hein and Bünemann 2009; Skinbjerg et al. 2012). It is not clear what factors influence the interaction between the G-protein and receptor, or if receptors are able to switch between high and low affinity states easily. However, assuming signals exist that can change the affinity state of dopamine D1 receptors, these signals would be able to alter dopamine D1 receptor activation and have the ability to modulate the striatal output.

The data in this thesis generated with our model only provide a global perspective of the average dopamine release site. We have shown that striatal dopamine has a low probability of release and that dopamine D1 receptors are not occupied under multiple dopamine release conditions. However, It is possible that distinct pockets exist throughout the striatum where other factors, such as receptors located on terminals, increase dopamine release probability and greatly increase the extracellular dopamine concentration. It is also possible that postsynaptic signals are able to increase the affinity of D1 receptors for dopamine, thus enhancing their signaling capability. As a modulatory neurotransmitter, dopamine has the ability to alter the output of the striatum through a variety of mechanisms, and the dopamine signal does not seem to be solely dependent on dopamine neuron firing rate. Based on the data in this thesis, we have shown that the traditional view of neurotransmission does not apply to the dopamine system in the striatum. Instead, it seems the system is designed to have low, tonic activity that can then be emphasized with local signals when necessary.

6.2. Future Perspectives

The results of this dissertation suggest interesting phenomena that need to be proven experimentally. This will require development of new technology. Dopamine is a modulatory neurotransmitter that activates G-protein coupled receptors, which initiate signaling cascades that indirectly affect membrane potential. This makes it difficult to directly measure fast changes in dopamine release. Electrochemistry and microdialysis techniques are helpful in looking at average dopamine concentrations, but are not small enough or precise enough to measure dopamine release from a single terminal. False fluorescent neurotransmitters have also been used to look at dopamine release, but the temporal sensitivity is not fast enough (Gubernator et al. 2009). More recently, however, new techniques have been developed that allow us to study dopamine release in real time.

Kress et al. used a dopamine-gated chloride channel from *C. elegans* to study dopamine release from terminals in the rat dorsal striatum. They were able to distinguish direct dopamine release, and even see dopamine release driven by nicotinic receptor activation (Kress et al. 2014). There are still limitations to this technique, though. The receptor has about a 6 μM affinity for dopamine, but also has a low sensitivity to norepinephrine and epinephrine. A lentiviral expression system was used to express the receptors on medium spiny neurons in striatal slices. Depending on the success of the technique, surface expression of the receptor could have had an impact on the results. One of the biggest limitations to this study, though, is the fact that it was performed in slices and dopamine release was elicited by electrical stimulation. This would not give us

data on tonic, baseline dopamine release *in vivo*. Even with the limitations of this experiment, the technology has the potential to be useful in providing further evidence that either supports or denies the conclusions of this thesis. If the dopamine-gated chloride channel could be transfected and electrophysiological readings taken *in vivo*, the system could potentially be used to determine what physiological dopamine release looks like in real time.

Another technique that has been recently used to look at dopamine D2 receptor occupation in real time utilizes G protein activated inwardly rectifying potassium channels (GIRK2) coupled to D2 receptors in the striatum (Marcott, Mamaligas, and Ford 2014). This group virally overexpressed the GIRK2 channels in mouse striatum and the outward currents were used as a sensor of dopamine D2 receptor activation. Again, measurements were taken from striatal slices, and dopamine release was either electrically or optogenetically evoked. If the electrophysiological readings could be taken *in vivo*, the system could potentially be used to determine what dopamine D2 receptor occupation looks like in real time, under multiple circumstances like those tested using our model.

While no current technique exists to look at dopamine D1 receptor occupation in real-time, the new techniques discussed above offer a framework for potential ways to monitor D1 receptor occupation, if a reporter with high specificity can be found. These techniques open up new avenues for investigating how modulatory neurotransmitter systems work in real-time and can supplement and improve our models of the dopamine terminal.

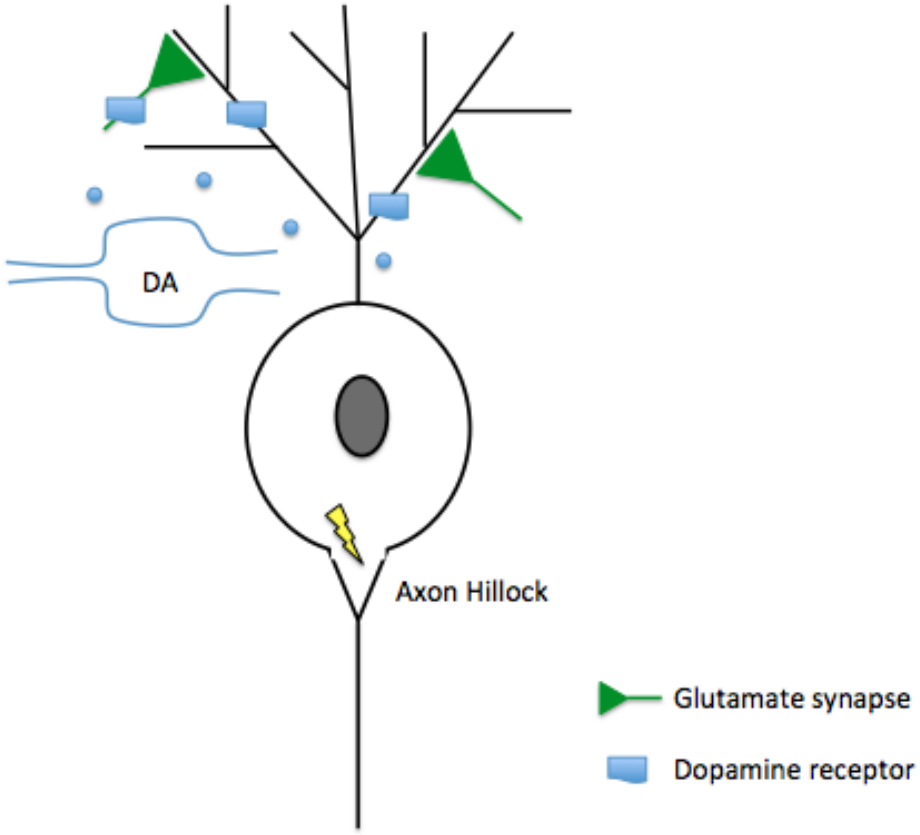

Figure 19: Dopamine modulation of striatal output.

The medium spiny neuron is the only output neuron in the striatum, and the pattern of action potentials initiated at the axon hillock provide the code for striatally regulated functions. In order to generate an action potential at the axon hillock, various glutamate inputs initiate small currents that must travel to the axon hillock. The amount of signal arriving can be modulated by varying leakiness of dendritic membranes. When the current reaching the axon hillock is strong enough to depolarize the membrane past the threshold, the neuron will fire. Dopamine signals in the striatum act both to modulate the magnitude of the glutamate input and the leakiness of the membrane. Ways in which this can be accomplished include the following. First, dopamine D2 receptors exist on glutamate inputs, which, when activated, reduce glutamate release. Second, postsynaptic signals may increase dopamine D1 receptor affinity for ligand, thus increasing D1 receptor signaling. Activation of dopamine D1 receptors expressed on the dendrites of the medium spiny neuron has been shown to increase phosphorylation of AMPA receptors and potentiate the current (G. L. Snyder et al. 2000). Signals acting at dopamine terminals, such as activation of nicotinic acetylcholine receptors or dopamine D2 receptors, would alter dopamine release probability, which would affect dopamine signaling. An additional potential effect of activation of D2 receptors is opening of potassium channels in dendrites with the effect of increasing membrane leakiness.

References

Abekawa, T., T. Ohmori, M. Honda, K. Ito, and T. Koyama. 2001. "Effect of Low Doses of L-NAME on Methamphetamine-Induced Dopaminergic Depletion in the Rat Striatum." *Journal of Neural Transmission (Vienna, Austria: 1996)* 108 (11): 1219–30.

Adrover, Martín F, Jung Hoon Shin, and Veronica A Alvarez. 2014. "Glutamate and Dopamine Transmission from Midbrain Dopamine Neurons Share Similar Release Properties but Are Differentially Affected by Cocaine." *The Journal of Neuroscience: The Official Journal of the Society for Neuroscience* 34 (9): 3183–92. doi:10.1523/JNEUROSCI.4958-13.2014.

Agnati, L F, M Zoli, I Strömberg, and K Fuxe. 1995. "Intercellular Communication in the Brain: Wiring versus Volume Transmission." *Neuroscience* 69 (3): 711–26.

Alcantara, A. A., L. Mrzljak, R. L. Jakab, A. I. Levey, S. M. Hersch, and P. S. Goldman-Rakic. 2001. "Muscarinic m1 and m2 Receptor Proteins in Local Circuit and Projection Neurons of the Primate Striatum: Anatomical Evidence for Cholinergic Modulation of Glutamatergic Prefronto-Striatal Pathways." *The Journal of Comparative Neurology* 434 (4): 445–60.

Andén, N. E., K. Hfuxe, B. Hamberger, and T. Hökfelt. 1966. "A Quantitative Study on the Nigro-Neostriatal Dopamine Neuron System in the Rat." *Acta Physiologica Scandinavica* 67 (3): 306–12. doi:10.1111/j.1748-1716.1966.tb03317.x.

Antipova, Veronica, Alexander Hawlitschka, Eilhard Mix, Oliver Schmitt, Désirée Dräger, Reiner Benecke, and Andreas Wree. 2013. "Behavioral and Structural Effects of Unilateral Intrastriatal Injections of Botulinum Neurotoxin a in the Rat Model of Parkinson's Disease." *Journal of Neuroscience Research* 91 (6): 838–47. doi:10.1002/jnr.23210.

Anzalone, Andrea, José E Lizardi-Ortiz, Maria Ramos, Claudia De Mei, F Woodward Hopf, Ciro Iaccarino, Briac Halbout, et al. 2012. "Dual Control of Dopamine Synthesis and Release by Presynaptic and Postsynaptic Dopamine D2 Receptors." *The Journal of Neuroscience: The Official Journal of the Society for Neuroscience* 32 (26): 9023–34. doi:10.1523/JNEUROSCI.0918-12.2012.

Araujo, D. M., P. A. Lapchak, and R. Quirion. 1991. "Heterogeneous Binding of [3H]4-DAMP to Muscarinic Cholinergic Sites in the Rat Brain: Evidence from Membrane Binding and Autoradiographic Studies." *Synapse (New York, N.Y.)* 9 (3): 165–76. doi:10.1002/syn.890090303.

Badiani, A., M. M. Oates, H. E. Day, S. J. Watson, H. Akil, and T. E. Robinson. 1998. "Amphetamine-Induced Behavior, Dopamine Release, and c-Fos mRNA Expression: Modulation by Environmental Novelty." *The Journal of*

Neuroscience: The Official Journal of the Society for Neuroscience 18 (24): 10579–93.

Bardullas, Ulises, Magda Giordano, and Verónica M. Rodríguez. 2011. "Chronic Atrazine Exposure Causes Disruption of the Spontaneous Locomotor Activity and Alters the Striatal Dopaminergic System of the Male Sprague–Dawley Rat." *Neurotoxicology and Teratology* 33 (2): 263–72. doi:10.1016/j.ntt.2010.09.001.

Beaulieu, Jean-Martin, and Raul R. Gainetdinov. 2011. "The Physiology, Signaling, and Pharmacology of Dopamine Receptors." *Pharmacological Reviews* 63 (1): 182–217. doi:10.1124/pr.110.002642.

Bello, Estefanía P., Yolanda Mateo, Diego M. Gelman, Daniela Noaín, Jung H. Shin, Malcolm J. Low, Verónica A. Alvarez, David M. Lovinger, and Marcelo Rubinstein. 2011. "Cocaine Supersensitivity and Enhanced Motivation for Reward in Mice Lacking Dopamine D2 Autoreceptors." *Nature Neuroscience* 14 (8): 1033–38. doi:10.1038/nn.2862.

Bennett, B. D., and J. P. Bolam. 1993. "Characterization of Calretinin-Immunoreactive Structures in the Striatum of the Rat." *Brain Research* 609 (1–2): 137–48. doi:10.1016/0006-8993(93)90866-L.

Bennett, B. D., and C. J. Wilson. 1999. "Spontaneous Activity of Neostriatal Cholinergic Interneurons in Vitro." *The Journal of Neuroscience: The Official Journal of the Society for Neuroscience* 19 (13): 5586–96.

Benoit-Marand, M, E Borrelli, and F Gonon. 2001. "Inhibition of Dopamine Release via Presynaptic D2 Receptors: Time Course and Functional Characteristics in Vivo." *The Journal of Neuroscience: The Official Journal of the Society for Neuroscience* 21 (23): 9134–41.

Benuck, M., A. Lajtha, and M. E. Reith. 1987. "Pharmacokinetics of Systemically Administered Cocaine and Locomotor Stimulation in Mice." *The Journal of Pharmacology and Experimental Therapeutics* 243 (1): 144–49.

Bhargava, H. N., A. Gulati, and P. Ramarao. 1989. "Effect of Chronic Administration of U-50,488H on Tolerance to Its Pharmacological Actions and on Multiple Opioid Receptors in Rat Brain Regions and Spinal Cord." *The Journal of Pharmacology and Experimental Therapeutics* 251 (1): 21–26.

Bianco, Laura E., Jason Wiesinger, Christopher J. Earley, Byron C. Jones, and John L. Beard. 2008. "Iron Deficiency Alters Dopamine Uptake and Response to L-DOPA Injection in Sprague-Dawley Rats." *Journal of Neurochemistry* 106 (1): 205–15. doi:10.1111/j.1471-4159.2008.05358.x.

Bidaut-Russell, M., W. A. Devane, and A. C. Howlett. 1990. "Cannabinoid Receptors and Modulation of Cyclic AMP Accumulation in the Rat Brain." *Journal of Neurochemistry* 55 (1): 21–26.

Birbeck, Johnna A, Madiha Khalid, and Tiffany A Mathews. 2014. "Potentiated Striatal Dopamine Release Leads to Hyperdopaminergia in Female Brain-Derived Neurotrophic Factor Heterozygous Mice." *ACS Chemical Neuroscience* 5 (4): 275–81. doi:10.1021/cn400157b.

Björklund, Anders, and Stephen B. Dunnett. 2007. "Dopamine Neuron Systems in the Brain: An Update." *Trends in Neurosciences* 30 (5): 194–202. doi:10.1016/j.tins.2007.03.006.

Boja, J. W., J. L. Cadet, T. A. Kopajtic, J. Lever, H. H. Seltzman, C. D. Wyrick, A. H. Lewin, P. Abraham, and F. I. Carroll. 1995. "Selective Labeling of the Dopamine Transporter by the High Affinity Ligand 3 Beta-(4-[125I]iodophenyl)tropane-2 Beta-Carboxylic Acid Isopropyl Ester." *Molecular Pharmacology* 47 (4): 779–86.

Bonnet, J J, P Protais, A Chagraoui, and J Costentin. 1986. "High-Affinity [3H]GBR 12783 Binding to a Specific Site Associated with the Neuronal Dopamine Uptake Complex in the Central Nervous System." *European Journal of Pharmacology* 126 (3): 211–22.

Bonsi, P., D. Cuomo, B. Picconi, G. Sciamanna, A. Tscherter, M. Tolu, G. Bernardi, P. Calabresi, and A. Pisani. 2007. "Striatal Metabotropic Glutamate Receptors as a Target for Pharmacotherapy in Parkinson's Disease." *Amino Acids* 32 (2): 189–95. doi:10.1007/s00726-006-0320-3.

Bozarth, M. A., and R. A. Wise. 1986. "Involvement of the Ventral Tegmental Dopamine System in Opioid and Psychomotor Stimulant Reinforcement." *NIDA Research Monograph* 67: 190–96.

Britt, Jonathan P., Faiza Benaliouad, Ross A. McDevitt, Garret D. Stuber, Roy A. Wise, and Antonello Bonci. 2012. "Synaptic and Behavioral Profile of Multiple Glutamatergic Inputs to the Nucleus Accumbens." *Neuron* 76 (4): 790–803. doi:10.1016/j.neuron.2012.09.040.

Britt, Jonathan P., and Daniel S. McGehee. 2008. "Presynaptic Opioid and Nicotinic Receptor Modulation of Dopamine Overflow in the Nucleus Accumbens." *The Journal of Neuroscience: The Official Journal of the Society for Neuroscience* 28 (7): 1672–81. doi:10.1523/JNEUROSCI.4275-07.2008.

Brown, L. L., D. M. Smith, and L. M. Goldbloom. 1998. "Organizing Principles of Cortical Integration in the Rat Neostriatum: Corticostriate Map of the Body Surface Is an Ordered Lattice of Curved Laminae and Radial Points." *The Journal of Comparative Neurology* 392 (4): 468–88.

Bucher, D., and J. M. Goaillard. 2011. "Beyond Faithful Conduction: Short-Term Dynamics, Neuromodulation, and Long-Term Regulation of Spike Propagation in the Axon." *Progress in Neurobiology* 94 (4): 307–46.

Bunney, B S, G K Aghajanian, and R H Roth. 1973. "Comparison of Effects of L-DOPA, Amphetamine and Apomorphine on Firing Rate of Rat Dopaminergic Neurones." *Nature: New Biology* 245 (143): 123–25.

Buu, N. T. 1989. "Vesicular Accumulation of Dopamine Following L-DOPA Administration." *Biochemical Pharmacology* 38 (11): 1787–92.

Cadet, J. L., and R. B. Rothman. 1986. "Decreased Striatal Opiate Delta-Receptors in the Rat Model of Persistent Dyskinesia Induced by Iminodipropionitrile." *Neuroscience Letters* 72 (1): 84–86.

Calipari, Erin S, Kimberly N Huggins, Tiffany A Mathews, and Sara R Jones. 2012. "Conserved Dorsal-Ventral Gradient of Dopamine Release and Uptake Rate in Mice, Rats and Rhesus Macaques." *Neurochemistry International* 61 (7): 986–91. doi:10.1016/j.neuint.2012.07.008.

Camp, D. M., K. E. Browman, and T. E. Robinson. 1994. "The Effects of Methamphetamine and Cocaine on Motor Behavior and Extracellular Dopamine

in the Ventral Striatum of Lewis versus Fischer 344 Rats." *Brain Research* 668 (1-2): 180–93.
Carboni, E., C. Spielewoy, C. Vacca, M. Nosten-Bertrand, B. Giros, and G. Di Chiara. 2001. "Cocaine and Amphetamine Increase Extracellular Dopamine in the Nucleus Accumbens of Mice Lacking the Dopamine Transporter Gene." *The Journal of Neuroscience: The Official Journal of the Society for Neuroscience* 21 (9): RC141: 1–4.
Carneiro, Ana M., Susan L. Ingram, Jean-Martin Beaulieu, Ava Sweeney, Susan G. Amara, Sheila M. Thomas, Marc G. Caron, and Gonzalo E. Torres. 2002. "The Multiple LIM Domain-Containing Adaptor Protein Hic-5 Synaptically Colocalizes and Interacts with the Dopamine Transporter." *The Journal of Neuroscience: The Official Journal of the Society for Neuroscience* 22 (16): 7045–54. doi:20026740.
Carta, M., R. Stancampiano, E. Tronci, M. Collu, A. Usiello, M. Morelli, and F. Fadda. 2006. "Vitamin A Deficiency Induces Motor Impairments and Striatal Cholinergic Dysfunction in Rats." *Neuroscience* 139 (4): 1163–72. doi:10.1016/j.neuroscience.2006.01.027.
Cartmell, J., C. R. Salhoff, K. W. Perry, J. A. Monn, and D. D. Schoepp. 2000. "Dopamine and 5-HT Turnover Are Increased by the mGlu2/3 Receptor Agonist LY379268 in Rat Medial Prefrontal Cortex, Nucleus Accumbens and Striatum." *Brain Research* 887 (2): 378–84.
Caruncho, H. J., I. Liste, and J. L. Labandeira-García. 1996. "GABAA Receptor Alpha 1-Subunit-Immunopositive Neurons in the Rat Striatum." *Brain Research* 722 (1-2): 185–89.
Cass, W A, and G A Gerhardt. 1994. "Direct in Vivo Evidence That D2 Dopamine Receptors Can Modulate Dopamine Uptake." *Neuroscience Letters* 176 (2): 259–63.
Castner, S. A., L. Xiao, and J. B. Becker. 1993. "Sex Differences in Striatal Dopamine: In Vivo Microdialysis and Behavioral Studies." *Brain Research* 610 (1): 127–34.
Catterall, William A. 2011. "Voltage-Gated Calcium Channels." *Cold Spring Harbor Perspectives in Biology* 3 (8). doi:10.1101/cshperspect.a003947.
Cerovic, Milica, Raffaele d'Isa, Raffaella Tonini, and Riccardo Brambilla. 2013. "Molecular and Cellular Mechanisms of Dopamine-Mediated Behavioral Plasticity in the Striatum." *Neurobiology of Learning and Memory*, MCCS 2013, 105 (October): 63–80. doi:10.1016/j.nlm.2013.06.013.
Chang, M. Y., S. H. Lee, J. H. Kim, K. H. Lee, Y. S. Kim, H. Son, and Y. S. Lee. 2001. "Protein Kinase C-Mediated Functional Regulation of Dopamine Transporter Is Not Achieved by Direct Phosphorylation of the Dopamine Transporter Protein." *Journal of Neurochemistry* 77 (3): 754–61.
Chen, N. H., Y. J. Lai, and W. H. Pan. 1997. "Effects of Different Perfusion Medium on the Extracellular Basal Concentration of Dopamine in Striatum and Medial Prefrontal Cortex: A Zero-Net Flux Microdialysis Study." *Neuroscience Letters* 225 (3): 197–200.
Chuhma, Nao, Kenji F. Tanaka, René Hen, and Stephen Rayport. 2011. "Functional Connectome of the Striatal Medium Spiny Neuron." *The Journal of*

Neuroscience: The Official Journal of the Society for Neuroscience 31 (4): 1183–92. doi:10.1523/JNEUROSCI.3833-10.2011.

Church, W. H., J. B. Justice, and L. D. Byrd. 1987. "Extracellular Dopamine in Rat Striatum Following Uptake Inhibition by Cocaine, Nomifensine and Benztropine." *European Journal of Pharmacology* 139 (3): 345–48.

Cobos, E.J, J.M Entrena, F.R Nieto, C.M Cendan, and E Del Pozo. 2008. "Pharmacology and Therapeutic Potential of Sigma1 Receptor Ligands." *Current Neuropharmacology* 6 (4): 344–66. doi:10.2174/157015908787386113.

Contant, C., D. Umbriaco, S. Garcia, K. C. Watkins, and L. Descarries. 1996. "Ultrastructural Characterization of the Acetylcholine Innervation in Adult Rat Neostriatum." *Neuroscience* 71 (4): 937–47.

Cossette, Martine, Frédéric Lecomte, and André Parent. 2005. "Morphology and Distribution of Dopaminergic Neurons Intrinsic to the Human Striatum." *Journal of Chemical Neuroanatomy* 29 (1): 1–11. doi:10.1016/j.jchemneu.2004.08.007.

Coury, A., C. D. Blaha, L. J. Atkinson, and A. G. Phillips. 1992. "Cocaine-Induced Changes in Extracellular Levels of Striatal Dopamine Measured Concurrently by Microdialysis with HPLC-EC and Chronoamperometry." *Annals of the New York Academy of Sciences* 654 (June): 424–27.

Cragg, Stephanie J. 2003. "Variable Dopamine Release Probability and Short-Term Plasticity between Functional Domains of the Primate Striatum." *The Journal of Neuroscience: The Official Journal of the Society for Neuroscience* 23 (10): 4378–85.

Crespo, Jose A, Katja Sturm, Alois Saria, and Gerald Zernig. 2006. "Activation of Muscarinic and Nicotinic Acetylcholine Receptors in the Nucleus Accumbens Core Is Necessary for the Acquisition of Drug Reinforcement." *The Journal of Neuroscience: The Official Journal of the Society for Neuroscience* 26 (22): 6004–10. doi:10.1523/JNEUROSCI.4494-05.2006.

Crippens, Donita, Dianne M. Camp, and Terry E. Robinson. 1993. "Basal Extracellular Dopamine in the Nucleus Accumbens during Amphetamine Withdrawal: A 'no Net Flux' Microdialysis Study." *Neuroscience Letters* 164 (1–2): 145–48. doi:10.1016/0304-3940(93)90878-O.

Cunha, R. A., B. Johansson, M. D. Constantino, A. M. Sebastião, and B. B. Fredholm. 1996. "Evidence for High-Affinity Binding Sites for the Adenosine A2A Receptor Agonist [3H] CGS 21680 in the Rat Hippocampus and Cerebral Cortex That Are Different from Striatal A2A Receptors." *Naunyn-Schmiedeberg's Archives of Pharmacology* 353 (3): 261–71.

Dai, M., and J. M. Tepper. 1998. "Do Silent Dopaminergic Neurons Exist in Rat Substantia Nigra in Vivo?" *Neuroscience* 85 (4): 1089–99.

Dal Toso, R., B. Sommer, M. Ewert, A. Herb, D. B. Pritchett, A. Bach, B. D. Shivers, and P. H. Seeburg. 1989. "The Dopamine D2 Receptor: Two Molecular Forms Generated by Alternative Splicing." *The EMBO Journal* 8 (13): 4025–34.

Dautan, Daniel, Icnelia Huerta-Ocampo, Ilana B. Witten, Karl Deisseroth, J. Paul Bolam, Todor Gerdjikov, and Juan Mena-Segovia. 2014. "A Major External Source of Cholinergic Innervation of the Striatum and Nucleus Accumbens Originates in the

Brainstem." *The Journal of Neuroscience: The Official Journal of the Society for Neuroscience* 34 (13): 4509–18. doi:10.1523/JNEUROSCI.5071-13.2014.
Descarries, L., K. C. Watkins, S. Garcia, O. Bosler, and G. Doucet. 1996. "Dual Character, Asynaptic and Synaptic, of the Dopamine Innervation in Adult Rat Neostriatum: A Quantitative Autoradiographic and Immunocytochemical Analysis." *The Journal of Comparative Neurology* 375 (2): 167–86. doi:10.1002/(SICI)1096-9861(19961111)375:2<167::AID-CNE1>3.0.CO;2-0.
Doucet, G, L Descarries, and S Garcia. 1986. "Quantification of the Dopamine Innervation in Adult Rat Neostriatum." *Neuroscience* 19 (2): 427–45.
Dreyer, Jakob K., Kjartan F. Herrik, Rune W. Berg, and Jørn D. Hounsgaard. 2010. "Influence of Phasic and Tonic Dopamine Release on Receptor Activation." *The Journal of Neuroscience* 30 (42): 14273–83. doi:10.1523/JNEUROSCI.1894-10.2010.
Dreyer, Jakob Kisbye, and Jørn Hounsgaard. 2013. "Mathematical Model of Dopamine Autoreceptors and Uptake Inhibitors and Their Influence on Tonic and Phasic Dopamine Signaling." *Journal of Neurophysiology* 109 (1): 171–82. doi:10.1152/jn.00502.2012.
Dubach, M., R. Schmidt, D. Kunkel, D. M. Bowden, R. Martin, and D. C. German. 1987. "Primate Neostriatal Neurons Containing Tyrosine Hydroxylase: Immunohistochemical Evidence." *Neuroscience Letters* 75 (2): 205–10.
Dubé, L., A. D. Smith, and J. P. Bolam. 1988. "Identification of Synaptic Terminals of Thalamic or Cortical Origin in Contact with Distinct Medium-Size Spiny Neurons in the Rat Neostriatum." *The Journal of Comparative Neurology* 267 (4): 455–71. doi:10.1002/cne.902670402.
Dubocovich, M. L., and N. R. Zahniser. 1985. "Binding Characteristics of the Dopamine Uptake Inhibitor [3H]nomifensine to Striatal Membranes." *Biochemical Pharmacology* 34 (8): 1137–44.
Durkin, M. M., C. A. Gunwaldsen, B. Borowsky, K. A. Jones, and T. A. Branchek. 1999. "An in Situ Hybridization Study of the Distribution of the GABA(B2) Protein mRNA in the Rat CNS." *Brain Research. Molecular Brain Research* 71 (2): 185–200.
Erikson, K. M., B. C. Jones, and J. L. Beard. 2000. "Iron Deficiency Alters Dopamine Transporter Functioning in Rat Striatum." *The Journal of Nutrition* 130 (11): 2831–37.
Eshleman, A J, R L Neve, A Janowsky, and K A Neve. 1995. "Characterization of a Recombinant Human Dopamine Transporter in Multiple Cell Lines." *The Journal of Pharmacology and Experimental Therapeutics* 274 (1): 276–83.
Euvrard, C., F. Javoy, A. Herbert, and J. Glowinski. 1977. "Effect of Quipazine, a Serotonin-like Drug, on Striatal Cholinergic Interneurones." *European Journal of Pharmacology* 41 (3): 281–89.
Everitt, Barry J., and Trevor W. Robbins. 2005. "Neural Systems of Reinforcement for Drug Addiction: From Actions to Habits to Compulsion." *Nature Neuroscience* 8 (11): 1481–89. doi:10.1038/nn1579.

Fadda, P., M. C. Martellotta, M. G. De Montis, G. L. Gessa, and W. Fratta. 1992. "Dopamine D1 and Opioid Receptor Binding Changes in the Limbic System of Sleep Deprived Rats." *Neurochemistry International* 20 Suppl (March): 153S – 156S.

Fawaz, Charbel S, Philippe Martel, Damiana Leo, and Louis-Eric Trudeau. 2009. "Presynaptic Action of Neurotensin on Dopamine Release through Inhibition of D(2) Receptor Function." *BMC Neuroscience* 10: 96. doi:10.1186/1471-2202-10-96.

Ferre, S., G. von Euler, B. Johansson, B. B. Fredholm, and K. Fuxe. 1991. "Stimulation of High-Affinity Adenosine A2 Receptors Decreases the Affinity of Dopamine D2 Receptors in Rat Striatal Membranes." *Proceedings of the National Academy of Sciences of the United States of America* 88 (16): 7238–41.

Ferris, Mark J, Erin S Calipari, Yolanda Mateo, James R Melchior, David C S Roberts, and Sara R Jones. 2012. "Cocaine Self-Administration Produces Pharmacodynamic Tolerance: Differential Effects on the Potency of Dopamine Transporter Blockers, Releasers, and Methylphenidate." *Neuropsychopharmacology: Official Publication of the American College of Neuropsychopharmacology* 37 (7): 1708–16. doi:10.1038/npp.2012.17.

Ferris, Mark J, Yolanda Mateo, David C S Roberts, and Sara R Jones. 2011. "Cocaine-Insensitive Dopamine Transporters with Intact Substrate Transport Produced by Self-Administration." *Biological Psychiatry* 69 (3): 201–7. doi:10.1016/j.biopsych.2010.06.026.

Fischer, J. F., and A. K. Cho. 1979. "Chemical Release of Dopamine from Striatal Homogenates: Evidence for an Exchange Diffusion Model." *The Journal of Pharmacology and Experimental Therapeutics* 208 (2): 203–9.

Fitoussi, A., F. Dellu-Hagedorn, and P. De Deurwaerdère. 2013. "Monoamines Tissue Content Analysis Reveals Restricted and Site-Specific Correlations in Brain Regions Involved in Cognition." *Neuroscience* 255: 233–45. doi:10.1016/j.neuroscience.2013.09.059.

Floresco, Stan B., Anthony R. West, Brian Ash, Holly Moore, and Anthony A. Grace. 2003. "Afferent Modulation of Dopamine Neuron Firing Differentially Regulates Tonic and Phasic Dopamine Transmission." *Nature Neuroscience* 6 (9): 968–73. doi:10.1038/nn1103.

Ford, C. P. 2014. "The Role of D2-Autoreceptors in Regulating Dopamine Neuron Activity and Transmission." *Neuroscience*, The Ventral Tegmentum and Dopamine: A New Wave of Diversity, 282 (December): 13–22. doi:10.1016/j.neuroscience.2014.01.025.

Fremeau, Robert T., Susan Voglmaier, Rebecca P. Seal, and Robert H. Edwards. 2004. "VGLUTs Define Subsets of Excitatory Neurons and Suggest Novel Roles for Glutamate." *Trends in Neurosciences* 27 (2): 98–103. doi:10.1016/j.tins.2003.11.005.

Fremeau, R. T., M. D. Troyer, I. Pahner, G. O. Nygaard, C. H. Tran, R. J. Reimer, E. E. Bellocchio, D. Fortin, J. Storm-Mathisen, and R. H. Edwards. 2001. "The Expression of Vesicular Glutamate Transporters Defines Two Classes of Excitatory Synapse." *Neuron* 31 (2): 247–60.

Fritschy, J. M., and H. Mohler. 1995. “GABAA-Receptor Heterogeneity in the Adult Rat Brain: Differential Regional and Cellular Distribution of Seven Major Subunits.” *The Journal of Comparative Neurology* 359 (1): 154–94. doi:10.1002/cne.903590111.

Fujiyama, Fumino, Jean-Marc Fritschy, F. Anne Stephenson, and J. Paul Bolam. 2000. “Synaptic Localization of GABAA Receptor Subunits in the Striatum of the Rat.” *The Journal of Comparative Neurology* 416 (2): 158–72. doi:10.1002/(SICI)1096-9861(20000110)416:2<158::AID-CNE3>3.0.CO;2-L.

Furay, Amy R., Ross A. McDevitt, Klaus A. Miczek, and John F. Neumaier. 2011. “5-HT1B mRNA Expression after Chronic Social Stress.” *Behavioural Brain Research* 224 (2): 350–57. doi:10.1016/j.bbr.2011.06.016.

Gao, X., and D. E. Dluzen. 2001. “Tamoxifen Abolishes Estrogen’s Neuroprotective Effect upon Methamphetamine Neurotoxicity of the Nigrostriatal Dopaminergic System.” *Neuroscience* 103 (2): 385–94.

Garreau, L., P. Emond, C. Belzung, D. Guilloteau, Y. Frangin, J. C. Besnard, and S. Chalon. 1997. “N-(3-Lodoprop-2E-Enyl)-2beta-Carbomethoxy-3beta-(3’,4’-Dichloro Phenyl)nortropane (beta-CDIT), a Tropane Derivative: Pharmacological Characterization as a Specific Ligand for the Dopamine Transporter in the Rodent Brain.” *The Journal of Pharmacology and Experimental Therapeutics* 282 (1): 467–74.

Garris, P A, and R M Wightman. 1994. “Different Kinetics Govern Dopaminergic Transmission in the Amygdala, Prefrontal Cortex, and Striatum: An in Vivo Voltammetric Study.” *The Journal of Neuroscience: The Official Journal of the Society for Neuroscience* 14 (1): 442–50.

Gauthier, J., M. Parent, M. Lévesque, and A. Parent. 1999. “The Axonal Arborization of Single Nigrostriatal Neurons in Rats.” *Brain Research* 834 (1-2): 228–32.

Gerfen, Charles R., and Charles J. Wilson. 1996. “Chapter II The Basal Ganglia.” In *Handbook of Chemical Neuroanatomy*, edited by A. BjÖrklund and T. Hökfelt L.W. Swanson, 12:371–468. Integraded Systems of the CNS, Part III Cerebellum, Basal Ganglia, Olfactory System. Elsevier. http://www.sciencedirect.com/science/article/pii/S0924819696800042.

Gether, Ulrik, Peter H. Andersen, Orla M. Larsson, and Arne Schousboe. 2006. “Neurotransmitter Transporters: Molecular Function of Important Drug Targets.” *Trends in Pharmacological Sciences* 27 (7): 375–83. doi:10.1016/j.tips.2006.05.003.

Gilbert, R. F., M. R. Hanley, and L. L. Iversen. 1979. “[3H]-Quinuclidinyl Benzilate Binding to Muscarinic Receptors in Rat Brain: Comparison of Results from Intact Brain Slices and Homogenates.” *British Journal of Pharmacology* 65 (3): 451–56.

Giros, B., P. Sokoloff, M. P. Martres, J. F. Riou, L. J. Emorine, and J. C. Schwartz. 1989. “Alternative Splicing Directs the Expression of Two D2 Dopamine Receptor Isoforms.” *Nature* 342 (6252): 923–26. doi:10.1038/342923a0.

Glick, S D, N Dong, R W Keller Jr, and J N Carlson. 1994. “Estimating Extracellular Concentrations of Dopamine and 3,4-Dihydroxyphenylacetic Acid in Nucleus Accumbens and Striatum Using Microdialysis: Relationships between in Vitro and in Vivo Recoveries.” *Journal of Neurochemistry* 62 (5): 2017–21.

Grace, Anthony A., Stan B. Floresco, Yukiori Goto, and Daniel J. Lodge. 2007. "Regulation of Firing of Dopaminergic Neurons and Control of Goal-Directed Behaviors." *Trends in Neurosciences*, Fifty years of dopamine research, 30 (5): 220–27. doi:10.1016/j.tins.2007.03.003.

Graveland, G. A., and M. Difiglia. 1985. "The Frequency and Distribution of Medium-Sized Neurons with Indented Nuclei in the Primate and Rodent Neostriatum." *Brain Research* 327 (1–2): 307–11. doi:10.1016/0006-8993(85)91524-0.

Graybiel, A. M., T. Aosaki, A. W. Flaherty, and M. Kimura. 1994. "The Basal Ganglia and Adaptive Motor Control." *Science* 265 (5180): 1826–31. doi:10.1126/science.8091209.

Guan, X. M., and W. J. McBride. 1988. "Amphetamine-Induced in Vivo Release of Dopamine in the Striatum Is Influenced by Local pH." *Life Sciences* 42 (25): 2625–31.

Gubernator, Niko G, Hui Zhang, Roland G W Staal, Eugene V Mosharov, Daniela B Pereira, Minerva Yue, Vojtech Balsanek, et al. 2009. "Fluorescent False Neurotransmitters Visualize Dopamine Release from Individual Presynaptic Terminals." *Science (New York, N.Y.)* 324 (5933): 1441–44. doi:10.1126/science.1172278.

Halimi, G., C. Devaux, O. Clot-Faybesse, J. Sampol, L. Legof, H. Rochat, and R. Guieu. 2000. "Modulation of Adenosine Concentration by Opioid Receptor Agonists in Rat Striatum." *European Journal of Pharmacology* 398 (2): 217–24.

Han, Dawn D., and Howard H. Gu. 2006. "Comparison of the Monoamine Transporters from Human and Mouse in Their Sensitivities to Psychostimulant Drugs." *BMC Pharmacology* 6: 6. doi:10.1186/1471-2210-6-6.

Harris, J. E., and R. J. Baldessarini. 1973. "Uptake of (3H)-Catecholamines by Homogenates of Rat Corpus Striatum and Cerebral Cortex: Effects of Amphetamine Analogues." *Neuropharmacology* 12 (7): 669–79.

Harrison, M. B., M. Tissot, and R. G. Wiley. 1996. "Expression of m1 and m4 Muscarinic Receptor mRNA in the Striatum Following a Selective Lesion of Striatonigral Neurons." *Brain Research* 734 (1-2): 323–26.

Härtig, W., K. Brauer, J. M. Fritschy, G. Brückner, and V. Bigl. 1995. "Regional and Cellular Expression Sites of the Alpha 1 Subunit of GABAA Receptors in the Rat Basal Forebrain: A Cytochemical Study with Glutamic Acid Decarboxylase, Choline Acetyltransferase, Calcium-Binding Proteins and Nitric Oxide Synthase as Second Markers." *Brain Research* 692 (1-2): 215–26.

Heien, M. L. a. V., and R. M. Wightman. 2006. "Phasic Dopamine Signaling during Behavior, Reward, and Disease States." *CNS & Neurological Disorders Drug Targets* 5 (1): 99–108.

Hein, Peter, and Moritz Bünemann. 2009. "Coupling Mode of Receptors and G Proteins." *Naunyn-Schmiedeberg's Archives of Pharmacology* 379 (5): 435–43. doi:10.1007/s00210-008-0383-7.

He, M, and T S Shippenberg. 2000. "Strain Differences in Basal and Cocaine-Evoked Dopamine Dynamics in Mouse Striatum." *The Journal of Pharmacology and Experimental Therapeutics* 293 (1): 121–27.

Hewett, Jeff, Peter Johanson, Nutan Sharma, David Standaert, and Aygul Balcioglu. 2010. “Function of Dopamine Transporter Is Compromised in DYT1 Transgenic Animal Model in Vivo.” *Journal of Neurochemistry* 113 (1): 228–35. doi:10.1111/j.1471-4159.2010.06590.x.

Hnasko, Thomas S., Nao Chuhma, Hui Zhang, Germaine Y. Goh, David Sulzer, Richard D. Palmiter, Stephen Rayport, and Robert H. Edwards. 2010. “Vesicular Glutamate Transport Promotes Dopamine Storage and Glutamate Corelease in Vivo.” *Neuron* 65 (5): 643–56. doi:10.1016/j.neuron.2010.02.012.

Hoffmann, Johann du, and Saleem M. Nicola. 2014. “Dopamine Invigorates Reward Seeking by Promoting Cue-Evoked Excitation in the Nucleus Accumbens.” *The Journal of Neuroscience: The Official Journal of the Society for Neuroscience* 34 (43): 14349–64. doi:10.1523/JNEUROSCI.3492-14.2014.

Hooks, M. S., P. Duffy, C. Striplin, and P. W. Kalivas. 1994. “Behavioral and Neurochemical Sensitization Following Cocaine Self-Administration.” *Psychopharmacology* 115 (1-2): 265–72.

Hooks, M S, J L Juncos, J B Justice Jr, S M Meiergerd, S L Povlock, J O Schenk, and P W Kalivas. 1994. “Individual Locomotor Response to Novelty Predicts Selective Alterations in D1 and D2 Receptors and mRNAs.” *The Journal of Neuroscience: The Official Journal of the Society for Neuroscience* 14 (10): 6144–52.

Horn, A. S. 1990. “Dopamine Uptake: A Review of Progress in the Last Decade.” *Progress in Neurobiology* 34 (5): 387–400.

Humphries, Mark D., Ric Wood, and Kevin Gurney. 2010. “Reconstructing the Three-Dimensional GABAergic Microcircuit of the Striatum.” *PLoS Computational Biology* 6 (11): e1001011. doi:10.1371/journal.pcbi.1001011.

Hyttel, J. 1987. “Age Related Decrease in the Density of Dopamine D1 and D2 Receptors in Corpus Striatum of Rats.” *Pharmacology & Toxicology* 61 (2): 126–29.

Ibáñez-Sandoval, Osvaldo, Fatuel Tecuapetla, Bengi Unal, Fulva Shah, Tibor Koós, and James M. Tepper. 2010. “Electrophysiological and Morphological Characteristics and Synaptic Connectivity of Tyrosine Hydroxylase-Expressing Neurons in Adult Mouse Striatum.” *The Journal of Neuroscience: The Official Journal of the Society for Neuroscience* 30 (20): 6999–7016. doi:10.1523/JNEUROSCI.5996-09.2010.

Inada, T., K. Polk, C. Jin, C. Purser, A. Hume, B. Hoskins, I. K. Ho, and R. W. Rockhold. 1992. “Cocaine Elevates Striatal Dopamine Efflux in Spontaneously Hypertensive and Wistar-Kyoto Rats.” *Brain Research Bulletin* 28 (2): 227–31.

Inada, T., K. Polk, C. Purser, A. Hume, B. Hoskins, I. K. Ho, and R. W. Rockhold. 1992. “Behavioral and Neurochemical Effects of Continuous Infusion of Cocaine in Rats.” *Neuropharmacology* 31 (7): 701–8.

Itokawa, M., Z. Lin, N. S. Cai, C. Wu, S. Kitayama, J. B. Wang, and G. R. Uhl. 2000. “Dopamine Transporter Transmembrane Domain Polar Mutants: DeltaG and DeltaDeltaG Values Implicate Regions Important for Transporter Functions.” *Molecular Pharmacology* 57 (6): 1093–1103.

Ito, Rutsuko, Trevor W Robbins, and Barry J Everitt. 2004. “Differential Control over Cocaine-Seeking Behavior by Nucleus Accumbens Core and Shell.” *Nature Neuroscience* 7 (4): 389–97. doi:10.1038/nn1217.

Janowsky, A., P. Berger, F. Vocci, R. Labarca, P. Skolnick, and S. M. Paul. 1986. "Characterization of Sodium-Dependent [3H]GBR-12935 Binding in Brain: A Radioligand for Selective Labelling of the Dopamine Transport Complex." *Journal of Neurochemistry* 46 (4): 1272–76.

Jones, I. W., J. P. Bolam, and S. Wonnacott. 2001. "Presynaptic Localisation of the Nicotinic Acetylcholine Receptor beta2 Subunit Immunoreactivity in Rat Nigrostriatal Dopaminergic Neurones." *The Journal of Comparative Neurology* 439 (2): 235–47.

Jones, S R, R R Gainetdinov, R M Wightman, and M G Caron. 1998. "Mechanisms of Amphetamine Action Revealed in Mice Lacking the Dopamine Transporter." *The Journal of Neuroscience: The Official Journal of the Society for Neuroscience* 18 (6): 1979–86.

Jones, S R, J D Joseph, L S Barak, M G Caron, and R M Wightman. 1999. "Dopamine Neuronal Transport Kinetics and Effects of Amphetamine." *Journal of Neurochemistry* 73 (6): 2406–14.

Kaddis, F. G., N. J. Uretsky, and L. J. Wallace. 1995. "DNQX in the Nucleus Accumbens Inhibits Cocaine-Induced Conditioned Place Preference." *Brain Research* 697 (1-2): 76–82.

Käenmäki, Mikko, Anne Tammimäki, Timo Myöhänen, Kaisa Pakarinen, Carolina Amberg, Maria Karayiorgou, Joseph A. Gogos, and Pekka T. Männistö. 2010. "Quantitative Role of COMT in Dopamine Clearance in the Prefrontal Cortex of Freely Moving Mice." *Journal of Neurochemistry* 114 (6): 1745–55. doi:10.1111/j.1471-4159.2010.06889.x.

Kalivas, P. W., and P. Duffy. 1993. "Time Course of Extracellular Dopamine and Behavioral Sensitization to Cocaine. I. Dopamine Axon Terminals." *The Journal of Neuroscience: The Official Journal of the Society for Neuroscience* 13 (1): 266–75.

Katona, István, and Tamás F. Freund. 2012. "Multiple Functions of Endocannabinoid Signaling in the Brain." *Annual Review of Neuroscience* 35: 529–58. doi:10.1146/annurev-neuro-062111-150420.

Kawaguchi, Y. 1993. "Physiological, Morphological, and Histochemical Characterization of Three Classes of Interneurons in Rat Neostriatum." *The Journal of Neuroscience* 13 (11): 4908–23.

Kennedy, R. T., S. R. Jones, and R. M. Wightman. 1992. "Dynamic Observation of Dopamine Autoreceptor Effects in Rat Striatal Slices." *Journal of Neurochemistry* 59 (2): 449–55.

Kerr, Rex A, Thomas M Bartol, Boris Kaminsky, Markus Dittrich, Jen-Chien Jack Chang, Scott B Baden, Terrence J Sejnowski, and Joel R Stiles. 2008. "Fast Monte Carlo Simulation Methods for Biological Reaction-Diffusion Systems in Solution and On Surfaces." *SIAM Journal on Scientific Computing: A Publication of the Society for Industrial and Applied Mathematics* 30 (6): 3126. doi:10.1137/070692017.

Kincaid, A. E., T. Zheng, and C. J. Wilson. 1998. "Connectivity and Convergence of Single Corticostriatal Axons." *The Journal of Neuroscience: The Official Journal of the Society for Neuroscience* 18 (12): 4722–31.

Kita, H., T. Kosaka, and C. W. Heizmann. 1990. “Parvalbumin-Immunoreactive Neurons in the Rat Neostriatum: A Light and Electron Microscopic Study.” *Brain Research* 536 (1–2): 1–15. doi:10.1016/0006-8993(90)90002-S.

Kitayama, S, S Shimada, H Xu, L Markham, D M Donovan, and G R Uhl. 1992. “Dopamine Transporter Site-Directed Mutations Differentially Alter Substrate Transport and Cocaine Binding.” *Proceedings of the National Academy of Sciences of the United States of America* 89 (16): 7782–85.

Koeltzow, T E, M Xu, D C Cooper, X T Hu, S Tonegawa, M E Wolf, and F J White. 1998. “Alterations in Dopamine Release but Not Dopamine Autoreceptor Function in Dopamine D3 Receptor Mutant Mice.” *The Journal of Neuroscience: The Official Journal of the Society for Neuroscience* 18 (6): 2231–38.

Koob, G. F., and F. E. Bloom. 1988. “Cellular and Molecular Mechanisms of Drug Dependence.” *Science (New York, N.Y.)* 242 (4879): 715–23.

Kress, Geraldine J., Hong-Jin Shu, Andrew Yu, Amanda Taylor, Ann Benz, Steve Harmon, and Steven Mennerick. 2014. “Fast Phasic Release Properties of Dopamine Studied with a Channel Biosensor.” *The Journal of Neuroscience* 34 (35): 11792–802. doi:10.1523/JNEUROSCI.2355-14.2014.

Kuhar, M. J., M. C. Ritz, and J. W. Boja. 1991. “The Dopamine Hypothesis of the Reinforcing Properties of Cocaine.” *Trends in Neurosciences* 14 (7): 299–302.

Kulagina, N. V., M. J. Zigmond, and A. C. Michael. 2001. “Glutamate Regulates the Spontaneous and Evoked Release of Dopamine in the Rat Striatum.” *Neuroscience* 102 (1): 121–28.

Kürschner, V. C., R. L. Petruzzi, G. T. Golden, W. H. Berrettini, and T. N. Ferraro. 1998. “Kainate and AMPA Receptor Binding in Seizure-Prone and Seizure-Resistant Inbred Mouse Strains.” *Brain Research* 780 (1): 1–8.

Kustova, Y., M. G. Espey, Y. Sei, and A. S. Basile. 1997. “Regional Decreases [corrected] in AMPA Receptor Density in Mice Infected with the LP-BM5 Murine Leukemia Virus.” *Neuroreport* 8 (5): 1243–47.

Kwok, K. H., Y. C. Tse, R. N. Wong, and K. K. Yung. 1997. “Cellular Localization of GluR1, GluR2/3 and GluR4 Glutamate Receptor Subunits in Neurons of the Rat Neostriatum.” *Brain Research* 778 (1): 43–55.

Lacey, C. J., J. Boyes, O. Gerlach, L. Chen, P. J. Magill, and J. P. Bolam. 2005. “GABAB Receptors at Glutamatergic Synapses in the Rat Striatum.” *Neuroscience* 136 (4): 1083–95. doi:10.1016/j.neuroscience.2005.07.013.

Land, B. R., W. V. Harris, E. E. Salpeter, and M. M. Salpeter. 1984. “Diffusion and Binding Constants for Acetylcholine Derived from the Falling Phase of Miniature Endplate Currents.” *Proceedings of the National Academy of Sciences* 81 (5): 1594–98.

Lapchak, P. A., D. M. Araujo, R. Quirion, and B. Collier. 1989a. “Effect of Chronic Nicotine Treatment on Nicotinic Autoreceptor Function and N-[3H]methylcarbamylcholine Binding Sites in the Rat Brain.” *Journal of Neurochemistry* 52 (2): 483–91.

Lapchak, P. A., D. M. Araujo, R. Quirion, and B. Collier. 1989b. “Binding Sites for [3H]AF-DX 116 and Effect of AF-DX 116 on Endogenous Acetylcholine Release from Rat Brain Slices.” *Brain Research* 496 (1-2): 285–94.

Lee, F. J., Z. B. Pristupa, B. J. Ciliax, A. I. Levey, and H. B. Niznik. 1996. "The Dopamine Transporter Carboxyl-Terminal Tail. Truncation/substitution Mutants Selectively Confer High Affinity Dopamine Uptake While Attenuating Recognition of the Ligand Binding Domain." *The Journal of Biological Chemistry* 271 (34): 20885–94.

Lin, Zhicheng, and George R. Uhl. 2002. "Dopamine Transporter Mutants with Cocaine Resistance and Normal Dopamine Uptake Provide Targets for Cocaine Antagonism." *Molecular Pharmacology* 61 (4): 885–91.

Lin, Zhicheng, and George R. Uhl. 2005. "Proline Mutations Induce Negative-Dosage Effects on Uptake Velocity of the Dopamine Transporter." *Journal of Neurochemistry* 94 (1): 276–87. doi:10.1111/j.1471-4159.2005.03196.x.

Liste, Isabel, Véronique Bernard, and Bertrand Bloch. 2002. "Acute and Chronic Acetylcholinesterase Inhibition Regulates in Vivo the Localization and Abundance of Muscarinic Receptors m2 and m4 at the Cell Surface and in the Cytoplasm of Striatal Neurons." *Molecular and Cellular Neurosciences* 20 (2): 244–56.

Livingstone, Phil D., Jayaraman Srinivasan, James N.C. Kew, Lee A. Dawson, Cecilia Gotti, Milena Moretti, Mohammed Shoaib, and Susan Wonnacott. 2009. "α7 and Non-α7 Nicotinic Acetylcholine Receptors Modulate Dopamine Release in Vitro and in Vivo in the Rat Prefrontal Cortex." *European Journal of Neuroscience* 29 (3): 539–50. doi:10.1111/j.1460-9568.2009.06613.x.

Lobo, Mary Kay. 2009. "Molecular Profiling of Striatonigral and Striatopallidal Medium Spiny Neurons Past, Present, and Future." *International Review of Neurobiology* 89: 1–35. doi:10.1016/S0074-7742(09)89001-6.

Loland, C. J., L. Norregaard, and U. Gether. 1999. "Defining Proximity Relationships in the Tertiary Structure of the Dopamine Transporter. Identification of a Conserved Glutamic Acid as a Third Coordinate in the Endogenous Zn(2+)-Binding Site." *The Journal of Biological Chemistry* 274 (52): 36928–34.

Loland, Claus Juul, Lene Norregaard, Thomas Litman, and Ulrik Gether. 2002. "Generation of an Activating Zn(2+) Switch in the Dopamine Transporter: Mutation of an Intracellular Tyrosine Constitutively Alters the Conformational Equilibrium of the Transport Cycle." *Proceedings of the National Academy of Sciences of the United States of America* 99 (3): 1683–88. doi:10.1073/pnas.032386299.

Luk, K. C, and A. F Sadikot. 2001. "GABA Promotes Survival but Not Proliferation of Parvalbumin-Immunoreactive Interneurons in Rodent Neostriatum: An in Vivo Study with Stereology." *Neuroscience* 104 (1): 93–103. doi:10.1016/S0306-4522(01)00038-0.

Mackey, W. B., and D. van der Kooy. 1985. "Neuroleptics Block the Positive Reinforcing Effects of Amphetamine but Not of Morphine as Measured by Place Conditioning." *Pharmacology, Biochemistry, and Behavior* 22 (1): 101–5.

Maher, C. E., D. E. Selley, and S. R. Childers. 2000. "Relationship of Mu Opioid Receptor Binding to Activation of G-Proteins in Specific Rat Brain Regions." *Biochemical Pharmacology* 59 (11): 1395–1401.

Maisonneuve, I. M., and M. J. Kreek. 1994. “Acute Tolerance to the Dopamine Response Induced by a Binge Pattern of Cocaine Administration in Male Rats: An in Vivo Microdialysis Study.” *The Journal of Pharmacology and Experimental Therapeutics* 268 (2): 916–21.

Maldonado, R., P. Robledo, A. J. Chover, S. B. Caine, and G. F. Koob. 1993. “D1 Dopamine Receptors in the Nucleus Accumbens Modulate Cocaine Self-Administration in the Rat.” *Pharmacology, Biochemistry, and Behavior* 45 (1): 239–42.

Mallet, Nicolas, Benjamin R. Micklem, Pablo Henny, Matthew T. Brown, Claire Williams, J. Paul Bolam, Kouichi C. Nakamura, and Peter J. Magill. 2012. “Dichotomous Organization of the External Globus Pallidus.” *Neuron* 74 (6): 1075–86. doi:10.1016/j.neuron.2012.04.027.

Mao, L., Y. S. Lau, E. Petroske, and J. Q. Wang. 2001. “Profound Astrogenesis in the Striatum of Adult Mice Following Nigrostriatal Dopaminergic Lesion by Repeated MPTP Administration.” *Brain Research. Developmental Brain Research* 131 (1-2): 57–65.

Marcott, Pamela F., Aphroditi A. Mamaligas, and Christopher P. Ford. 2014. “Phasic Dopamine Release Drives Rapid Activation of Striatal D2-Receptors.” *Neuron* 84 (1): 164–76. doi:10.1016/j.neuron.2014.08.058.

Marshall, J. F, S. J O’Dell, R. Navarrete, and A. J Rosenstein. 1990. “Dopamine High-Affinity Transport Site Topography in Rat Brain: Major Differences between Dorsal and Ventral Striatum.” *Neuroscience* 37 (1): 11–21.

Martin-Fardon, R., F. Sandillon, J. Thibault, A. Privat, and J. Vignon. 1997. “Long-Term Monitoring of Extracellular Dopamine Concentration in the Rat Striatum by a Repeated Microdialysis Procedure.” *Journal of Neuroscience Methods* 72 (2): 123–35.

Mateo, Yolanda, Evgeny A Budygin, Carrie E John, Matthew L Banks, and Sara R Jones. 2004. “Voltammetric Assessment of Dopamine Clearance in the Absence of the Dopamine Transporter: No Contribution of Other Transporters in Core or Shell of Nucleus Accumbens.” *Journal of Neuroscience Methods* 140 (1-2): 183–87. doi:10.1016/j.jneumeth.2004.05.018.

Matsuda, Wakoto, Takahiro Furuta, Kouichi C. Nakamura, Hiroyuki Hioki, Fumino Fujiyama, Ryohachi Arai, and Takeshi Kaneko. 2009. “Single Nigrostriatal Dopaminergic Neurons Form Widely Spread and Highly Dense Axonal Arborizations in the Neostriatum.” *The Journal of Neuroscience: The Official Journal of the Society for Neuroscience* 29 (2): 444–53. doi:10.1523/JNEUROSCI.4029-08.2009.

May, L J, and R M Wightman. 1989. “Effects of D-2 Antagonists on Frequency-Dependent Stimulated Dopamine Overflow in Nucleus Accumbens and Caudate-Putamen.” *Journal of Neurochemistry* 53 (3): 898–906.

McGeorge, A. J., and R. L. M. Faull. 1989. “The Organization of the Projection from the Cerebral Cortex to the Striatum in the Rat.” *Neuroscience* 29 (3): 503–37. doi:10.1016/0306-4522(89)90128-0.

McGregor, A., and D. C. Roberts. 1993. “Dopaminergic Antagonism within the Nucleus Accumbens or the Amygdala Produces Differential Effects on Intravenous

Cocaine Self-Administration under Fixed and Progressive Ratio Schedules of Reinforcement." *Brain Research* 624 (1-2): 245–52.
Melikian, Haley E. 2004. "Neurotransmitter Transporter Trafficking: Endocytosis, Recycling, and Regulation." *Pharmacology & Therapeutics* 104 (1): 17–27. doi:10.1016/j.pharmthera.2004.07.006.
Mendes de Freitas, Rivelilson, Lissiana M. V. Aguiar, Silvânia M. M. Vasconcelos, Francisca C. F. Sousa, Glauce S. B. Viana, and Marta M. F. Fonteles. 2005. "Modifications in Muscarinic, Dopaminergic and Serotonergic Receptors Concentrations in the Hippocampus and Striatum of Epileptic Rats." *Life Sciences* 78 (3): 253–58. doi:10.1016/j.lfs.2005.04.045.
Mennicken, F., M. Savasta, R. Peretti-Renucci, and C. Feuerstein. 1992. "Autoradiographic Localization of Dopamine Uptake Sites in the Rat Brain with 3H-GBR 12935." *Journal of Neural Transmission. General Section* 87 (1): 1–14.
Meredith, G. E., R. Agolia, M. P. Arts, H. J. Groenewegen, and D. S. Zahm. 1992. "Morphological Differences between Projection Neurons of the Core and Shell in the Nucleus Accumbens of the Rat." *Neuroscience* 50 (1): 149–62.
Meredith, G. E., T. Farrell, P. Kellaghan, Y. Tan, D. S. Zahm, and S. Totterdell. 1999. "Immunocytochemical Characterization of Catecholaminergic Neurons in the Rat Striatum Following Dopamine-Depleting Lesions." *The European Journal of Neuroscience* 11 (10): 3585–96.
Miller, H. H., P. A. Shore, and D. E. Clarke. 1980. "In Vivo Monoamine Oxidase Inhibition by D-Amphetamine." *Biochemical Pharmacology* 29 (10): 1347–54.
Mithani, S., M. T. Martin-Iverson, A. G. Phillips, and H. C. Fibiger. 1986. "The Effects of Haloperidol on Amphetamine- and Methylphenidate-Induced Conditioned Place Preferences and Locomotor Activity." *Psychopharmacology* 90 (2): 247–52.
Moll, G. H., C. Mehnert, M. Wicker, N. Bock, A. Rothenberger, E. Rüther, and G. Huether. 2000. "Age-Associated Changes in the Densities of Presynaptic Monoamine Transporters in Different Regions of the Rat Brain from Early Juvenile Life to Late Adulthood." *Brain Research. Developmental Brain Research* 119 (2): 251–57.
Monsma, F. J., L. D. McVittie, C. R. Gerfen, L. C. Mahan, and D. R. Sibley. 1989. "Multiple D2 Dopamine Receptors Produced by Alternative RNA Splicing." *Nature* 342 (6252): 926–29. doi:10.1038/342926a0.
Mortensen, Ole V., and Susan G. Amara. 2003. "Dynamic Regulation of the Dopamine Transporter." *European Journal of Pharmacology* 479 (1-3): 159–70.
Murrin, L. C., and W. Zeng. 1986. "Postnatal Ontogeny of Dopamine D2 Receptors in Rat Striatum." *Biochemical Pharmacology* 35 (7): 1159–62.
Nakayama, M., T. Koyama, and I. Yamashita. 1993. "Long-Lasting Decrease in Dopamine Uptake Sites Following Repeated Administration of Methamphetamine in the Rat Striatum." *Brain Research* 601 (1-2): 209–12.
Narayanan, Sanju, Christophe Mesangeau, Jacques H Poupaert, and Christopher R McCurdy. 2011. "Sigma Receptors and Cocaine Abuse." *Current Topics In Medicinal Chemistry* 11 (9): 1128–50.

Near, J. A., J. C. Bigelow, and R. M. Wightman. 1988. “Comparison of Uptake of Dopamine in Rat Striatal Chopped Tissue and Synaptosomes.” *The Journal of Pharmacology and Experimental Therapeutics* 245 (3): 921–27.

Ng, Tony K.Y., and Ken K.L. Yung. 2001. “Differential Expression of GABABR1 and GABABR2 Receptor Immunoreactivity in Neurochemically Identified Neurons of the Rat Neostriatum.” *The Journal of Comparative Neurology* 433 (4): 458–70. doi:10.1002/cne.1153.

Nicolaysen, Lance C., Hwai-Tzong Pan, and Joseph B. Justice Jr. 1988. “Extracellular Cocaine and Dopamine Concentrations Are Linearly Related in Rat Striatum.” *Brain Research* 456 (2): 317–23. doi:10.1016/0006-8993(88)90234-X.

Nonaka, R., and T. Moroji. 1984. “Quantitative Autoradiography of Muscarinic Cholinergic Receptors in the Rat Brain.” *Brain Research* 296 (2): 295–303.

Oorschot, Dorothy E. 1996. “Total Number of Neurons in the Neostriatal, Pallidal, Subthalamic, and Substantia Nigral Nuclei of the Rat Basal Ganglia: A Stereological Study Using the Cavalieri and Optical Disector Methods.” *The Journal of Comparative Neurology* 366 (4): 580–99. doi:10.1002/(SICI)1096-9861(19960318)366:4<580::AID-CNE3>3.0.CO;2-0.

Oude Ophuis, Ralph J. A., Arjen J. Boender, Andrea J. van Rozen, and Roger A. H. Adan. 2014. “Cannabinoid, Melanocortin and Opioid Receptor Expression on DRD1 and DRD2 Subpopulations in Rat Striatum.” *Frontiers in Neuroanatomy* 8: 14. doi:10.3389/fnana.2014.00014.

Owesson-White, Catarina A, Mitchell F Roitman, Leslie A Sombers, Anna M Belle, Richard B Keithley, Jessica L Peele, Regina M Carelli, and R Mark Wightman. 2012. “Sources Contributing to the Average Extracellular Concentration of Dopamine in the Nucleus Accumbens.” *Journal Of Neurochemistry* 121 (2): 252–62. doi:10.1111/j.1471-4159.2012.07677.x.

Parsons, L. H., and J. B. Justice. 1992. “Extracellular Concentration and in Vivo Recovery of Dopamine in the Nucleus Accumbens Using Microdialysis.” *Journal of Neurochemistry* 58 (1): 212–18.

Parsons, L H, A D Smith, and J B Justice Jr. 1991a. “Basal Extracellular Dopamine Is Decreased in the Rat Nucleus Accumbens during Abstinence from Chronic Cocaine.” *Synapse (New York, N.Y.)* 9 (1): 60–65. doi:10.1002/syn.890090109.

Parsons, L H, A D Smith, and J B Justice Jr. 1991b. “The in Vivo Microdialysis Recovery of Dopamine Is Altered Independently of Basal Level by 6-Hydroxydopamine Lesions to the Nucleus Accumbens.” *Journal of Neuroscience Methods* 40 (2-3): 139–47.

Patyal, Robin, Evan Y Woo, and Stephanie L Borgland. 2012. “Local Hypocretin-1 Modulates Terminal Dopamine Concentration in the Nucleus Accumbens Shell.” *Frontiers in Behavioral Neuroscience* 6: 82. doi:10.3389/fnbeh.2012.00082.

Peña, Ike Dela, Ruzanna Gevorkiana, and Wei-Xing Shi. 2015. “Psychostimulants Affect Dopamine Transmission through Both Dopamine Transporter-Dependent and Independent Mechanisms.” *European Journal of Pharmacology* 764 (July): 562–70. doi:10.1016/j.ejphar.2015.07.044.

Perez, Xiomara A., Tanuja Bordia, J. Michael McIntosh, and Maryka Quik. 2010. “α6ß2* and α4ß2* Nicotinic Receptors Both Regulate Dopamine Signaling with

Increased Nigrostriatal Damage: Relevance to Parkinson's Disease." *Molecular Pharmacology* 78 (5): 971–80. doi:10.1124/mol.110.067561.
Petroske, E., G. E. Meredith, S. Callen, S. Totterdell, and Y. S. Lau. 2001. "Mouse Model of Parkinsonism: A Comparison between Subacute MPTP and Chronic MPTP/probenecid Treatment." *Neuroscience* 106 (3): 589–601.
Phillipson, O. T., and A. C. Griffiths. 1985. "The Topographic Order of Inputs to Nucleus Accumbens in the Rat." *Neuroscience* 16 (2): 275–96.
Pierce, R. Christopher, and Vidhya Kumaresan. 2006. "The Mesolimbic Dopamine System: The Final Common Pathway for the Reinforcing Effect of Drugs of Abuse?" *Neuroscience and Biobehavioral Reviews* 30 (2): 215–38. doi:10.1016/j.neubiorev.2005.04.016.
Pierce, R. Christopher, and Louk J. M. J. Vanderschuren. 2010. "Kicking the Habit: The Neural Basis of Ingrained Behaviors in Cocaine Addiction." *Neuroscience and Biobehavioral Reviews* 35 (2): 212–19. doi:10.1016/j.neubiorev.2010.01.007.
Pisani, Valerio, Graziella Madeo, Annalisa Tassone, Giuseppe Sciamanna, Mauro Maccarrone, Paolo Stanzione, and Antonio Pisani. 2011. "Homeostatic Changes of the Endocannabinoid System in Parkinson's Disease." *Movement Disorders: Official Journal of the Movement Disorder Society* 26 (2): 216–22. doi:10.1002/mds.23457.
Pissadaki, Eleftheria K., and J. Paul Bolam. 2013. "The Energy Cost of Action Potential Propagation in Dopamine Neurons: Clues to Susceptibility in Parkinson's Disease." *Frontiers in Computational Neuroscience* 7: 13. doi:10.3389/fncom.2013.00013.
Ponzio, F., G. Achilli, G. Calderini, P. Ferretti, C. Perego, G. Toffano, and S. Algeri. 1984. "Depletion and Recovery of Neuronal Monoamine Storage in Rats of Different Ages Treated with Reserpine." *Neurobiology of Aging* 5 (2): 101–4.
Porritt, M. J., P. E. Batchelor, A. J. Hughes, R. Kalnins, G. A. Donnan, and D. W. Howells. 2000. "New Dopaminergic Neurons in Parkinson's Disease Striatum." *Lancet* 356 (9223): 44–45. doi:10.1016/S0140-6736(00)02437-5.
Prensa, L, and A Parent. 2001. "The Nigrostriatal Pathway in the Rat: A Single-Axon Study of the Relationship between Dorsal and Ventral Tier Nigral Neurons and the Striosome/matrix Striatal Compartments." *The Journal of Neuroscience: The Official Journal of the Society for Neuroscience* 21 (18): 7247–60.
Qin, Kou, Chunmin Dong, Guangyu Wu, and Nevin A. Lambert. 2011. "Inactive-State Preassembly of G(q)-Coupled Receptors and G(q) Heterotrimers." *Nature Chemical Biology* 7 (10): 740–47. doi:10.1038/nchembio.642.
Reith, M. E., M. Benuck, and A. Lajtha. 1987. "Cocaine Disposition in the Brain after Continuous or Intermittent Treatment and Locomotor Stimulation in Mice." *The Journal of Pharmacology and Experimental Therapeutics* 243 (1): 281–87.
Rice, Margaret E., and Stephanie J. Cragg. 2008. "Dopamine Spillover after Quantal Release: Rethinking Dopamine Transmission in the Nigrostriatal Pathway." *Brain Research Reviews* 58 (2): 303–13. doi:10.1016/j.brainresrev.2008.02.004.
Richfield, E. K., J. B. Penney, and A. B. Young. 1989. "Anatomical and Affinity State Comparisons between Dopamine D1 and D2 Receptors in the Rat Central Nervous System." *Neuroscience* 30 (3): 767–77.

Robson, Matthew J, Bahar Noorbakhsh, Michael J Seminerio, and Rae R Matsumoto. 2012. “Sigma-1 Receptors: Potential Targets for the Treatment of Substance Abuse.” *Current Pharmaceutical Design* 18 (7): 902–19.

Rocha, B. A., F. Fumagalli, R. R. Gainetdinov, S. R. Jones, R. Ator, B. Giros, G. W. Miller, and M. G. Caron. 1998. “Cocaine Self-Administration in Dopamine-Transporter Knockout Mice.” *Nature Neuroscience* 1 (2): 132–37. doi:10.1038/381.

Romero, J., L. García, J. J. Fernández-Ruiz, M. Cebeira, and J. A. Ramos. 1995. “Changes in Rat Brain Cannabinoid Binding Sites after Acute or Chronic Exposure to Their Endogenous Agonist, Anandamide, or to Delta 9-Tetrahydrocannabinol.” *Pharmacology, Biochemistry, and Behavior* 51 (4): 731–37.

Rossetti, Z. L., P. S. D’Aquila, Y. Hmaidan, G. L. Gessa, and G. Serra. 1991. “Repeated Treatment with Imipramine Potentiates Cocaine-Induced Dopamine Release and Motor Stimulation.” *European Journal of Pharmacology* 201 (2-3): 243–45.

Rothman, R. B., M. H. Baumann, C. M. Dersch, D. V. Romero, K. C. Rice, F. I. Carroll, and J. S. Partilla. 2001. “Amphetamine-Type Central Nervous System Stimulants Release Norepinephrine More Potently than They Release Dopamine and Serotonin.” *Synapse (New York, N.Y.)* 39 (1): 32–41. doi:10.1002/1098-2396(20010101)39:1<32::AID-SYN5>3.0.CO;2-3.

Rothman, R. B., J. L. Cadet, H. C. Akunne, M. L. Silverthorn, M. H. Baumann, F. I. Carroll, K. C. Rice, B. R. de Costa, J. S. Partilla, and J. B. Wang. 1994. “Studies of the Biogenic Amine Transporters. IV. Demonstration of a Multiplicity of Binding Sites in Rat Caudate Membranes for the Cocaine Analog [125I]RTI-55.” *The Journal of Pharmacology and Experimental Therapeutics* 270 (1): 296–309.

Rymar, Vladimir V., Rachel Sasseville, Kelvin C. Luk, and Abbas F. Sadikot. 2004. “Neurogenesis and Stereological Morphometry of Calretinin-Immunoreactive GABAergic Interneurons of the Neostriatum.” *The Journal of Comparative Neurology* 469 (3): 325–39. doi:10.1002/cne.11008.

Samanin, R., T. Mennini, A. Ferraris, C. Bendotti, and F. Borsini. 1980. “Hyper- and Hyposensitivity of Central Serotonin receptors:[3H]serotonin Binding and Functional Studies in the Rat.” *Brain Research* 189 (2): 449–57.

Sam, P. M., and J. B. Justice. 1996. “Effect of General Microdialysis-Induced Depletion on Extracellular Dopamine.” *Analytical Chemistry* 68 (5): 724–28.

Savica, Rodolfo, and Eduardo E. Benarroch. 2014. “Dopamine Receptor Signaling in the Forebrain Recent Insights and Clinical Implications.” *Neurology* 83 (8): 758–67. doi:10.1212/WNL.0000000000000719.

Schmitz, Y, C J Lee, C Schmauss, F Gonon, and D Sulzer. 2001. “Amphetamine Distorts Stimulation-Dependent Dopamine Overflow: Effects on D2 Autoreceptors, Transporters, and Synaptic Vesicle Stores.” *The Journal of Neuroscience: The Official Journal of the Society for Neuroscience* 21 (16): 5916–24.

Schmitz, Yvonne, Marianne Benoit-Marand, Fran&ccedil Gonon, ois, and David Sulzer. 2003. “Presynaptic Regulation of Dopaminergic Neurotransmission.” *Journal of Neurochemistry* 87 (2): 273–89.

Schönfuss, D., T. Reum, P. Olshausen, T. Fischer, and R. Morgenstern. 2001. "Modelling Constant Potential Amperometry for Investigations of Dopaminergic Neurotransmission Kinetics in Vivo." *Journal of Neuroscience Methods* 112 (2): 163–72.

Schultz, Wolfram. 2002. "Getting Formal with Dopamine and Reward." *Neuron* 36 (2): 241–63.

Schwartz, J. C., J. Diaz, R. Bordet, N. Griffon, S. Perachon, C. Pilon, S. Ridray, and P. Sokoloff. 1998. "Functional Implications of Multiple Dopamine Receptor Subtypes: The D1/D3 Receptor Coexistence." *Brain Research. Brain Research Reviews* 26 (2-3): 236–42.

Schwartz, R. D., J. Lehmann, and K. J. Kellar. 1984. "Presynaptic Nicotinic Cholinergic Receptors Labeled by [3H]acetylcholine on Catecholamine and Serotonin Axons in Brain." *Journal of Neurochemistry* 42 (5): 1495–98.

Sesack, S. R., A. Y. Deutch, R. H. Roth, and B. S. Bunney. 1989. "Topographical Organization of the Efferent Projections of the Medial Prefrontal Cortex in the Rat: An Anterograde Tract-Tracing Study with Phaseolus Vulgaris Leucoagglutinin." *The Journal of Comparative Neurology* 290 (2): 213–42. doi:10.1002/cne.902900205.

Sharp, T., T. Zetterström, and U. Ungerstedt. 1986. "An in Vivo Study of Dopamine Release and Metabolism in Rat Brain Regions Using Intracerebral Dialysis." *Journal of Neurochemistry* 47 (1): 113–22.

Shen, Haowei, Susan R. Sesack, Shigenobu Toda, and Peter W. Kalivas. 2008. "Automated Quantification of Dendritic Spine Density and Spine Head Diameter in Medium Spiny Neurons of the Nucleus Accumbens." *Brain Structure and Function* 213 (1-2): 149–57. doi:10.1007/s00429-008-0184-2.

Siciliano, Cody A, Erin S Calipari, Mark J Ferris, and Sara R Jones. 2014. "Biphasic Mechanisms of Amphetamine Action at the Dopamine Terminal." *The Journal of Neuroscience: The Official Journal of the Society for Neuroscience* 34 (16): 5575–82. doi:10.1523/JNEUROSCI.4050-13.2014.

Silberberg, Gilad, and J. Paul Bolam. 2015. "Local and Afferent Synaptic Pathways in the Striatal Microcircuitry." *Current Opinion in Neurobiology* 33 (August): 182–87. doi:10.1016/j.conb.2015.05.002.

Skinbjerg, Mette, David R. Sibley, Jonathan A. Javitch, and Anissa Abi-Dargham. 2012. "Imaging the High-Affinity State of the Dopamine D2 Receptor in Vivo: Fact or Fiction?" *Biochemical Pharmacology* 83 (2): 193–98. doi:10.1016/j.bcp.2011.09.008.

Smith, A D, R J Olson, and J B Justice Jr. 1992. "Quantitative Microdialysis of Dopamine in the Striatum: Effect of Circadian Variation." *Journal of Neuroscience Methods* 44 (1): 33–41.

Smith, A D, and F Weiss. 1999. "Ethanol Exposure Differentially Alters Central Monoamine Neurotransmission in Alcohol-Preferring versus -Nonpreferring Rats." *The Journal of Pharmacology and Experimental Therapeutics* 288 (3): 1223–28.

Smith, Yoland, and André Parent. 1986. "Neuropeptide Y-Immunoreactive Neurons in the Striatum of Cat and Monkey: Morphological Characteristics, Intrinsic

Organization and Co-Localization with Somatostatin." *Brain Research* 372 (2): 241–52. doi:10.1016/0006-8993(86)91131-5.
Snyder, G. L., P. B. Allen, A. A. Fienberg, C. G. Valle, R. L. Huganir, A. C. Nairn, and P. Greengard. 2000. "Regulation of Phosphorylation of the GluR1 AMPA Receptor in the Neostriatum by Dopamine and Psychostimulants in Vivo." *The Journal of Neuroscience: The Official Journal of the Society for Neuroscience* 20 (12): 4480–88.
Snyder, S. H., and J. T. Coyle. 1969. "Regional Differences in H3-Norepinephrine and H3-Dopamine Uptake into Rat Brain Homogenates." *The Journal of Pharmacology and Experimental Therapeutics* 165 (1): 78–86.
Soghomonian, J. J., L. Descarries, and K. C. Watkins. 1989. "Serotonin Innervation in Adult Rat Neostriatum. II. Ultrastructural Features: A Radioautographic and Immunocytochemical Study." *Brain Research* 481 (1): 67–86.
Soghomonian, J. J., G. Doucet, and L. Descarries. 1987. "Serotonin Innervation in Adult Rat Neostriatum. I. Quantified Regional Distribution." *Brain Research* 425 (1): 85–100.
Sora, I., C. Wichems, N. Takahashi, X. F. Li, Z. Zeng, R. Revay, K. P. Lesch, D. L. Murphy, and G. R. Uhl. 1998. "Cocaine Reward Models: Conditioned Place Preference Can Be Established in Dopamine- and in Serotonin-Transporter Knockout Mice." *Proceedings of the National Academy of Sciences of the United States of America* 95 (13): 7699–7704.
Speth, R. C., F. M. Chen, J. M. Lindstrom, R. M. Kobayashi, and H. I. Yamamura. 1977. "Nicotinic Cholinergic Receptors in Rat Brain Identified by [125I]Naja Naja Siamensis Alpha-Toxin Binding." *Brain Research* 131 (2): 350–55.
Spyraki, C., H. C. Fibiger, and A. G. Phillips. 1982a. "Cocaine-Induced Place Preference Conditioning: Lack of Effects of Neuroleptics and 6-Hydroxydopamine Lesions." *Brain Research* 253 (1-2): 195–203.
Spyraki, C., H. C. Fibiger, and A. G. Phillips. 1982b. "Dopaminergic Substrates of Amphetamine-Induced Place Preference Conditioning." *Brain Research* 253 (1-2): 185–93.
Staal, Roland G W, Eugene V Mosharov, and David Sulzer. 2004. "Dopamine Neurons Release Transmitter via a Flickering Fusion Pore." *Nature Neuroscience* 7 (4): 341–46. doi:10.1038/nn1205.
Stefani, A., Q. Chen, J. Flores-Hernandez, Y. Jiao, A. Reiner, and D. J. Surmeier. 1998. "Physiological and Molecular Properties of AMPA/Kainate Receptors Expressed by Striatal Medium Spiny Neurons." *Developmental Neuroscience* 20 (2-3): 242–52.
Stiles, JR, and TM Bartol. 2001. "Monte Carlo Methods for Simulating Realistic Synaptic Microphysiology Using MCell." In *Computational Neuroscience: Realistic Modeling for Experimentalists*, De Schutter, 87–127. Boca Raton (FL): CRC Press.
Stiles, J R, D Van Helden, T M Bartol Jr, E E Salpeter, and M M Salpeter. 1996. "Miniature Endplate Current Rise Times Less than 100 Microseconds from Improved Dual Recordings Can Be Modeled with Passive Acetylcholine

Diffusion from a Synaptic Vesicle." *Proceedings of the National Academy of Sciences of the United States of America* 93 (12): 5747–52.
Strange, P. G. 1993. "New Insights into Dopamine Receptors in the Central Nervous System." *Neurochemistry International* 22 (3): 223–36.
Takahashi, N, L L Miner, I Sora, H Ujike, R S Revay, V Kostic, V Jackson-Lewis, S Przedborski, and G R Uhl. 1997. "VMAT2 Knockout Mice: Heterozygotes Display Reduced Amphetamine-Conditioned Reward, Enhanced Amphetamine Locomotion, and Enhanced MPTP Toxicity." *Proceedings of the National Academy of Sciences of the United States of America* 94 (18): 9938–43.
Tarazi, F. I., and R. J. Baldessarini. 1999. "Regional Localization of Dopamine and Ionotropic Glutamate Receptor Subtypes in Striatolimbic Brain Regions." *Journal of Neuroscience Research* 55 (4): 401–10.
Tempel, A., and R. S. Zukin. 1987. "Neuroanatomical Patterns of the Mu, Delta, and Kappa Opioid Receptors of Rat Brain as Determined by Quantitative in Vitro Autoradiography." *Proceedings of the National Academy of Sciences of the United States of America* 84 (12): 4308–12.
Tepper, James M, and J Paul Bolam. 2004. "Functional Diversity and Specificity of Neostriatal Interneurons." *Current Opinion in Neurobiology* 14 (6): 685–92. doi:10.1016/j.conb.2004.10.003.
Thorne, Robert G., and Charles Nicholson. 2006. "In Vivo Diffusion Analysis with Quantum Dots and Dextrans Predicts the Width of Brain Extracellular Space." *Proceedings of the National Academy of Sciences* 103 (14): 5567–72. doi:10.1073/pnas.0509425103.
Threlfell, Sarah, and Stephanie Jane Cragg. 2011. "Dopamine Signaling in Dorsal versus Ventral Striatum: The Dynamic Role of Cholinergic Interneurons." *Frontiers in Systems Neuroscience* 5: 11. doi:10.3389/fnsys.2011.00011.
Threlfell, Sarah, Tatjana Lalic, Nicola J Platt, Katie A Jennings, Karl Deisseroth, and Stephanie J Cragg. 2012. "Striatal Dopamine Release Is Triggered by Synchronized Activity in Cholinergic Interneurons." *Neuron* 75 (1): 58–64. doi:10.1016/j.neuron.2012.04.038.
Tritsch, Nicolas, and Bernardo L Sabatini. 2012. "Dopaminergic Modulation of Synaptic Transmission in Cortex and Striatum." *Neuron* 76 (1): 33–50.
Usiello, A., J. H. Baik, F. Rougé-Pont, R. Picetti, A. Dierich, M. LeMeur, P. V. Piazza, and E. Borrelli. 2000. "Distinct Functions of the Two Isoforms of Dopamine D2 Receptors." *Nature* 408 (6809): 199–203. doi:10.1038/35041572.
Van Bockstaele, E. J., and V. M. Pickel. 1995. "GABA-Containing Neurons in the Ventral Tegmental Area Project to the Nucleus Accumbens in Rat Brain." *Brain Research* 682 (1-2): 215–21.
van Dongen, Yvette C., Philippe Mailly, Anne-Marie Thierry, Henk J. Groenewegen, and Jean-Michel Deniau. 2008. "Three-Dimensional Organization of Dendrites and Local Axon Collaterals of Shell and Core Medium-Sized Spiny Projection Neurons of the Rat Nucleus Accumbens." *Brain Structure and Function* 213 (1-2): 129–47. doi:10.1007/s00429-008-0173-5.
van Wieringen, Jan-Peter, Jan Booij, Vladimir Shalgunov, Philip Elsinga, and Martin C. Michel. 2012. "Agonist High- and Low-Affinity States of Dopamine D2

Receptors: Methods of Detection and Clinical Implications." *Naunyn-Schmiedeberg's Archives of Pharmacology* 386 (2): 135–54. doi:10.1007/s00210-012-0817-0.

Varona, Adolfo, Javier Gil, Gonzalo Saracibar, Jose Luis Maza, Enrique Echevarria, and Jon Irazusta. 2003. "Effects of Imipramine Treatment on Delta-Opioid Receptors of the Rat Brain Cortex and Striatum." *Arzneimittel-Forschung* 53 (1): 21–25. doi:10.1055/s-0031-1297065.

Vathy, I., A. Rimanóczy, and R. Slamberová. 2000. "Prenatal Exposure to Morphine Differentially Alters Gonadal Hormone Regulation of Delta-Opioid Receptor Binding in Male and Female Rats." *Brain Research Bulletin* 53 (6): 793–800.

Vaughan, Roxanne A., and James D. Foster. 2013. "Mechanisms of Dopamine Transporter Regulation in Normal and Disease States." *Trends in Pharmacological Sciences* 34 (9): 489–96. doi:10.1016/j.tips.2013.07.005.

Veeneman, Maartje M. J., Mark H. Broekhoven, Ruth Damsteegt, and Louk J. M. J. Vanderschuren. 2012. "Distinct Contributions of Dopamine in the Dorsolateral Striatum and Nucleus Accumbens Shell to the Reinforcing Properties of Cocaine." *Neuropsychopharmacology: Official Publication of the American College of Neuropsychopharmacology* 37 (2): 487–98. doi:10.1038/npp.2011.209.

Vezina, P., G. Blanc, J. Glowinski, and J. P. Tassin. 1992. "Nicotine and Morphine Differentially Activate Brain Dopamine in Prefrontocortical and Subcortical Terminal Fields: Effects of Acute and Repeated Injections." *The Journal of Pharmacology and Experimental Therapeutics* 261 (2): 484–90.

Voorn, Pieter, Louk J. M. J Vanderschuren, Henk J Groenewegen, Trevor W Robbins, and Cyriel M. A Pennartz. 2004. "Putting a Spin on the Dorsal–ventral Divide of the Striatum." *Trends in Neurosciences* 27 (8): 468–74. doi:10.1016/j.tins.2004.06.006.

Waldvogel, H. J., Y. Kubota, S. C. Trevallyan, Y. Kawaguchi, J. M. Fritschy, H. Mohler, and R. L. Faull. 1997. "The Morphological and Chemical Characteristics of Striatal Neurons Immunoreactive for the alpha1-Subunit of the GABA(A) Receptor in the Rat." *Neuroscience* 80 (3): 775–92.

Wallace, Lane J, and Rachel M Hughes. 2008. "Computational Analysis of Stimulated Dopaminergic Synapses Suggests Release Largely Occurs from a Single Pool of Vesicles." *Synapse (New York, N.Y.)* 62 (12): 909–19. doi:10.1002/syn.20572.

Wall, Nicholas R., Mauricio De La Parra, Edward M. Callaway, and Anatol C. Kreitzer. 2013. "Differential Innervation of Direct- and Indirect-Pathway Striatal Projection Neurons." *Neuron* 79 (2): 347–60. doi:10.1016/j.neuron.2013.05.014.

Walters, D. E., and L. A. Carr. 1988. "Perinatal Exposure to Cannabinoids Alters Neurochemical Development in Rat Brain." *Pharmacology, Biochemistry, and Behavior* 29 (1): 213–16.

Wassum, Kate M., Sean B. Ostlund, and Nigel T. Maidment. 2012. "Phasic Mesolimbic Dopamine Signaling Precedes and Predicts Performance of a Self-Initiated Action Sequence Task." *Biological Psychiatry* 71 (10): 846–54. doi:10.1016/j.biopsych.2011.12.019.

Watson, M., H. I. Yamamura, and W. R. Roeske. 1983. "A Unique Regulatory Profile and Regional Distribution of [3H]pirenzepine Binding in the Rat Provide

Evidence for Distinct M1 and M2 Muscarinic Receptor Subtypes." *Life Sciences* 32 (26): 3001–11.
Westerink, B. H., and J. Korf. 1976. "Regional Rat Brain Levels of 3,4-Dihydroxyphenylacetic Acid and Homovanillic Acid: Concurrent Fluorometric Measurement and Influence of Drugs." *European Journal of Pharmacology* 38 (2): 281–91.
Wewers, M. E., R. K. Dhatt, T. A. Snively, and G. A. Tejwani. 1999. "The Effect of Chronic Administration of Nicotine on Antinociception, Opioid Receptor Binding and Met-Enkelphalin Levels in Rats." *Brain Research* 822 (1-2): 107–13.
Wigestrand, Mattis B., Yann S. Mineur, Christopher J. Heath, Frode Fonnum, Marina R. Picciotto, and Sven Ivar Walaas. 2011. "Decreased α4β2 Nicotinic Receptor Number in the Absence of mRNA Changes Suggests Post-Transcriptional Regulation in the Spontaneously Hypertensive Rat Model of ADHD." *Journal of Neurochemistry* 119 (1): 240–50. doi:10.1111/j.1471-4159.2011.07415.x.
Willuhn, Ingo, Amanda Tose, Matthew J. Wanat, Andrew S. Hart, Nick G. Hollon, Paul E. M. Phillips, Rainer K. W. Schwarting, and Markus Wöhr. 2014. "Phasic Dopamine Release in the Nucleus Accumbens in Response to Pro-Social 50 kHz Ultrasonic Vocalizations in Rats." *The Journal of Neuroscience* 34 (32): 10616–23. doi:10.1523/JNEUROSCI.1060-14.2014.
Wilson, C. J., and P. M. Groves. 1980. "Fine Structure and Synaptic Connections of the Common Spiny Neuron of the Rat Neostriatum: A Study Employing Intracellular Inject of Horseradish Peroxidase." *The Journal of Comparative Neurology* 194 (3): 599–615. doi:10.1002/cne.901940308.
Wilson, C. J., and Y. Kawaguchi. 1996. "The Origins of Two-State Spontaneous Membrane Potential Fluctuations of Neostriatal Spiny Neurons." *The Journal of Neuroscience* 16 (7): 2397–2410.
Wise, Roy A. 2004. "Dopamine, Learning and Motivation." *Nature Reviews. Neuroscience* 5 (6): 483–94. doi:10.1038/nrn1406.
Wouterlood, Floris G., Wolfgang Härtig, Henk J. Groenewegen, and Pieter Voorn. 2012. "Density Gradients of Vesicular Glutamate- and GABA Transporter-Immunoreactive Boutons in Calbindinand μ-Opioid Receptor-Defined Compartments in the Rat Striatum." *The Journal of Comparative Neurology* 520 (10): 2123–42. doi:10.1002/cne.23031.
Wu, Q., M. E. Reith, M. J. Kuhar, F. I. Carroll, and P. A. Garris. 2001. "Preferential Increases in Nucleus Accumbens Dopamine after Systemic Cocaine Administration Are Caused by Unique Characteristics of Dopamine Neurotransmission." *The Journal of Neuroscience: The Official Journal of the Society for Neuroscience* 21 (16): 6338–47.
Xenias, Harry S., Osvaldo Ibáñez-Sandoval, Tibor Koós, and James M. Tepper. 2015. "Are Striatal Tyrosine Hydroxylase Interneurons Dopaminergic?" *The Journal of Neuroscience: The Official Journal of the Society for Neuroscience* 35 (16): 6584–99. doi:10.1523/JNEUROSCI.0195-15.2015.
Xie, Xiaobin, Vickram Ramkumar, and Linda A. Toth. 2007. "Adenosine and Dopamine Receptor Interactions in Striatum and Caffeine-Induced Behavioral Activation." *Comparative Medicine* 57 (6): 538–45.

Yang, Guang, Cora Sau Wan Lai, Joseph Cichon, Lei Ma, Wei Li, and Wen-Biao Gan. 2014. "Sleep Promotes Branch-Specific Formation of Dendritic Spines after Learning." *Science (New York, N.Y.)* 344 (6188): 1173–78. doi:10.1126/science.1249098.

Yorgason, Jordan T, Mark J Ferris, Scott C Steffensen, and Sara R Jones. 2014. "Frequency-Dependent Effects of Ethanol on Dopamine Release in the Nucleus Accumbens." *Alcoholism, Clinical and Experimental Research* 38 (2): 438–47. doi:10.1111/acer.12287.

Yuan, J., B. T. Callahan, U. D. McCann, and G. A. Ricaurte. 2001. "Evidence against an Essential Role of Endogenous Brain Dopamine in Methamphetamine-Induced Dopaminergic Neurotoxicity." *Journal of Neurochemistry* 77 (5): 1338–47.

Yu, L., Y. M. Kuo, and C. F. Cherng. 2001. "Opioid Peptides Alleviated While Naloxone Potentiated Methamphetamine-Induced Striatal Dopamine Depletion in Mice." *Journal of Neural Transmission (Vienna, Austria: 1996)* 108 (11): 1231–37.

Yung, K. K., T. K. Ng, and C. K. Wong. 1999. "Subpopulations of Neurons in the Rat Neostriatum Display GABABR1 Receptor Immunoreactivity." *Brain Research* 830 (2): 345–52.

Zapata, A., and T. S. Shippenberg. 2002. "D(3) Receptor Ligands Modulate Extracellular Dopamine Clearance in the Nucleus Accumbens." *Journal of Neurochemistry* 81 (5): 1035–42.

Zhang, Lifen, William M Doyon, Jeremy J Clark, Paul E M Phillips, and John A Dani. 2009. "Controls of Tonic and Phasic Dopamine Transmission in the Dorsal and Ventral Striatum." *Molecular Pharmacology* 76 (2): 396–404. doi:10.1124/mol.109.056317.

Zhang, Yiyue, Gloria E. Meredith, Nasya Mendoza-Elias, David J. Rademacher, Kuei Y. Tseng, and Kathy Steece-Collier. 2013. "Aberrant Restoration of Spines and Their Synapses in L-DOPA-Induced Dyskinesia: Involvement of Corticostriatal but Not Thalamostriatal Synapses." *The Journal of Neuroscience: The Official Journal of the Society for Neuroscience* 33 (28): 11655–67. doi:10.1523/JNEUROSCI.0288-13.2013.

Zheng, T., and C. J. Wilson. 2002. "Corticostriatal Combinatorics: The Implications of Corticostriatal Axonal Arborizations." *Journal of Neurophysiology* 87 (2): 1007–17.

Zhou, Feng C., Robert N. Sahr, Youssef Sari, and Kamran Behbahani. 2006. "Glutamate and Dopamine Synaptic Terminals in Extended Amygdala after 14-Week Chronic Alcohol Drinking in Inbred Alcohol-Preferring Rats." *Alcohol* 39 (1): 39–49. doi:10.1016/j.alcohol.2006.06.013.

Zhu, J., and M. E. A. Reith. 2008. "Role of the Dopamine Transporter in the Action of Psychostimulants, Nicotine, and Other Drugs of Abuse." *CNS & Neurological Disorders Drug Targets* 7 (5): 393–409.

Zoli, M, C Torri, R Ferrari, A Jansson, I Zini, K Fuxe, and L F Agnati. 1998. "The Emergence of the Volume Transmission Concept." *Brain Research. Brain Research Reviews* 26 (2-3): 136–47.

Zuber, Benoît, Irina Nikonenko, Paul Klauser, Dominique Muller, and Jacques Dubochet. 2005. "The Mammalian Central Nervous Synaptic Cleft Contains a High Density

of Periodically Organized Complexes." *Proceedings of the National Academy of Sciences of the United States of America* 102 (52): 19192–97. doi:10.1073/pnas.0509527102.